THE ROLE OF METAL METABOLISM AND HEAT SHOCK PROTEIN GENES ON REPLICATIVE LIFESPAN OF THE BUDDING YEAST, *SACCHAROMYCES CEREVISIAE*

A Thesis Submitted to the College of

Graduate Studies and Research

In Partial Fulfillment of the Requirements

For the Degree of Master of Science

In the Department of Anatomy and Cell Biology

University of Saskatchewan

Saskatoon

By

Martin Prusinkiewicz

Permission to Use

In presenting this thesis in partial fulfilment of the requirements for a Postgraduate degree from the University of Saskatchewan, I agree that the Libraries of this University may make it freely available for inspection. I further agree that permission for copying of this thesis in any manner, in whole or in part, for scholarly purposes may be granted by the professor or professors who supervised my thesis work or, in their absence, by the Head of the Department or the Dean of the College in which my thesis work was done. It is understood that any copying or publication or use of this thesis or parts thereof for financial gain shall not be allowed without my written permission. It is also understood that due recognition shall be given to me and to the University of Saskatchewan in any scholarly use which may be made of any material in my thesis.

Requests for permission to copy or to make other use of material in this thesis in whole or part should be addressed to:

Head of the Department of Anatomy and Cell Biology
107 Wiggins Road, University of Saskatchewan
Saskatoon, Saskatchewan (S7N 5E5)

Abstract

A variety of genes that influence aging have been identified in a broad selection of organisms including *Saccharomyces cerevisiae* (yeast), *Caenorhabditis elegans* (worms), *Drosophila* (fruit flies), *Macaca Mulatta* (rhesus monkeys), and even *Homo sapiens*. Many of these genes, such the *TOR'*s, *FOXO'*s, *AKT'*s, and *S6K'*s are conserved across different organisms. All of these genes participate in nutrient sensing networks. Other conserved genetic networks may similarly affect lifespan. In this thesis, I explored genes from an iron metabolism family and a heat shock protein (HSP) gene family that have been identified, but not confirmed, to influence lifespan.

Yeast is a reliable model for mitotic (replicative) aging. Using yeast, I tested whether the *FET*-genes, encoding a family of iron importer-related genes, are required for mitotic lifespan. I also tested whether another family of genes, the yeast *SSA* HSP70-encoding genes, related to mammalian HSP70s, influence mitotic aging. I primarily used the replicative lifespan (RLS) assay, in which I measured the mitotic capacity of multiple *FET* and *SSA* yeast mutants. I hypothesize that aging occurs when iron transport is misregulated, which may lead to an over-reliance on HSPs for lifespan maintenance.

The results presented in this thesis support the hypothesis. First, *FET3* was primarily involved in lifespan maintenance under normal conditions (2% glucose), while *FET5* was primarily involved in the cellular lifespan extension characteristic of caloric restriction (0.01% glucose), a known anti-aging intervention. In addition, *SSA2* appeared to facilitate lifespan maintenance in the absence of *FET4*, while the presence of *SSA1* limited lifespan length. That the aging genes identified in this study are involved in iron metabolism or heat stress suggests that protein aggregation or reactive oxidative species production are common processes through which these genes interact.

Acknowledgements

I would like to thank Dr. Troy Harkness for supervising me over the course of my thesis project. Your guidance and the opportunity you gave me as a member of your lab has been an invaluable experience for me. I learned a wealth of information about working with yeast and the general practice of science. I appreciate your commitment to my project, your helpful comments regarding my work and your support of my future academic interests.

I would like to acknowledge the members of my supervisory committee, Dr. Julia Boughner and Dr. Brian Eames. Thank you both for your valuable insight and feedback throughout the course of this project. As the newest faculty members in the Department of Anatomy and Cell Biology, you are both great inspirations to me, who hopes to one day have a career in academia.

I would also like to extend my thanks to the members of Harkness laboratory including Dr. Ata Ghavidel, for your work on the yeast longevity screen; Mackenzie Malo, for your technical guidance (and good discussions) and Dr. Gerald Davies, Dr. Spike Postnikoff and Johannes Menzel for your general advice.

I appreciate the funding that I have received over the course of this project and I would like to acknowledge funding support from the Government of Saskatchewan, NSERC, University of Saskatchewan Graduate Student Scholarships/Travel Awards and the generous financial support of Dr. Troy Harkness.

I would like to thank my family, specifically my parents, you both inspired my love of science; my brother, you always are willing to impart words of wisdom when I need them; and my wife, thanks for your endless encouragement and putting up with my writing process!

Finally, thanks to all my friends.

Table of Contents

List of Tables

List of Figures

List of Abbreviations

Abbreviation	
AKT	Protein Kinase B (gene/protein designation)
AMPK	AMP-activated protein kinase (gene/protein designation)
APP	Amyloid precursor protein (gene/protein designation)
Bp	(DNA) base pairs
COT	Cobalt toxicity (gene/protein designation)
CpG	Cytosine phosphate guanine
CR	Caloric restriction
DAF	Dauer formation (gene/protein designation)
DMT	Divalent metal cation transporter (gene/protein designation)
ER	Endoplasmic reticulum
ERC	Extrachromosomal rDNA circle
FET	Ferrous transport (gene/protein designation)
FDA	Food and Drug Administration
FKH	Forkhead (gene/protein designation)
FOXO	Forkhead box O (gene/protein designation)
FTH	FTR1 homolog (gene/protein designation)
FTR	Fe transporter (gene/protein designation)
GPA	G protein alpha subunit (gene/protein designation)
GPR	G-protein coupled receptor (gene/protein designation)
•HO	Hydroxyl radical
HAP	Heme activator protein (gene/protein designation)
HIS	Histidine biosynthesis (gene/protein designation)
HSP	Heat shock protein (gene/protein designation)
HXK	Hexokinase (gene/protein designation)
IGF	Insulin-like growth factor (gene/protein designation)
KanMX	Kanamycin resistance marker (gene/protein designation)
LEU	Leucine biosynthesis (gene/protein designation)
LKB	A Serine/threonine protein kinase (gene/protein designation)
LYS	Lysine biosynthesis (gene/protein designation)
MAT	Mating type locus (A or α) (gene/protein designation)
MMT	Mitochondrial metal transporter (gene/protein designation)
MET	Methionine biosynthesis (gene/protein designation)
MSC	Meiotic sister-chromatid recombination (gene/protein designation)
mTORC	Mammalian target of rapamycin complex
O_2•$^-$	Superoxide radical
ORF	Open Reading Frame
PCR	Polymerase chain reaction
PKA	Protein kinase A (gene/protein designation)
qPCR	Quantitative polymerase chain reaction
R	R-statistics software
rDNA	Ribosomal deoxyribonucleic acid

ResGen	Research Genetics (company)
RLS	Replicative lifespan
ROS	Reactive oxidative species
SCH	Yeast AKT homolog (gene/protein designation)
SIR	Silent information regulator (gene/protein designation)
SIRT	Silent mating type information regulation 2 homolog (gene/protein designation)
SNF	Sucrose non-fermenting (gene/protein designation)
SOD	Superoxide dismutase (gene/protein designation)
S6K	S6 Kinase (gene/protein designation)
SSA	Stress-seventy subfamily A (gene/protein designation)
SSE	Stress-seventy subfamily E (gene/protein designation)
Taq	*Thermus aquaticus* bacteria
TOR	Target of rapamycin (gene/protein designation)
URA	Uracil biosynthesis (gene/protein designation)
UV	Ultraviolet
YP-	Yeast extract peptone no sugar growth media
YPD	Yeast extract peptone dextrose growth media
VNTR	Variable number tandem repeat
ZRC	Zinc resistance conferring (gene/protein designation)

1. Introduction

The eukaryotic model organism, the budding yeast *S. cerevisiae*, is a unicellular and predominantly haploid microorganism useful for elucidating major conserved biological pathways found across many other eukaryotic organisms, including *Homo sapiens* (Botstein et al., 1997). Aging is a phenomenon that affects all living organisms and culminates in a cessation of biological and metabolic activity known as death (Lopez-Otin et al., 2013). Understanding the natural causes for this cessation of biological activity may be the key to extending lifespan, if these causes can be reversed or limited.

1.1 Rationale

Extending human lifespan, which is the absolute number of years lived, and healthspan, which is the number of high-quality and fully active years lived, is an area of research that is gaining wide public attention from biotechnology start-ups, investors, government funding agencies (e.g. National Institute of Aging in the USA) and the aging population (Scott and DeFrancesco, 2015). Currently, one of the most reliable methods of lifespan extension is caloric restriction (CR), but this method is associated with biological trade-offs, such as slower, stunted growth, and impaired wound healing and immunity, perhaps all leading to a decrease in quality of life (Fontana et al., 2010). A variety of genes such as *SIR2* and *TOR1* have been associated with CR lifespan extension, but altering expression of these genes to extend lifespan without CR can produce health defects (de Cabo et al., 2014). These health defects include immunosuppression, glucose intolerance and hyperlipidemia (Roth and Ingram, 2015). For this reason it is important to

explore the variety of other genetic processes modified by CR to determine whether another set of genes or metabolic processes are more tractable targets for viable lifespan extension. Metal metabolism and protein misfolding have both been related to lifespan due to the toxic effects of protein aggregation (Leal et al., 2012). For example, excess free iron within the cell can induce the formation of reactive oxidative species (ROS) (Batista-Nascimento et al., 2012). ROS can interact with protein aggregations within the cell to induce additional misfolding of surrounding proteins that leads to an increase in aggregate size (Batista-Nascimento et al., 2012). Free iron can also interact with misfolded proteins directly to induce aggregation (Batista-Nascimento et al., 2012). Also, protein aggregate induction and removal can be linked to genes corresponding to metal transporters and heat shock proteins (HSPs) respectively, whose expression is modified by CR (Lin et al., 2002). Based on these past studies, it is likely that, when examined more closely, heat shock protein-encoding and metal metabolism genes will affect lifespan of *S. cerevisiae*.

1.2 Replicative (Mitotic) Aging in *S. cerevisiae*

S. cerevisiae can serve as a model for two types of cellular aging, replicative aging and chronological aging. These two aging-patterns are represented by two main populations of cells in higher eukaryotes, differentiated or senescent cells, and pluripotent stem cells. Chronological, or post-mitotic, aging of yeast is most similar to the aging pattern of differentiated or senescent cells of higher eukaryotes. Chronological aging affects all of the metabolic activities of a cell that occur once the cell no longer replicates (Austriaco, 1996; Gershon and Gershon, 2000; Kaeberlein, 2010; Piper, 2006). This process usually culminates in apoptosis, also known as programmed cell death (Fröhlich

and Madeo, 2000; Herker et al., 2004; Kaeberlein, 2010). Examples of cell types for which chronological aging can be modeled in *S. cerevisiae* include neurons, and fibroblasts in wound healing (van Deursen, 2014).

The second type of yeast aging is replicative, or mitotic, aging, which resembles the aging pattern of pluripotent stem cells in higher eukaryotes. (Austriaco, 1996; Gershon and Gershon, 2000; Lopez-Otin et al., 2013; Piper, 2006). Cells are replicatively aged when they lose the capacity to mitotically divide and sequester damaging cellular features, such as protein aggregates and reactive oxidative species, away from daughter cells (Bufalino et al., 2013; Pattabiraman and Kaganovich, 2014). Eventually replicatively aging cells accumulate so much damage as to become mitotically non-functional. Replicative aging differs distinctly from chronological aging as cells are in a post-replicative state once their chronological lifespan begins (Kaeberlein, 2010; Katajisto et al., 2015; Zhou et al., 2014). In addition, the RLS length (i.e. number of mitotic divisions) of yeast cells does not correlate with a unit of time (e.g. minutes, hours) (Molon et al., 2015). Extending the replicative or mitotic capacity of certain cells, such as human stem cells, may extend the lifespan of a multi-cellular organism (Fontana et al., 2010). Yeast cells are technically the easiest experimental model of replicative cellular aging because it is possible to clearly count the divisions of each yeast cell using a micromanipulator dissection microscope. This microscope allows the user to remove daughter cells from the mother cell with ease as they bud every 1.5 to 2 hours. The daughter cell from a mitotic budding event in *S. cerevisiae* is always smaller. Another method of determining RLS in yeast, which involves staining and counting bud scars on a mother cell, is limited by the maximum number of divisions that can be accurately

counted (Kim et al., 1996). Counting bud scars is therefore a less precise measurement of RLS. In addition, the causes of replicative cellular aging, such as aging factors (e.g. an accumulation of misfolded or damaged proteins and reactive oxidative species) and actions of specific genes, are consistently conserved across a variety of organisms (Steinkraus et al., 2008). This conservation of aging features from yeast to higher eukaryotes is important because it means that results from yeast research (e.g. a molecular pathway) are likely applicable to higher eukaryotes. However, a primary concern with the assay is that it is time-consuming, since every individual cell division for a sample of yeast must be manually counted (Steinkraus et al., 2008). Despite this, it is well suited for thorough study of putative aging-related genes identified from previously performed screens because it can be used to study a multitude of genetic interactions and provide quantitative lifespan data.

The daughter cell from a yeast mitotic event cannot be renewed indefinitely. Certain harmful components in the cytoplasm of yeast cells segregate asymmetrically in the dividing mother cell (Egilmez and Jazwinski, 1989). This asymmetry ensures that the new daughter cell contains virtually no harmful factors that can negatively affect its replicative capacity (Egilmez and Jazwinski, 1989). In this way, replicative aging in a daughter yeast cell is influenced more by genotype than by the accumulated damage of the mother cell. However, segregation of harmful factors is imperfect and does have consequences: daughter cells from older mothers do have reduced lifespans although these are still greater than that of the mother cell (Kennedy et al., 1994). However, via as-yet unknown mechanisms, the grand-daughters of an aged mother cell do not exhibit a reduced lifespan (Kennedy et al., 1994). The renewal capacity of the second-generation

daughter cells indicates that the damage faced by aging mother cells is unlikely to be permanent DNA damage, as one would expect such damage to persist throughout successive generations (Kennedy et al., 1994). Very old mother cells do have a hyper-mutation phenotype which contributes to a breakdown in this daughter-cell renewal capacity (Burhans and Weinberger, 2012).

When using *S. cerevisiae* to model aging, strains must be carefully selected: for example, naturally short-lived *S. cerevisiae* strains, such as W303R, KAY446, YPHDF-1A, YPK9 and PSY316, may show lifespans effects for certain genes that, when examined in naturally long-lived strains, such as BY4741 or BY4742, have no discernable effect on lifespan (Kaeberlein et al., 2005b). One possible explanation of lifespan differences between yeast strains could be variable untranslated regions in the transcriptome of each strain (Sardu et al., 2014). BY4741 was the strain selected for the present study because, first, a deletion library is available for every non-essential gene found in this strain (Winzeler et al., 1999) and, second, BY4741 is less likely to accumulate spontaneous genetic mutations or aneuploidies that suppress the mutation of interest (Kaeberlein et al., 2005b).

1.3 Genetic pathways contributing to replicative aging in *S. cerevisiae*

1.3.1 The Forkhead (FOXO) transcription factors

In *S. cerevisiae* and other eukaryotic models, conserved pathways related to nutrient sensing have been identified that contribute to cellular aging and the CR response. One example is the insulin/IGF-1 signaling pathway, which has a variety of targets, such as the FOXO transcription factor (DAF-16 in worms) shown to shorten lifespan in *C. elegans* when deleted or reduced, and to extend lifespan when

overexpressed (Gami and Wolkow, 2006). The yeast orthologs of FOXO, *FKH1* and *FKH2* also extend lifespan when overexpressed (Postnikoff et al., 2012). In humans, an allele of *FOXO3A* is associated with long lifespan: mRNA levels of *FOXO3A* are increased in individuals with this version (Banasik et al., 2011; Flachsbart et al., 2009; Willcox et al., 2008). This lifespan extension likely occurs through increased transcription of stress resistance genes, subsequently reducing the production of aging factors (Gami and Wolkow, 2006). These aging factors will be discussed below in the "causes of replicative aging" section.

1.3.2 Sirtuin nutrient-sensing

Another major aging gene is *SIR2*, part of the nutrient-sensing signaling pathway (Ha and Huh, 2011). *SIR2* encodes a histone deacetylase with genomic silencing functions. As yeast cells age, *SIR2* is downregulated, contributing to dysregulation of genes at certain loci (e.g., the yeast mating type locus leading to pseudodiploid states and sterility) (Imai et al., 2000; Smeal et al., 1996). Yeast strains lacking *SIR2* have shorter lifespans and cannot segregate damaging aging factors such as oxidized proteins away from the daughter cell (Aguilaniu et al., 2003). Although *SIR2* has been associated with telomeres, telomeres appear to maintain a constant length during yeast aging (D'Mello and Jazwinski, 1991). In mice, overexpression of *SIRT6*, a *SIR2* ortholog, extends lifespan of male mice, but inexplicably not that of female mice (Kanfi et al., 2012). Note that the females of the CB6F1 mouse strain used in this study are naturally longer lived than the males (Kanfi et al., 2012). The maximum lifespan of the male *SIRT6* overexpression strains approximated the wild type female maximum lifespans of 1,200 days (Kanfi et al., 2012). Upregulation of *SIRT6* in male mice was associated with a

decrease in serum IGF1, a major signaling protein associated with aging (Kanfi et al., 2012). Certain alleles of a human *SIR2* ortholog, *SIRT3,* are associated with long life. One, the TT genotype, is more prevalent in aged humans (Rose et al., 2003). A second allele contains an enhancer region (VNTR) that was present at high incidences in people older than 90 years (Bellizzi et al., 2005).

1.3.3 Glucose metabolism

A variety of microarray studies have been performed in order to identify expression differences between young and old yeast cells (Kamei et al., 2014; Lesur and Campbell, 2004; Lin et al., 2001). The consensus that has emerged from these high-throughput studies is that pathways involved in glucose metabolism, as well as the citric acid cycle and amino acid catabolism, are upregulated in aging cells. For example, deletion of certain genes involved in glucose metabolism, such as *HXK2* (which encodes a hexokinase predominantly found when yeast cells are grown on glucose-based media) can extend RLS (Ahuatzi et al., 2004). Hexokinase inhibition can also extend worm and mouse lifespan (Roth et al., 2009; Schmeisser et al., 2011). Reducing expression of genes involved in nutrient-response signaling pathways, such as the genes that comprise the TOR and PKA complexes, or genes encoding proteins which function upstream or downstream of these complexes, can extend lifespan in yeast (Garay et al., 2014). For example, deletion of *GPR1* or *GPA2,* which encode upstream G-protein activators of PKA increased mean yeast lifespan by 40% (Steinkraus et al., 2008). Although these genes were not examined in this thesis, they could be examined in combination with the mutants generated in this thesis as part of a future project to further understand how the metal metabolism genes affect nutrient sensing.

1.3.4 TORC nutrient-sensing

Drugs that limit the activities of certain proteins in nutrient sensing pathways have also experimentally extended lifespan. For example, deletion of *TOR1* extends yeast lifespan, and similarly the drug rapamycin, which acts to suppress the TOR1 complex (TORC1), can extend yeast lifespan (Kaeberlein et al., 2005c). In mice, rapamycin inhibits the mammalian-complex analogous to TORC1, mTOR-complex 1 (mTORC1), and increases lifespan (Harrison et al., 2009; Miller et al., 2014). The mTORC1 is comprised of the proteins mTOR, raptor, PRAS40 and mLSTB (Yip et al., 2010). In contrast, mTORC2 is comprised of mTOR, rictor, mSIN1, Protor-1 and mLSTB (Yip et al., 2010). Rapamycin can act on mTORC2, but the lifespan extending effects of the drug occur through mTORC1 (Lamming et al., 2012). Although rapamycin is approved for human use to treat cancer, its many side effects exclude its ethical use as an anti-aging intervention. These side effects include severe metabolic deregulation (Soefje et al., 2011) and may be related to the drug's effects on mTORC2, rather than mTORC1 (Lamming et al., 2012). Thus creating a drug that targets only mTORC1 may be a viable anti-aging intervention (Longo et al., 2015).

1.3.5 Insulin signaling

While yeast do not respond to insulin in a manner similar to human cells (one of the major metabolic pathways affected by anti-aging interventions), yeast do encode insulin responsive signaling components (Müller et al., 1998). Yeast *SCH9* is similar to both human *AKT* and *S6K*. These two kinases upregulate human insulin signaling which shortens lifespan (Fontana et al., 2010). Deletion of *SCH9* in *S. cerevisiae* extends yeast

lifespan (Kaeberlein et al., 2005c). In *C. elegans*, inhibition of either AKT or RSK-1 (SCH9) extends worm lifespan (Hansen et al., 2007; Paradis and Ruvkun, 1998). A mutant strain of mice, the Snell dwarf mouse, has an extended lifespan due to lower expression and activity levels of AKT compared to aged matched controls leading to reduced transcription of insulin-response genes (Hsieh and Papaconstantinou, 2004). In a human study where decreased AKT expression was associated with CR (discussed in more detail below), individuals had skeletal muscle transcriptional profiles that resembled those of younger control individuals rather than same-aged control individuals (Mercken et al., 2013). Additionally, healthy women with below-average IGF-1 levels had longer lifespans compared to other healthy women (Milman et al., 2014). This effect was not observed in healthy men with below-average IGF-1 levels when compared to healthy men with average IGF-1 levels (Milman et al., 2014). Again, these genes and their corresponding proteins are other potential areas of future research in combination with the mutants produced in this thesis in order to better understand how metal metabolism genes affect nutrient sensing.

1.3.6 Oxidative phosphorylation (respiration)

A decrease in fermentative glucose metabolism, such as glycolysis, is associated with a longer lifespan in yeast and, potentially, in humans. However, as living cells always demand energy, another type of energy metabolism is required, such as oxidative phosphorylation (also referred to mitochondrial respiration) or ketosis (energy production from fatty acids). Increased oxidative phosphorylation may play a role in extending lifespan. For instance, in yeast, increasing cellular respiration has been associated with longer lifespan (Lin et al., 2002). AMPK (called SNF1-protein kinase in yeast) is a kinase

involved in transcriptionally enacting the transition to oxidative phosphorylation in both yeast and humans under conditions of low glucose (Haurie et al., 2003; Polge and Thomas, 2007). In humans, AMPK stimulates fatty acid oxidation under low glucose conditions (Winder and Hardie, 1999). In yeast, SNF1 is involved in inducing oxidative phosphorylation on any non-glucose carbon source (Hedbacker and Carlson, 2008). Snf1/AMPK also encourages mitochondrial biogenesis (Zong et al., 2002). Over-expression of AMPK has reported lifespan-extending effects. In worms, overexpression of an AMPK-subunit gene extends lifespan (Apfeld et al., 2004). In fruit flies, overexpression of, *LKB1*, which encodes a kinase that phosphorylates AMPK, extends lifespan (Funakoshi et al., 2011). However, in yeast, SNF1 overexpression, deletion and constitutive activity all decrease lifespan on 2% glucose (normal yeast growth) conditions (Ashrafi et al., 2000; Lin et al., 2003; Lorenz et al., 2009). Alternatively, a recent study showed that under stress conditions constitutive activation of *SNF1* leads to lifespan extension (Jiao et al., 2015). This suggests that *SNF1* expression must be tightly regulated in order to promote lifespan maintenance or extension depending on the extracellular environment.

There is evidence that AMPK/SNF1 interact with the major aging proteins discussed above. In mice, AMPK promotes SIRT1 (an ortholog of yeast *SIR2*) activity (Canto et al., 2009). In a mouse cell model, AMPK phosphorylated FOXO3, leading to the transcription of genes beneficial under conditions of respiration, namely oxidative stress resistance genes, such as *Gadd45a,* metallothionein I and II, and glutathione *S*-transferase μ-1 (Greer et al., 2007). Other experiments using a variety of cellular models showed that AMPK inhibited mTORC1 by phosphorylation of an mTORC1 subunit

(Gwinn et al., 2008). Certain compounds have been identified to activate AMPK, such as resveratrol (a polyphenol) and the diabetes drug, metformin (Canto and Auwerx, 2009; Hawley et al., 2010). Resveratrol can increase lifespan in yeast, flies and worms (Howitz et al., 2003; Viswanathan et al., 2005; Wood et al., 2004). In yeast, resveratrol extends lifespan by stimulating Sir2 (Howitz et al., 2003). Sir2 activation can occur through an increased NAD/NADH ratio from mitochondrial respiration or by Pnc1 consumption of nicotinamide, which inhibits Sir2 (Guarente, 2007). In worms, this lifespan extension occurs though AMPK phosphorylation of SIR2 (Greer and Brunet, 2009). However, resveratrol is only capable of extending lifespan for mice on a fatty diet relative to untreated mice on a fatty diet (Baur et al., 2006). There was no lifespan effect for mice on a balanced, lower calorie diet (Pearson et al., 2008). This fine-tuning of AMPK/SNF1 to mediate lifespan extension is a good reason to explore the many downstream targets of AMPK to determine which of these genes alter lifespan. *FET3*, which is a target of the study presented in this thesis, is upregulated by AMPK when cells are grown on low glucose media (the yeast form of CR) (Haurie et al., 2003). *FET3* and its related family of genes may help extend lifespan under CR conditions.

1.4 Phenotypic characteristics of replicative aging in *S. cerevisiae*

S. cerevisiae is a perfect model for replicative aging because the number of mitotic divisions can be counted directly using the RLS. Yeast cells divide asymmetrically; a unique feature which makes it simple to accurately and repeatedly distinguish and pick the daughters away from the parental cell using a dissection microscope as they bud (Mortimer and Johnston, 1959; Postnikoff and Harkness, 2014; Steffen et al., 2009). Despite that yeast is a unicellular eukaryote, the genes identified to

alter yeast lifespan, such as *SCH9*, *TOR*, *SIR2* and *FKH*, are conserved in humans, emphasizing the usefulness of the yeast model to understand fundamental aging processes in humans if not other primates (Bishop and Guarente, 2007; Fontana et al., 2010; Kenyon, 2010). For example, when the human homolog of the yeast regulatory kinase *Sch9*, *AKT*, is functionally knocked-out in human endothelial cells, an increased cellular population doubling capacity occurs (Miyauchi et al., 2004). This is similar to how yeast *sch9Δ* strains have a longer replicative lifespan compared to the corresponding wild type background (Kaeberlein et al., 2005c). Additionally, cellular aging factors found in human cells, such as protein aggregates and reactive oxidative species (ROS), are also found in aging yeast cells. Thus it is likely that the cellular mechanisms that remove these potentially toxic factors are also conserved across yeast and human organisms (Blagosklonny, 2014; Grune et al., 2004; Kaeberlein, 2010). Because the yeast RLS is short (cell division stops after 20-30 divisions) and yeast can grow consistently in a variety of experimental conditions, lifespan experiments in yeast can be performed in rapid succession and with ease when compared to longer-lived model cell types or organisms. *S. cerevisiae* is also easily genetically modifiable, meaning that putative lifespan genes and genetic interactions can be readily tested for lifespan effects (Fontana et al., 2010; Michal Jazwinski et al., 1989; Postnikoff and Harkness, 2014; Steinkraus et al., 2008).

1.5 Caloric restriction in *S. cerevisiae*

One of the most reliable lifespan extension mechanisms known to date is CR (Bishop and Guarente, 2007; Jiang et al., 2000; Lin et al., 2004). CR is defined as, at a minimum, a 30% reduction in the overall caloric or energy intake of an organism when

compared to *ad libitum* feeding (de Cabo et al., 2014). In yeast, this can be mimicked by reducing the glucose concentration in the yeast growth media to at least 0.5% (Jiang et al., 2000). *Ad libitum* feeding in yeast is considered the standard growth conditions of 2% glucose at which yeast divide most rapidly. In a wide variety of model organisms, not only yeast, but in *Drosophila, C. elegans*, mice, and potentially the rhesus monkey, CR increases organismal lifespan without major deleterious health effects (de Cabo et al., 2014).

1.5.1 Genetic effectors of caloric restriction

Interestingly, many of the proteins discussed above as regulators of replicative aging (section 2.1.1) have modified expression under CR. For example, TOR1 is downregulated under CR, as are AKT, insulin and IGF-1 (Fontana et al., 2010). Downregulating these proteins increases lifespan (Fontana et al., 2010). In addition, genes whose upregulation is associated with an increase in lifespan, such as *FOXO*s, are increased under CR (Fontana et al., 2010). Yeast high-throughput datasets are a valuable starting point for finding novel genes, networks and mechanisms to extend cellular and perhaps even organismal lifespans (Ghavidel et al., 2015; Lin et al., 2002; Sharma et al., 2011).

Characterizing individual genes involved in aging is an important task because as an anti-aging regime, CR may have developmental consequences that outweigh the benefits of a longer life. For every model organism in which CR has been well defined (i.e., *Drosophila, C. elegans*, and *M. musculus*) the organisms have slower and stunted growth when CR is administered from birth (Fontana et al., 2010; Pugh et al., 1999). Due to the potential unpleasantness of drastically restricting one's food intake, CR to extend

lifespan is unappealing. Characterizing genetic pathways that could extend human lifespan may reveal therapeutic targets that can be manipulated by simple means, such as mineral or dietary supplementation (Scott and DeFrancesco, 2015).

1.5.2 Cellular pathways triggered by caloric restriction

A variety of conserved cellular pathways that extend lifespan have already been elucidated for many model organisms. These pathways include the target of rapamycin (TOR*)* (Kapahi et al., 2010), the various homologues of the S6K and AKT kinases (Fontana et al., 2010) as well as the FOXO homologues (van der Horst and Burgering, 2007). An understanding of how aging related genes are regulated is important, since increased expression of an aging associated gene does not necessarily lead to lifespan extension. For example, rapamycin, can inhibit TORC1, a nutrient-sensing complex that can regulate transcription of genes involve in metabolic pathways. This extends lifespan and causes broader phenotypic effects similar to those observed in organisms on a CR regime. These effects include reduced growth, rather than extending lifespan in isolation of any other effects (Fontana et al., 2010). This thesis contributes a solution to this problem in searching for new classes of genes that are linked to nutrient or mineral metabolism. The expression of the iron metabolism genes examined in this project may be more easily modifiable through macronutrient supplementation, and offer a viable path to lifespan extension, or in the very least healthspan extension. Healthspan is an increase in the length of quality of life in an aged individual without a numerical lifespan extension.

As will be discussed below, iron metabolism is linked to a variety of aging factors and pathways including mitochondrial function, ROS production, genome stability and

glucose metabolism. As shown by yeast microarray analysis and qPCR analysis (Lin et al., 2002; Sharma et al., 2011), the *FET* family of iron transporters is upregulated under conditions of CR. Only the RLS effects for *fet3Δ* have been briefly explored in the literature (Botta et al., 2011). In addition, searches of lifespan and yeast databases show little lifespan data for these lifespan-associated metal metabolism genes identified here (*FET3-5*, *MSC2*, *SOD1* and *MMT1*) (Ghavidel et al., 2015). For example, the Aging Factor Database (Huhne et al., 2014) which incorporates aging data from a variety of sources including Science of Aging Lifespan Observation Database (http://lifespandb.sageweb.org), the Aging Gene Database (Tacutu et al., 2013) and the Dietary Restriction Gene Database (Wuttke et al., 2012), only finds hits for searches of *FET3* and *SOD1*. Seaching the *Saccharomyces* Genome Database (Cherry et al., 2012) supplements these hits with lifespan data about *MSC2*. However, the *FET3* and *MSC2* data only relates to chronological lifespan. None of these databases have hits for *FET4, FET5* or *MMT1*. Characterizing how these genes interact to affect RLS is an important and novel task.

1.6 Aging factors: the multiple causes of replicative aging addressed in this study

One of the main reasons replicative aging occurs in yeast cells is the accumulation of toxic or non-functional cellular components that interfere with normal cellular functions and replication machinery (Kaeberlein, 2010; Nystrom and Liu, 2014; Steinkraus et al., 2008). Three major components that build up in old, mitotically dividing yeast cells can lead to cellular senescence: protein aggregates (Nyström and Liu, 2014), ROS (Jakubowski et al., 2000), and extrachromosomal rDNA circles (ERCs) (Sinclair and Guarente, 1997). These three components are briefly discussed here and

described in-depth further below. Protein aggregates and ROS have been linked to cellular aging in higher eukaryotes (Squier, 2001). Although ERCs are likely a yeast-specific cause of aging (Nystrom and Liu, 2014), genomic instability at rDNA loci, rather than circularization itself, are linked with premature aging in higher eukaryotes (Ganley and Kobayashi, 2014; Shibata et al., 2012). Instability of the genome on a broad scale is suggested to be cause of aging for multicellular organisms (Vijg and Suh, 2013). Interestingly, a higher number of these aging-factor components segregate to the mother cell than the daughter cell after mitosis in a controlled manner that can be disrupted by deletion of certain genes, such as *SIR2* (Aguilaniu et al., 2003).

1.6.1 Protein aggregation increases risk of aging, especially by disrupting heat shock proteins

A protein aggregate is a structure composed of a variety of misfolded proteins (Squier, 2001). Protein aggregates start when misfolded proteins have exposed residues that induce other misfolded proteins of the same or different type to clump together and form an aggregate nucleus (Brundin et al., 2010). This nucleus increases in size as more misfolded proteins adhere to it (Brundin et al., 2010). Many protein aggregates can form within a cell. Older cells usually contain more protein aggregates, perhaps due to a breakdown in the protein synthesis machinery as cells age or a loss in the cellular ability to fix and remove aggregates (Kaeberlein, 2010). One way protein aggregates can be harmful to a cell is by potentiating the formation of ROS, usually by capturing free metal ions within the cell that become oxidized when attached to a protein aggregate (Leal et al., 2012).

Protein aggregates can encourage the misfolding and aggregation of other proteins that interact with the aggregate (Leal et al., 2012). Ironically, despite aiding protein refolding and the prevention of protein aggregates, HSPs are sensitive to misfolding due to oxidation (Cabiscol et al., 2014). This may make HSPs especially sensitive to conditions that can rapidly produce high levels of ROS, such as misregulated iron metabolism or transport.

1.6.2 Oxidative Stress is a major contributor to aging

Perhaps one of the most toxic components that can build up in an aging cell is reactive oxidative species (ROS). ROS are small molecules that contain an extra electron, which can either alter the chemical identity of a larger biologically significant structure to which it belongs or transfer the electron to a cellular location where it would be harmful (Kaeberlein, 2010). ROS are commonly formed when the electron transport chain reduces oxygen during respiration. This can form a superoxide radical ($O_2^{\bullet -}$). Superoxide dismutases (SODs), one of which, Sod1, is a topic of research in this thesis, changes the superoxide radical into hydrogen peroxide (H_2O_2) and water (Sturtz et al., 2001). This H_2O_2 product can interact with free cellular ferrous iron (Fe^{2+}) and be oxidized by hydrogen peroxide (H_2O_2) to produce ferric iron (Fe^{3+}) and the toxic hydroxyl radical ($^{\bullet}HO$), which is highly reactive (Winterbourn, 1995).This is called the Fenton reaction. SOD1 plays a major role in neutralizing ROS production in the mitochondria as it is found in the mitochondrial intermembrane space, in addition to the cytoplasm (Sturtz et al., 2001). At a low baseline level, ROS within the cell are ubiquitous signaling molecules. At levels that exceed the cell's ability to detoxify them, ROS can cause toxic

oxidation of biomolecules that either causes or, at the very least, furthers cellular aging (D'Autreaux and Toledano, 2007).

Hormesis is beneficial stress-resistance that occurs from short, repeated exposure to a toxin (Hekimi et al., 2011). Since ROS is normally a signaling molecule at low levels, this may be how ROS has a hormetic effect (Schieber and Chandel, 2014). ROS can regulate kinases, phosphatases and other co-regulatory factors at key cysteine residues through oxidation and reduction (Groeger et al., 2009). ROS plays a role in insulin signaling (Mahadev et al., 2001), which is linked to lifespan as discussed above. ROS becomes toxic when, as a natural course of aging, it accumulates to a point where it outnumbers ROS removal mechanisms (Hekimi et al., 2011). Toxic levels of ROS can change the properties of nearly every macromolecule within the cell, including DNA (Ralph et al., 2010), proteins (Leal et al., 2012) and lipids (Hekimi et al., 2011). Dysregulation of metal metabolism in yeast may potentiate the formation of ROS due to Fenton reaction chemistry (De Freitas et al., 2003). For example, if a deletion of a metal metabolism gene leads to an increase of free iron in the cytoplasm of the mutant cell, this can lead to more opportunities for the toxic hydroxyl radical to be produced. Additionally, disruption of iron-sulfur clusters in the mitochondria can lead to increased iron uptake providing another cellular opportunity for Fenton chemistry to occur (Lill et al., 2012).

ROS is linked to protein aggregation in that the reactive metal ions found within protein aggregates can lead to protein carbonylation through production of a hydroxyl radical by Fenton chemistry. Protein carbonylation occurs when an amino acid side chain, such as cysteine, lysine or histidine, becomes alkylated through oxidation (Curtis et al.,

2012). These carbonylated proteins cannot be easily degraded and are prone to toxic aggregation (Cabiscol et al., 2014).

1.6.3 Extrachromosomal rDNA circles negatively affect lifespan

As yeast cells age, the ribosomal DNA (rDNA) found within the nucleolus begins to form extrachromosomal rDNA circles (ERCs) as a result of incomplete homologous recombination events (Kaeberlein, 2010). The increased presence of ERCs in a mutant yeast strain leads to a shorter RLS when compared to an age-matched wild type (Sinclair and Guarente, 1997). ERCs may compete with transcription factors and other proteins that are meant to bind and transcribe the rDNA (Kaeberlein, 2010). It is the rDNA instability and the inability of the cell to repair it, rather than their circularized structure, that contributes to cellular aging (Ganley and Kobayashi, 2014). These rDNA fragments do not contain the complete rDNA of the nucleolus. They are essentially non-functional competitors of rDNA and interfere with the normal function of rDNA and its components. For example, one way rDNA instability occurs is through a decrease of CpG island methylation on rDNA, due to DNA methyltransferase inactivation, which leads to a toxic accumulation of unprocessed rDNA (Gagnon-Kugler et al., 2009). In addition, rDNA genomic instability and an increase in potentially harmful genome recombination can occur when iron-sulfur cluster biosynthesis is impaired through deletion of *ZIM17* (Diaz de la Loza Mdel et al., 2011). *ZIM17* encodes a mitochondrial chaperone that is involved in iron-sulfur cluster assembly, but *ZIM17* also interacts with a Replicative Factor C-like complex that regulates progression into S-phase during mitotic division (Diaz de la Loza Mdel et al., 2011). In this way, iron metabolism and its associated genes

are one of the causes of rDNA instability in eukaryotes, linking yet another aging factor to functional iron metabolism.

1.6.4 Mitochondria are a major consumer of cellular iron and can influence replicative lifespan

Another aging factor that segregates to the mother cell rather than the daughter cell and accumulates with each mitotic division in the mother cell are dysfunctional mitochondria (Jazwinski, 2005). ROS are a by-product of oxidative phosphorylation, which is carried out in mitochondria. Mitochondria are a crucial component of lifespan extension due to the upregulation of many mitochondrial genes under conditions of CR (Lin et al., 2002). In addition, increasing expression of *HAP4*, which encodes a transcription factor for a variety of nuclear-encoded mitochondria-localized proteins required for respiration, increases RLS (Lin et al., 2004). The role of mitochondria in increasing lifespan, including under CR conditions, is suggested to be independent of mitochondria's ability to perform oxidative phosphorylation, which suggests that respiration may not be necessary for CR (Kaeberlein et al., 2005a; Petti et al., 2011). Other mitochondrial or cellular factors may be responsible for the CR response.

Some of the metal metabolism genes examined in this thesis are repressed by a family of kinases that also repress mitochondrial genes, until the yeast growth conditions transition from being a fermentable to a non-fermentable carbon source, such as when growth media is depleted of nutrients by prolonged yeast growth. For example, *FET3* is upregulated under non-fermentable conditions (Robertson et al., 2000) and *fet3Δ* is insensitive to CR lifespan extension in chronological lifespan assays (Matecic et al., 2010). *FET5* is involved in the yeast cell transition from growth on an easily fermentable

carbon-source to a non-fermentable carbon source either from nutrient depletion due to an extended growing period or from physical relocation of the yeast culture. This transition is hampered by the absence of *FET5* despite compensatory upregulation of *FET3* (Urbanowski and Piper, 1999). The upregulation of iron transport genes in conjunction with upregulation of mitochondrial activity is likely due to the presence of iron-sulfur cluster co-factors within mitochondrial proteins on a non-fermentable (non-glucose based) carbon source.

1.7 Putative genes associated with lifespan extension in *S. cerevisiae*

The novel genes recently identified (Ghavidel et al., 2015) to potentially affect RLS in yeast will be discussed in this section (Table 1; Figure 1). These genes were selected from a screen that identified whether non-lethal single deletion yeast mutants had an altered lifespan compared to the wild type (Ghavidel et al., 2015). The hidden mating-type locus, which is derepressed when yeast cells near the end of their replicative lifespans, was replaced with a *URA3* gene that encoded a toxic substrate for yeast growth in 5-fluoroortic acid (5-FOA) (Ghavidel et al., 2015). The abundance of yeast mutants, as identified using a genetic barcode and microarray, at different time points in relation to their abundance in growth media lacking 5-FOA characterized the screened strains as short-lived or long-lived (Ghavidel et al., 2015). A subset of the screen-identified genes that were examined in this thesis are: 1) *FET4*, which encodes a low-affinity plasma membrane iron transporter; 2) *FET3*, which encodes the ferroxidase portion of a high-affinity plasma membrane iron transporter complex; 3) *FET5,* which encodes the ferroxidase portion of a vacuolar iron transporter complex; 4) *MMT1*, which encodes a mitochondrial iron transporter; 5) *MSC2*, which encodes an endoplasmic reticulum zinc

transporter; 6) *SOD1,* which encodes a superoxide dismutase that neutralizes ROS and utilizes a copper and zinc cofactor; and 7) *SSA1-4*, members of the yeast HSP70-encoding gene family that encode protein chaperones responsible for proper protein folding and destroying toxic protein aggregates.

Table 1.1: Genes examined in this thesis and their functions

S. cerevisiae **Gene Name**	**Protein Product Localization**	**Protein Function**	**Expression Timing**
FET3	Plasma membrane (Philpott, 2012)	Ferroxidase protein of iron import complex (Askwith et al., 1994)	Low intracellular iron conditions (Askwith et al., 1994)
FET4	Plasma membrane (Philpott, 2012)	Divalent metal ion importer (Hassett et al., 2000)	High intracellular iron conditions (Dix et al., 1994)
FET5	Vacuolar membrane (Philpott, 2012)	Ferroxidase protein of vacuole-to-cytosol iron transporter complex (Spizzo et al., 1997)	Low intracellular iron/stress conditions (Philpott, 2012)
MMT1	Mitochondrial membrane (Li et al., 2014)	Iron export from mitochondria (Li et al., 2014)	Possibly high mitochondrial iron (not well characterized) (Li et al., 2014)
MSC2	Endoplasmic reticulum (ER) (Ellis et al., 2004)	Zinc import to ER (Ellis et al., 2004)	ER unfolded protein response (Ellis et al., 2004)
SOD1	Cytosol, mitochondrial inner membrane space, nucleus (Barker et al., 1999; Sturtz et al., 2001)	Neutralizes cellular reactive oxidative species (De Freitas et al., 2000)	Constitutive (Barker et al., 1999)
SSA1	Cytosol (Hasin et al., 2014)	Heat shock protein 70 (Hasin et al., 2014)	Constitutive (Hasin et al., 2014)
SSA2	Cytosol (Hasin et al., 2014)	Heat shock protein 70 (Hasin et al., 2014)	Constitutive (Hasin et al., 2014)
SSA3	Cytosol (Hasin et al., 2014)	Heat shock protein 70 (Hasin et al., 2014)	Inducible (Hasin et al., 2014)
SSA4	Cytosol (Hasin et al., 2014)	Heat shock protein 70 (Hasin et al., 2014)	Inducible (Hasin et al., 2014)
SSE2	Cytosol (Hideyuki et al., 1993)	Heat shock protein 70 (Hasin et al., 2014)	Age-inducible (Soti and Csermely, 2007)

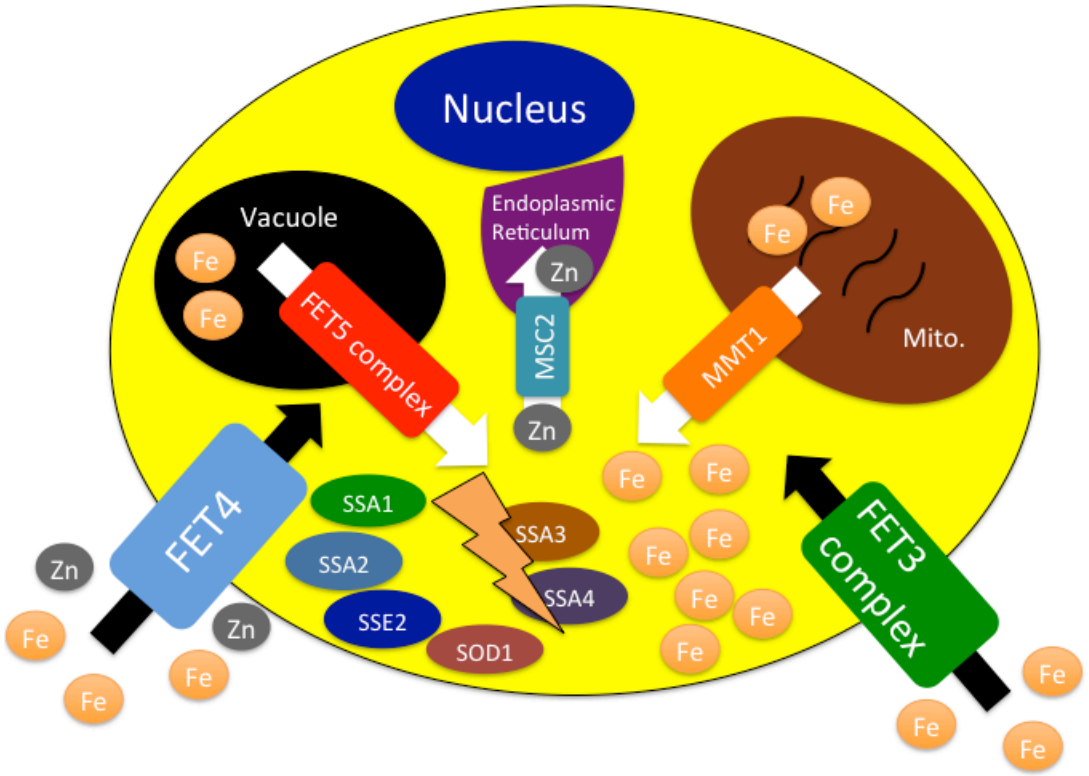

Figure 1: Localization of protein products encoded by genes studied in this thesis. Both Fet3 and Fet4 are located at the plasma membrane and are responsible for iron import. Fet5 is located at the vacuolar membrane. Mmt1 is located at the mitochondrial membrane. Msc2 is located at the endoplasmic reticulum. Ssa1-4, Sse2 and Sod1 are all predominantly cytosolic.

1.7.1 *FET4* encodes a plasma membrane iron transporter

Perhaps the simplest iron transporter in yeast is the Fet4 low-affinity plasma membrane divalent metal ion importer (Dix et al., 1994). The gene for this protein, *FET4*, is usually activated under conditions of high iron, when iron does not need to be scavenged by an iron exclusive high-affinity importer (Dix et al., 1994). However, because Fet4 has relatively broad specificity for divalent metal ions, it can also transport Cu^{2+} (Hassett et al., 2000), Zn^{2+} and Co^{2+} (Li and Kaplan, 1998) in addition to Fe^{2+}. Fet4

is related to the human divalent metal cation transporter DMT1 found in the intestine, which has been implicated in iron overload disorders (Garrick et al., 2003).

This study hypothesizes that the presence of *FET4* will likely be tied to the RLS of a yeast cell under nutrient rich growth conditions since these are the conditions when Fet4 is the primary yeast divalent metal ion transporter. Since yeast rely on divalent metal ions for the normal functioning of a variety of biological processes, including mitochondrial function, endoplasmic reticulum function and ROS scavenging, if expression of *FET4* is removed, the RLS of the yeast cell may be negatively affected due to an increase in aging-related factors such as protein aggregates or ROS. However, due to the many redundancies in cellular metal transport, alterations solely in *FET4* expression may not be sufficient to drastically alter lifespan.

1.7.2 *FET3* encodes part of a plasma membrane iron transport complex and has putative roles in replicative lifespan

Under iron-scarce conditions, the yeast cell will obtain iron through the Fet3 iron importer complex (Askwith et al., 1994). This complex consists of a transmembrane iron transporter, Ftr1, and a ferroxidase, Fet3 (Stearman et al., 1996). Fet3 is responsible for converting the reactive form of iron, Fe^{2+}, to its less reactive, oxidized form, Fe^{3+}, so that it can enter the Ftr1 transporter and pass through the plasma membrane into the cytosol (Stearman et al., 1996). Fet3 is orthologous to the mammalian ferroxidase Ceruloplasmin, which is responsible for converting Fe^{2+} to Fe^{3+} as it crosses the intestinal lumen (de Silva et al., 1997). Inactivation mutations in Ceruloplasmin cause neurological iron overload diseases in humans with dire consequences for survival if not appropriately treated (Vassiliev et al., 2005). Ceruloplasmin, and by extension Fet3, is functionally

related to another disease associated ferroxidase, β-amyloid protein precursor (APP) (Duce et al., 2010). This protein has been implicated as a contributing agent to Alzheimer's disease and functions similarly to Fet3 because the Fet3/Ftr1 transport complex converts transported Fe^{2+} to Fe^{3+}. Fet3/Ftr1 functions differently from APP in that, for APP, Fe^{2+} travels from the neuronal cytoplasm to the extracellular space where it is then oxidized by APP to Fe^{3+} (Duce et al., 2010) as opposed to being oxidized in the extracellular space and traveling to the cytoplasm. APP is an iron exporter, rather than an iron importer like Fet3, but there is a functional resemblance, which may extend Fet3 findings to humans. Interestingly, the Fet3 human ortholog Ceruloplasmin is mainly a serum circulating ferroxidase, but there are instances, such as in macrophages, where Ceruloplasmin is membrane bound. It is possible that cellular lifespan data for Fet3 in yeast may be applicable to the lifespans of more complex eukaryotic cells, such as macrophages (Lawen and Lane, 2013). *FET3* is the most highly upregulated *FET* gene in yeast under conditions of CR or low-iron (Sharma et al., 2011). *FET3* mRNA is upregulated 10-fold under CR (Sharma et al., 2011). FET3 protein is 1.5-fold higher in the wild type under CR than under normal conditions (Sharma et al., 2011).

The relationship between *FET3* and RLS has been explored in more detail than the other *FET* genes, for which RLS data is virtually non-existent. RLS data for *FET3* shows that under conditions requiring oxidative phosphorylation (i.e. on a glycerol carbon source), iron supplementation extends lifespan in the presence of Fet3, but not when *FET3* is deleted (Botta et al., 2011). Rather, *fet3Δ* on normal growth conditions (2% glucose) has a lifespan comparable to wild type (Kaeberlein et al., 2005c). Clearly

FET3 is implicated in RLS of yeast, but how Fet3 ties into other anti-aging pathways or mechanisms, such as CR, is unknown and warrants further investigation.

1.7.3 *FET5* encodes the ferroxidase portion of a vacuolar membrane iron transport complex that exports iron into the cytoplasm

Another *FET* gene shown to be upregulated (two-fold) under conditions of CR or low-iron is *FET5* (Sharma et al., 2011). The Fet5 protein is very similar to Fet3 in that it is the ferroxidase portion of an iron transporter complex (Spizzo et al., 1997). In concert with the transmembrane channel protein Fth1, Fet5 is responsible for moving iron from the vacuole (yeast lysosome) to the cytosol (Urbanowski and Piper, 1999). The vacuole is thought to be the iron storage center of the yeast cell since the yeast cell lacks Ferritin, a protein implicated in iron storage in mammalian, plant and algal cells (Briat et al., 2010; Raguzzi et al., 1988). In addition, the vacuole is the yeast equivalent of the lysosome in mammalian cells, which is the site of protein degradation (van den Hazel et al., 1996). Fet5 overexpression is able to rescue growth defects of a *fet3Δ fet4Δ* double mutant due to its similarity to Fet3 whereby Fet5 can localize to the plasma membrane in the absence of Fet3 (Spizzo et al., 1997). Thus Fet5 is another target of the present study.

1.7.4 Other genes possibly associated with lifespan

MMT1, MSC2 and *SOD1* are three other lifespan-associated genes that affect metal metabolism or use a metal co-factor (Ghavidel et al. 2015). *MMT1* encodes a mitochondrial iron exporter that is homologous to the protein product of *MMT2*, which also encodes a mitochondrial iron exporter (Li et al., 2014). *MMT2* arose from an evolutionary duplication of *MMT1* in the ancestral yeast genome (Li et al., 2014). *MSC2*

encodes an endoplasmic reticulum zinc importer (Ellis et al., 2004). *SOD1* encodes a cytoplasmic, nuclear, and mitochondrial intermembrane space copper and zinc containing superoxide dismutase that is responsible for negating the harmful effect of ROS by converting any ROS containing hydroxyls to non-toxic products (De Freitas et al., 2000; Sturtz et al., 2001). RLS data about *SOD1* has been previously published in the literature and *SOD1* deletion is shown to drastically shorten RLS (Barker et al., 1999). This is likely due to the role of Sod1 in neutralizing toxic superoxides by preventing the formation of hydroxyl radicals. Single deletion mutants of these three genes were examined in detail for this project, because of their role in aging-factor related processes.

1.8 *S. cerevisiae* heat shock proteins

1.8.1. The SSA heat shock protein family is implicated in aging

Another class of genes implicated in aging encode HSP70s (Chichester et al., 2015; Morimoto, 2011; Murshid et al., 2013; Tower, 2011). The yeast SSA HSPs are related to human HSP70s (Daugaard et al., 2007). HSP70s are responsible for ensuring that nascent proteins fold into their proper final conformation (Malyshev, 2013). HSP70s are also responsible for correcting misfolded proteins, contributing to their folding back into a native conformation (Malyshev, 2013). The SSA proteins are cytoplasmic HSPs and although they have many overlapping targets, high-throughput binding assays have shown that there are a variety of unique targets for each of the SSA proteins (Brownridge et al., 2013) some of which we hypothesize will impinge on lifespan regulation, hence their inclusion in this study.

1.8.2 The putative intersection between heat shock proteins, metal induced protein aggregates and metal metabolism

Both HSPs (Malyshev, 2013) and metal metabolism are implicated in the formation of protein aggregates (Leal et al., 2012). For example, in Alzheimer's disease metal ions such as zinc, copper and iron can potentiate the growth of protein aggregates by transferring electrons to or from existing misfolded proteins (Leal et al., 2012). These abnormal electron compositions can induce the misfolding of other proteins around the aggregate, which in turn can induce more electron exchange between free metal ions and the growing number of misfolded proteins within a cell (Leal et al., 2012). HSPs can potentially alleviate this process by preventing misfolding or refolding the misfolded proteins (Malyshev, 2013). However, it is likely that HSPs within a cell can become overwhelmed due to a combination of limited HSP numbers and an increasing rate of protein misfolding, aggregation and an inability to repair large aggregates (Malyshev, 2013). Some SSA HSPs may be more involved in this process than others. We hypothesize that the constitutively active SSA proteins, SSA1 and SSA2, will have the greatest effect on lifespan due to their removal of aging-factors produced by excess metal ions and ROS. We will test this by combining metal metabolism mutations with SSA HSP mutations.

1.9. Central hypothesis and objectives

I hypothesize that aging occurs when iron transport is misregulated, which may lead to an over-reliance on HSPs for lifespan maintenance. This hypothesis will be queried by exploring the follow aims:

1) Determining whether iron metabolism genes promote lifespan

2) Determining whether HSP-encoding genes promote lifespan

3) Determine if HSP and iron metabolism genes interact to affect lifespan

2. Materials and Methods

2.1. Yeast strains and culture conditions

The initial strains used in this study were obtained from the *KanMX* deletion library, which confers resistance to kanamycin and the drug G418 (genticin), a cheaper alternative to kanamycin (Wach et al., 1994). G418 was used as a selectable marker in this thesis. This library contains every non-lethal single deletion mutant that can be made in *S. cerevisiae* (Brachmann et al., 1998). The strains used specifically in this study are described in Table 3.1. In general, cultures were grown in growth media containing yeast extract, peptone and 2% glucose (YPD) unless other specific culture conditions were required by the experiment. Cultures were permanently stored at -80°C in a solution containing 60% glycerol and streaked on YPD plates when they were required for each experiment.

Table 2.2: *S. cerevisiae* strains used in this study
(? denotes selectable marker present in one parent strain, but not verified in offspring mutant strain listed. Presence or absence of this marker mutation has no impact on this study)

Strain	**Genotype**	**Source/reference**
BY4741	*MAT***a** *his3Δ1 Δleu2 Δmet15 Δura3*	Research Genetics (ResGen)
BY4742	*MATα his3Δ leu2Δ lys2Δ ura3Δ*	ResGen
fet3Δ	BY4741 *fet3Δ*::*KanMX6*	ResGen
fet4Δ	BY4741 *fet4Δ*::*KanMX6*	W. Xiao, ResGen
fet5Δ	BY4741 *fet5Δ*::*KanMX6*	W. Xiao, ResGen
mmt1Δ	BY4741 *mmt1Δ*::*KanMX6*	W. Xiao, ResGen
msc2Δ	BY4741 *msc2Δ*::*KanMX6*	W. Xiao, ResGen
sod1Δ	BY4741 *sod1Δ*::*KanMX6*	W. Xiao, ResGen
ssa1Δ	BY4741 *ssa1Δ*::*KanMX6*	W. Xiao, ResGen
ssa2Δ	BY4741 *ssa2Δ*::*KanMX6*	W. Xiao, ResGen

ssa3Δ	BY4741 *ssa3Δ::KanMX6*	W. Xiao, ResGen
ssa4Δ	BY4741 *ssa4Δ::KanMX6*	W. Xiao, ResGen
sse2Δ	BY4741 *sse2Δ::KanMX6*	W. Xiao, ResGen
fet3Δ α	*MATα his3Δ Δleu2 lys2Δ(?) Δmet15(?) Δura3 fet3Δ::KanMX6*	This study
fet4Δ α	*MATα his3Δ Δleu2 lys2Δ(?) Δmet15(?) Δura3 fet4Δ::KanMX6*	This study
ssa1Δ α	*MATα his3Δ Δleu2 lys2Δ(?) Δmet15(?) Δura3 ssa1Δ::KanMX6*	This study
fet3Δ fet4Δ	*MATα his3Δ Δleu2 lys2Δ(?) Δmet15(?) Δura3 fet3Δ::KanMX6 fet4Δ::KanMX6*	This study
fet3Δ fet5Δ	*MATα his3Δ Δleu2 lys2Δ(?) Δmet15(?) Δura3 fet3Δ::KanMX6 fet5Δ::KanMX6*	This study
fet4Δ fet5Δ	*MATα his3Δ Δleu2 lys2Δ(?) Δmet15(?) Δura3 fet4Δ::KanMX6 fet5Δ::KanMX6*	This study
$fet4^{+/-}$ $fet5^{+/-}$	*MAT***a***/α his3Δ Δleu2 lys2Δ(?) Δmet15(?) Δura3* $fet4^{+/-}$ $fet5^{+/-}$	This study
fet3Δ fet4Δ fet5Δ	*MATα his3Δ Δleu2 lys2Δ(?) Δmet15(?) Δura3 fet3Δ::KanMX6 fet4Δ::KanMX6 fet5Δ::KanMX6*	This study
mmt1Δ fet4Δ	*MAT(?) his3Δ Δleu2 lys2Δ(?) Δmet15(?) Δura3 mmt1Δ::KanMX6 fet4Δ::KanMX6*	This study
ssa1Δ ssa2Δ	*MAT(?) his3Δ Δleu2 lys2Δ(?) Δmet15(?) Δura3 ssa1Δ::KanMX6 ssa2Δ::KanMX6*	This study
ssa1Δ fet4Δ	*MAT(?) his3Δ Δleu2 lys2Δ(?) Δmet15(?) Δura3 ssa1Δ::KanMX6 fet4Δ::KanMX6*	This study
ssa2Δ fet4Δ	*MAT(?) his3Δ Δleu2 lys2Δ(?) Δmet15(?) Δura3 ssa2Δ::KanMX6 fet4Δ::KanMX6*	This study

2.2 Mating of Yeast

To cross yeast strains (Treco and Winston, 2008), strains of opposite mating types *MAT**a*** and *MATα* were plated on overlapping patches on a YPD plate and incubated overnight at 30°C. This patch was restreaked from the YPD plate onto a sporulation plate and incubated at 25°C for at least three days. After three days, tetrad formation was observed under a light microscope. A tetrad, which is a tight ascus containing four small spores, resembles a small diamond or pyramid of cells (Lindegren and Lindegren, 1943). Once this structure was observed, a small amount of cells was transferred to a 1:10 solution of lyticase for 20 minutes to ensure digestion of the ascus surrounding the tetrad

for easier spore dissection. Once the ascus was digested, cells were streaked onto the side of a YPD plate and whole tetrads (i.e. tretads in which every spore was accounted for) were dissected using an MSM1000 dissection microscope equiped with a fine glass needle. Spores from dissected tetrads were distrubuted in rows among the plate and incubated at 30°C until colonies were visible to the naked eye. Complete rows of four spore-based colonies were selected for further genotyping. Prior to genotyping the mutants did not look significantly different to the naked eye.

To generate yeast double and triple deletion mutants, strains from the *KanMX* deletion library used in this study, of which all were *MAT**a***, were first crossed with a corresponding wild type of opposite mating type, strain BY4742 (*MATα*), to generate *MATα* deletion strains (Hawthorne, 1963). Single deletion mutants of opposite mating type were crossed to generate the desired double mutants. Crossing a double deletion mutant with a single deletion mutant generated triple mutants.

2.3 Strain verification

Strains generated from crosses were verified first by plating colonies grown from spores onto G418 containing plates to ensure that a selectable marker, which was a *KanMX* insert, was present within the deletion mutants. Once grown on G418, colonies from the same tetrad which showed either a 2:2 or 3:1 segregation (Lindegren, 1949) of *KanMX* containing to non-*KanMX* containing colonies were inoculated in liquid YPD for genomic DNA extraction and confirmation PCR.

2.3.1 Genomic DNA extraction

In order to confirm whether deletion mutants were crossed successfully, genomic DNA of putative mutants was extracted according to the following protocol. Yeast cells from an overnight liquid YPD culture were pelleted and media discarded. Cells were resuspended in breaking buffer and a 25:24:1 solution of phenol:chloroform:isoamyl alcohol. Glass beads were added and cells were placed on a bead beater homogenizer for one minute to rupture the cells. The lysate was centrifuged and the topmost supernatant was transferred to a clean tube. Chloroform was added to the mixture, which was then briefly vortexed. After centrifuging for three minutes, the uppermost supernatant was transferred to a fresh tube. At this point, 3M NaAc pH 4.8 at a volume of $1/10^{th}$ was added to the volume of supernatant in the new tube. Next, three times the volume of 95% ethanol was added to the tube. DNA was pelleted at 4°C. The 95% ethanol solution was removed and the DNA pellet was washed once with 70% ethanol. The 70% ethanol was removed and the pellet was allowed to dry before its re-suspension in sterile water. At this point DNA was ready for PCR confirmation.

2.3.2 Confirmation PCR

PCR was used to confirm the genotype of strains generated from crosses. For each reaction of 20 µL, 16 µL of water, 2.0 µL of 10x Taq polymerase buffer (New England BioLabs), 0.5 µL of 10 mM dNTPs (BioBasics), 0.4 µL each of 5 µM forward and reverse primers, 0.4 µL of $5x10^3$ units/ml Taq polymerase enzyme (New England BioLabs) and 0.5 µL of 10mM genomic DNA were combined in a PCR tube. A list of primers used can be found in Table 3.2. The PCR program used was as follows: Step 1) 95°C denaturing for 5:00 minutes; Step 2) 95°C denaturing for 45 seconds, Step 3) 54°C

annealing for 55 seconds; Step 4) 72°C extension for 1:30 minutes; Step 5) Repeat step 2 to 4 for 34 cycles; Step 6) 72°C extension for 8:00 minutes; Step 7) Hold at 4°C. Amplified DNA was analyzed on a 1% agarose gel made with TAE buffer and a $1{:}2x10^4$ dilution of GelRed (Froggabio) to show DNA with a UV fluorescence imager. Strains showing amplified bands the size of *KanMX* insertions as opposed to the gene of interest were considered confirmed deletions and used for further experiments.

Table 2.3: Primers used in this study

	Primer name	Primer sequence
1	*FET5* forward (-450 bp external of ORF)	5'- TCAAGAACGGTGGAACAG
2	*FET5* reverse (+450 bp external of ORF)	5'- CTAGTGTCAATATCGCCG
3	*MMT1* forward (-400 bp external of ORF)	5'- AGACACCCCAGAATCTAG
4	*MMT1* reverse (+500 bp external of ORF)	5'- CAGTATCTACGATCTGGG
5	*MSC2* forward (-520 bp external of ORF)	5'- TTCTCGGTGGTATCCTTG
6	*MSC2* reverse (+480 bp external of ORF)	5'- TACGCCTGATGACGTACG
7	*SOD1* forward (-580 bp external of ORF)	5'- CACTGCGACTCATCCATG
8	*SOD1* reverse (+450 bp external of ORF)	5'- CGACAAGGAACACATGGG
9	*SSA1* forward (-300 bp external of ORF)	5'- CTTCCAAGAACCAATTGGAA
10	*SSA1* reverse (+300 bp external of ORF)	5'- AGGAAGACATCAATTAGTAC
11	*SSA2* forward (-400 bp external of ORF)	5'- GATATCGAAAAGATGGTTGC
12	*SSA2* reverse (+300 bp external of ORF)	5'- GCGTATATACACATTGTATA
13	*SSA3* forward (-100 bp external of ORF)	5'- AAGGGTATATAAAGTGACTG

14	*SSA4* forward (-250 bp external of ORF)	5'- TAGAAGTTCCTAGAACCTTA
15	*SSA4* reverse (+200 bp external of ORF)	5'- TGTATATGAACGCGAAATCG
16	*SSE2* forward (-130 bp external of ORF)	5'- TAGATTTTGGAAATATCCCT
17	*KanC* forward internal (600 bp from end of ORF)	5'-TGATTTTGATGACGAGCGTAAT
18	*KanB* reverse internal (250 bp from start of ORF)	5'- CTGCAGCGAGGAGCCGTAAT

2.4 Lifespan assay

The purpose of this particular assay was to examine the cell division characteristics of iron and HSP mutants of *S. cerevisiae*. As presented earlier in this thesis, one of the most accurate assays with which to characterize mitotic growth in yeast is the RLS assay (Mortimer and Johnston, 1959).

2.4.1. Replicative lifespan Assay

The target strain was inoculated into 50 µL of water from solid media. The 50 µL culture was pipetted near the edge of an agar plate containing the desired growth media. The plate was tilted to run the spot in a straight line along the plate to disperse the cells. The plate was covered and left to dry at room temperature. After an overnight incubation time at 30°C, the plate was set-up for the RLS assay. Using an MSM1000 dissection microscope, 15 holes were poked into the media using the attached glass needle at regular intervals. Two budding yeast cells were moved from the streak at the side of the plate to beside each hole using the glass needle. The cells were neither excessively tiny, which may indicate a growth defect, or excessively large, which may indicate a cell nearing the end of its lifespan. These cells were allowed to divide for four hours exactly, at which

time newly budded cells, which themselves had not yet budded, were used as the founding mother cells for the assay. Approximately 30 founding mother cells were used for each strain per assay.

These mother cells were monitored for growth every 1.5 to 2 hours and any new daughter cells were tallied and removed to a discard region. If more than one daughter cell had budded from the mother, the cells were counted according to 2^n rules of mitosis where *n* is the number of cell divisions. For example, if two cells were visible (i.e. the mother cell and its bud) this was counted as one division, since $2^1 = 2$ cells and n = 1 division. If four cells were visible (e.g. the mother cell, two daughter buds from the mother cell, and one grand-daughter bud from one of the daughter buds) this was counted as 2 divisions, since $2^2 = 4$ cells, where n = 2 divisions. Counting more than two mother cell divisions in this fashion was avoided to maintain accuracy of results and deter counting or estimation errors. The founding mother cell was easy to pick out from its daughter buds since it was always larger than the daughters, an established characteristic of yeast growth. Mitotic divisions for each cell were counted in this manner until divisions of the mother cells ceased.

In haploid yeast, the different mating types do not produce a significant difference in RLS from one another, while diploid yeast have a longer RLS relative to haploid strains. Note that mating type was determined using PCR (Silverman, 1996).

2.4.2 Statistical analysis of replicative lifespan assay

After data for the RLS assays were collected, the total number of cell divisions for each cell within a strain was tabulated in Microsoft® Excel as an unorganized list (Figure 2A). For example, if an experiment followed the divisions of 4 yeast cells with total

divisions of 25, 19, 21 and 15, they were tabulated as such. Once tabulated, the Microsoft® Excel formula "=COUNTIF($column$row:$column$row, ">="&generationscolumnrow)/COUNT($column$row:$column$row)*100" was used alongside an ascending list of numbers starting at 0 and ending at the maximum number of cell divisions of the assayed strain (Figure 3A). This formula counts the number of cells in the initial table that have reached a certain number of divisions and divides this value by the total number of cells assayed. Note that the "$" function in Excel ensures that the correct row and columns are counted by the software when copying the formula across all cells. This gives a percentage of mother cells that have reached a certain number of cell divisions. This procedure is repeated for each strain. These percentages are used to make a lifespan curve (Figure 3B) for each strain where the percentage of mother cells which have reached a certain number of divisions are on the y-axis and the corresponding number of mitotic divisions for that percentage of mother cells is on the x-axis. These curves can give a visual indication whether one strain had a longer or shorter RLS than another when curves for multiple strains are placed on the same graph.

To determine whether two strains had a statistically significant difference in RLS, I used the Student's T-test, which is used widely in the literature to test for differences in RLS between two different strains (Botta et al., 2011; McFaline-Figueroa et al., 2011; Steffen et al., 2009). This test determines whether two populations are the same (null hypothesis) or significantly different (alternative hypothesis) from one another. A significance value of $p < 0.05$ was chosen since this is a standard in the field. This *p*-value indicates that 1 result out of 20 would be expected to be false. If a *p*-value is less than or equal to 0.05, then the two populations would be considered significantly

different. In general, this test compares the rank of a certain collected value from one group, in this case a specific RLS for one cell from a tested sample of cells, to every value from another group and assigns a score (Mann, 1945). Higher values receive a higher rank. The total score of each comparison for one set is compared to the total score of each comparison for the second set. A *p*-value related to the scores can be calculated that reflects the probability that a certain result would be a false.

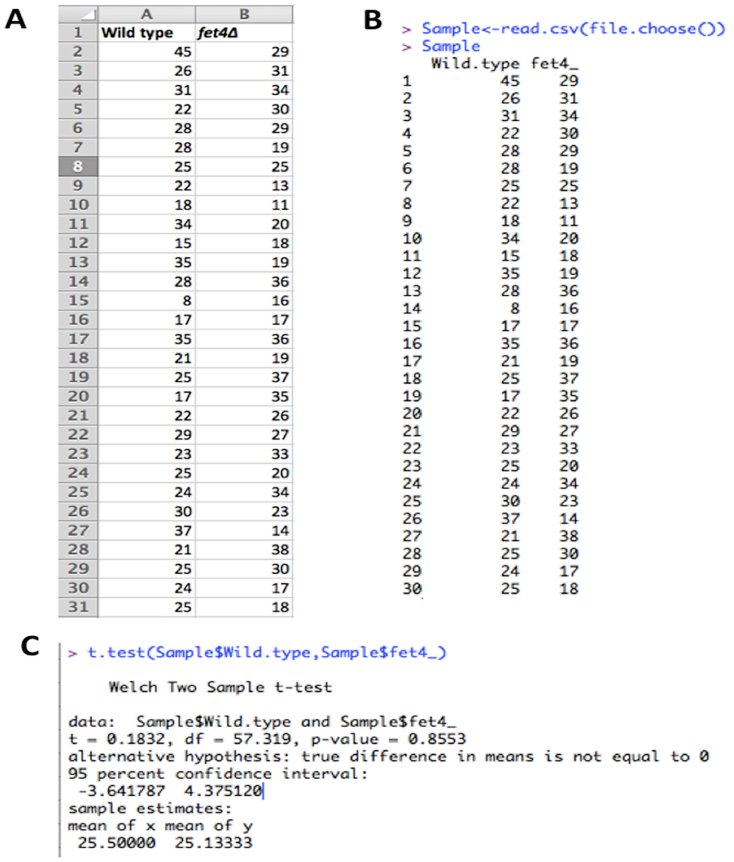

	A	B
1	Wild type	*fet4Δ*
2	45	29
3	26	31
4	31	34
5	22	30
6	28	29
7	28	19
8	25	25
9	22	13
10	18	11
11	34	20
12	15	18
13	35	19
14	28	36
15	8	16
16	17	17
17	35	36
18	21	19
19	25	37
20	17	35
21	22	26
22	29	27
23	23	33
24	25	20
25	24	34
26	30	23
27	37	14
28	21	38
29	25	30
30	24	17
31	25	18

	Wild.type	fet4_
1	45	29
2	26	31
3	31	34
4	22	30
5	28	29
6	28	19
7	25	25
8	22	13
9	18	11
10	34	20
11	15	18
12	35	19
13	28	36
14	8	16
15	17	17
16	35	36
17	21	19
18	25	37
19	17	35
20	22	26
21	29	27
22	23	33
23	25	20
24	24	34
25	30	23
26	37	14
27	21	38
28	25	30
29	24	17
30	25	18

Figure 2: Example of raw replicative lifespan data and statistical analysis.
(A) Unordered counts of replicative lifespan for each assayed mother cell in a wild type and mutant strains in Microsoft Excel. (B) The Excel chart is saved as a .csv file and imported into R using the formula "Sample<-read.csv(file.choose())", where "Sample" is the named assigned to the data table. Typing "Sample" shows the table in R. (C) The formula "t.test(Sample$Wild.type,Sample$fet4_)" which uses the table name and column titles to indicate from which data the Student's T-test is to be performed. The output shows a p-value of 0.8553, which means the two sets of data are not significantly different.

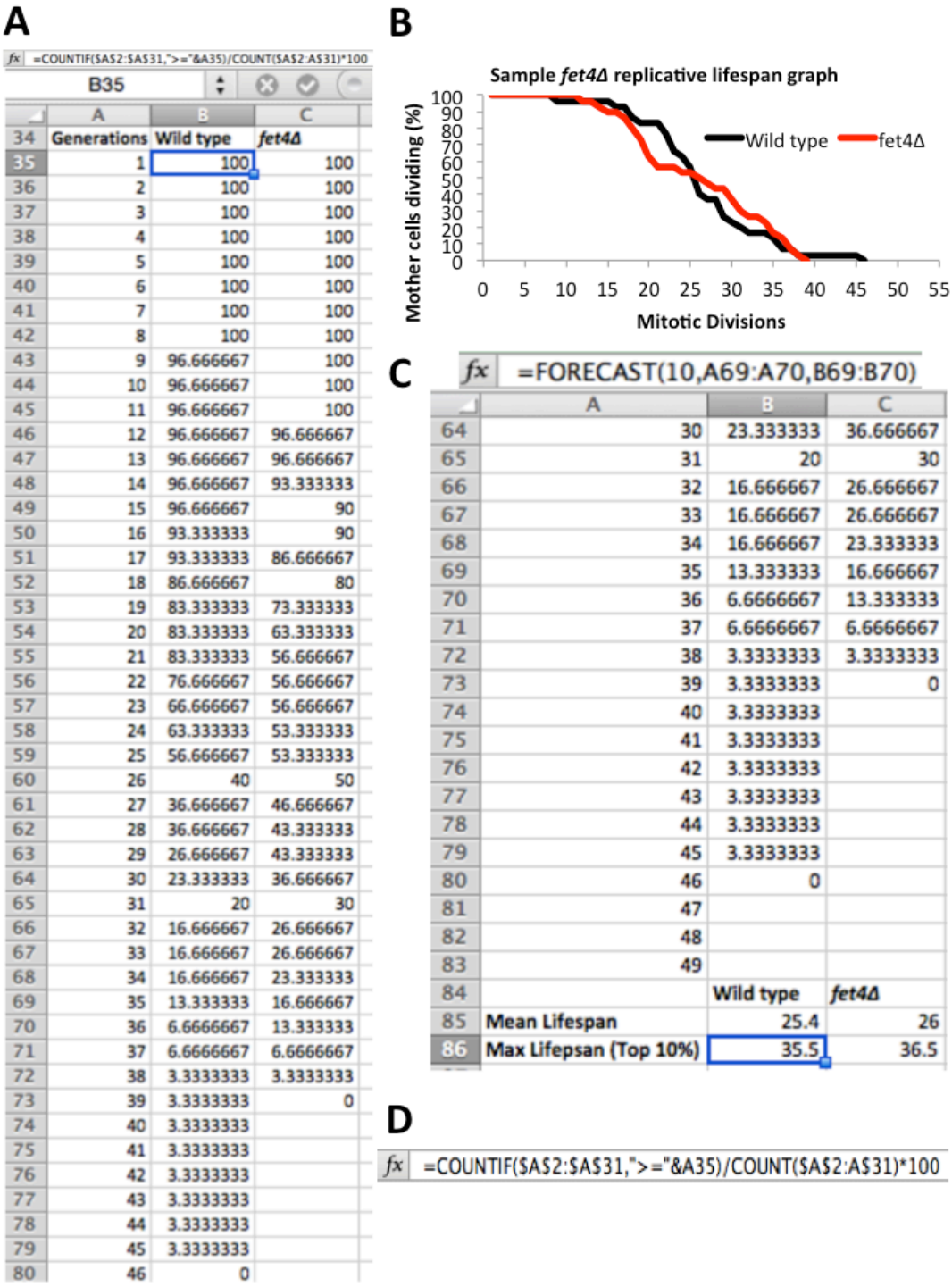

Figure 3: Example of replicative lifespan curve construction in Excel.
(A) The raw data in Excel is converted to survival percentages for each generation. The formula "=COUNTIF($A$2:$A$31,">="&A35)/COUNT($A$2:A$31)*100" gives the percentage of wild type mother cells that have divided once. (B) A line graph representation of the survival percentages for each strain. (C) Mean and maximum lifespan calculation using survival percentage. The formula "=FORECAST(10,A69:A70,B69:B70) gives the maximum wild type RLS (where only 10% of cells are still dividing). (D) The survival formula from A) enlarged.

The statistical software package used to execute the Student's T-test was R (R Core Team, 2012). To input data into R, a table of an unorganized list of cell divisions for each strain is saved as a comma separated values document (.csv). This file is loaded into R using the formula "title<-read.csv(file.choose())" where title can be any data title the user wishes (Figure 2B). Once the table was entered into R, the following formula is used: "t.test(title$item1,title$item2)" where "title" is the title of the inputted table, "Sample" in figure 2B,C, and "item1" and "item2" are the names of the strains within the dataset, "Wild.type" and "fet4_" in the example above (Figure 2C). This test gives mean values and the corresponding variances for a dataset and compares them to another strain's dataset to give a p value. A p value > 0.05 indicates there is no significant difference between the compared strains and a value < 0.05 indicates there is a significant difference between compared strains.

Other parameters determined for the datasets included "mean lifespan" (standard terminology for the field), which is the number of cell divisions 50% of the mother cells have reached. The maximum lifespan was defined as the number of cell divisions the highest 10% of dividing mother cells reached instead of the single highest-dividing cell. The excel formula used to calculate the mean or maximum RLS of a certain strain was "=FORECAST(x, known y's, known x's)" where x was either 50 for mean lifespan or 10 for maximum lifespan of the top 10% (Menzel et al., 2014) (Figure 3C). Known Y values were the mitotic divisions of the cells at values above or below the desired X value. The known X values were the corresponding percentage of mother cells that reached the certain number of divisions given in the known Y values.

The percent difference in mean lifespan between tested strains and the wild type was calculated using the formula "(tested strain mean lifespan/wild type strain mean lifespan) x 100 – 100". This will give a positive value for an increase in mean RLS and a negative value for a decrease in mean RLS.

2.5 Spot Dilutions

Growth characteristics of yeast mutants were determined using the spot dilution assay (Hampsey, 1997). An overnight culture of liquid yeast cells grown in 2% YPD was diluted to an OD_{600} of 0.5 in water. This corresponded to a cell concentration of approximately 10^7 yeast cells per milliliter. Cultures were further diluted to concentrations of 10^6, 10^5, 10^4, and 10^3 cells per milliliter. On a plate, each strain and its corresponding descending dilutions were spotted out in rows on the desired growth media conditions. In general, 3 µl of cells were spotted onto 2% YPD to assay growth under normal conditions, but for some experiments cultures were spotted onto media containing 3% YP glycerol to give an indirect indication of mitochondrial function (Hampsey, 1997). Plates were incubated at 30°C, which is the normal growth temperature for yeast, or 37°C to assay strain resistance to a stressor, in this case heat stress. Plates were scanned to produce a digital image, usually between one to three days of growth for strains grown on 2% YPD, and after approximately three to seven days for strains grown on slow growth media, such as 3% YP glycerol.

3. Results I – Growth and replicative lifespans of *fetΔ* and other metal-related mutants under glucose and carbon-source replete conditions

3.1 Spot dilution assays of single *fetΔ* metal metabolism mutants highlighted a growth deficit of *fet3Δ* on glycerol

To characterize growth ability of the single metal metabolism mutants and test the hypothesis that metal-metabolism related genes affect fitness of yeast, spot dilution assays were performed on 2% YP Glucose (YPD [dextrose]) at 30°C (normal conditions), 2% YPD at 37°C (heat stress conditions), YP Glycerol (YPG) at 30°C (forced mitochondrial respiration conditions), and YPG at 37°C (heat stress and forced mitochondrial respiration conditions). These spot dilutions could give preliminary insight to RLS effects of these mutations since growth ability is sometimes correlated with viability and RLS (Mirisola et al., 2014). Under normal conditions, impaired growth was not detected in any of the single mutants (Figure 4A). This corresponded to the RLS findings to come below, in which none of the single *fetΔ* mutants, nor the *msc2Δ* mutant, had a shortened RLS compared to the wild type on 2% YPD. None of the single *fetΔ, msc2Δ* or *sod1Δ* mutants were negatively affected by heat stress because all of the cells formed colonies in a manner that was visually similar to the wild type at 37°C (Figure 4B).

Under glycerol conditions at 30°C (Figure 5A), which forced mitochondrial respiration and was used to test the hypothesis that the studied metal metabolism genes have a significant role in oxidative phosphorylation, *fet3Δ* had growth impairment. The *fet4Δ* and *fet5Δ* mutants had less perceptible growth defects if any (Figure 5A). The *sod1Δ* and *msc2Δ* mutants grew similarly to the wild type on glycerol at 30°C. The impaired growth of the *fet3Δ, fet4Δ* and *fet5Δ* mutants was worsened on 37°C glycerol

(Figure 5B). In addition, the *sod1Δ* mutant showed a glycerol growth defect at 37°C. The *msc2Δ* mutant still grew as well as the wild type on glycerol at 37°C.

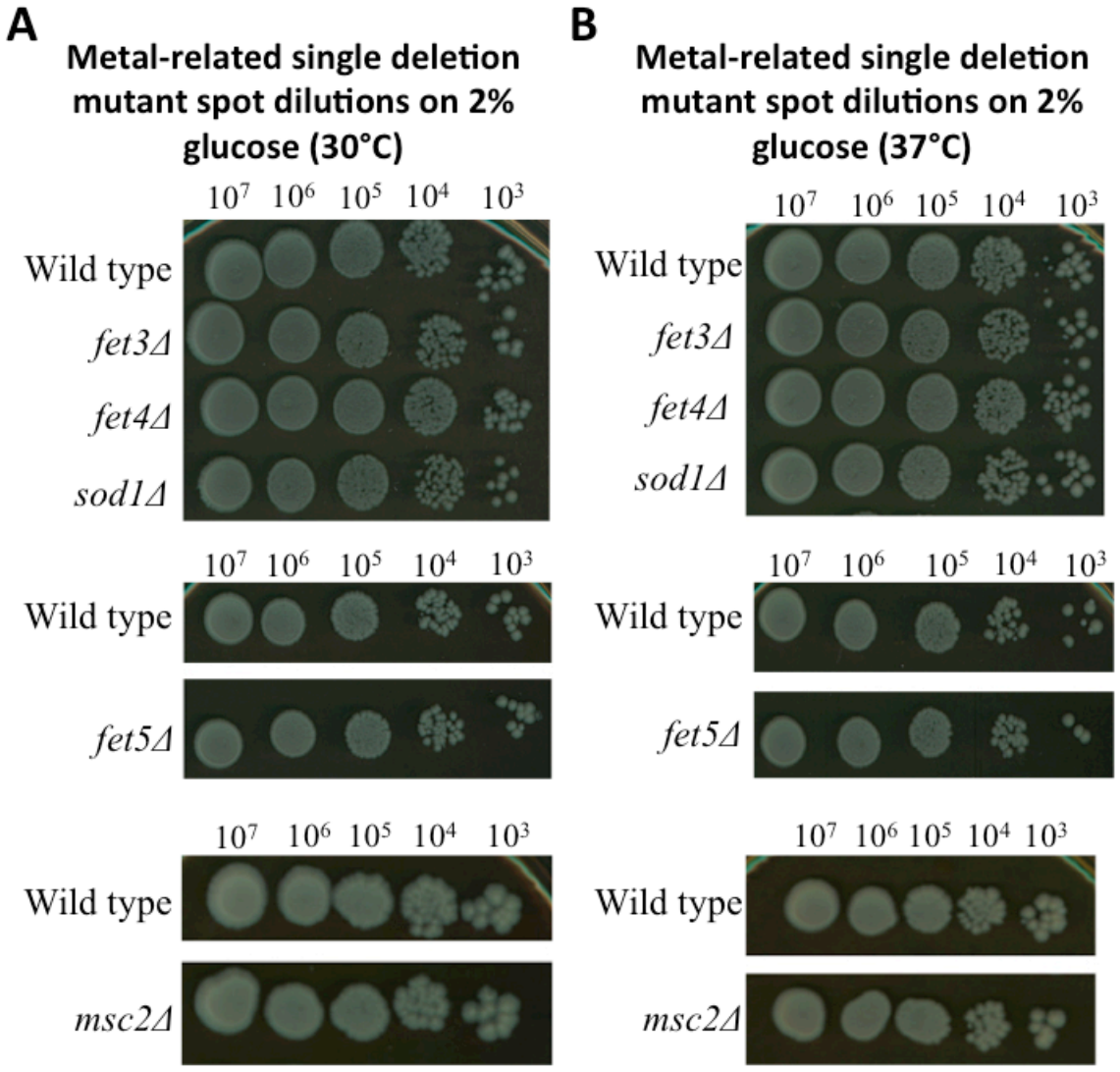

Figure 4: Spot dilutions for *fet4Δ, msc2Δ* and *sod1Δ* single mutants on YPD at 30°C and 37°C.
(A) None of *fet3Δ*, *fet4Δ*, *fet5Δ*, *sod1Δ*, or *msc2Δ* appeared to grow differently than the wild type on 2% glucose (YPD) at ideal growth temperatures (30°C) or (B) at 37°C.

When *fet3Δ* and *fet4Δ* mutants were further tested on galactose (also a poor carbon source that thus induces respirative growth), the *fet3Δ* deletion mutant had reduced growth under both normal (Figure 6A) and heat stressed (Figure 6B) galactose

conditions, indicating a reduced ability to utilize galactose. The growth of the *fet4Δ* mutant was comparable to wild type (Figure 6A,B).

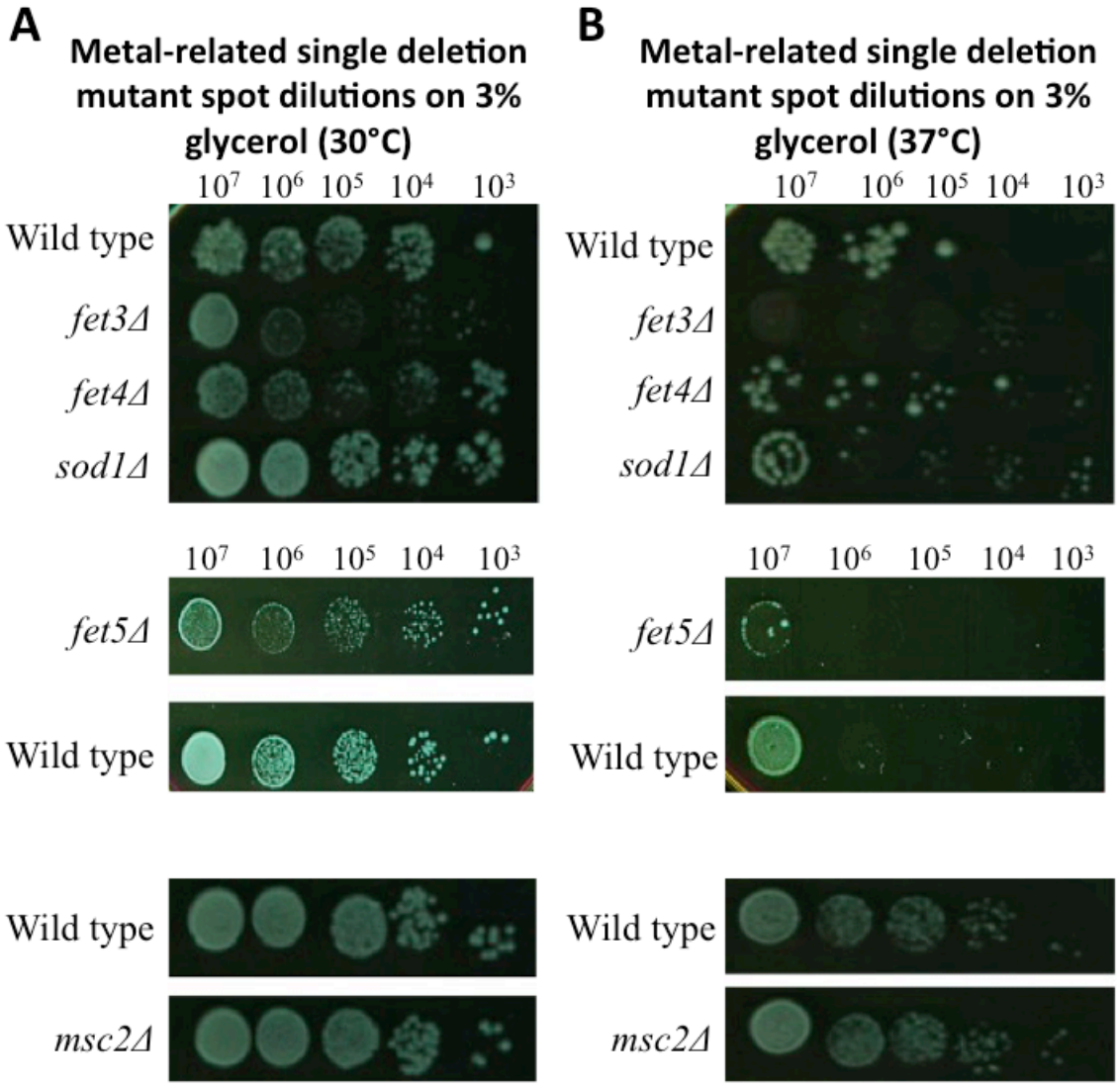

Figure 5: Spot dilutions of *fetΔ*, *msc2Δ* and *sod1Δ* single deletion mutants on 3% glycerol at 30°C and 37°C.
(A) The single mutant *fet3Δ* showed less growth than the wild type on glycerol at 30°C. The *fet4Δ* and *fet5Δ* single mutants may have less growth than the wild type. (B) At higher temperatures (37°C) on glycerol, *fet4Δ, fet5Δ* and *sod1Δ* showed drastically less growth than the wild type while *fet3Δ* showed nearly no growth. The *msc2Δ* mutant did not appear to grow differently than the wild type.

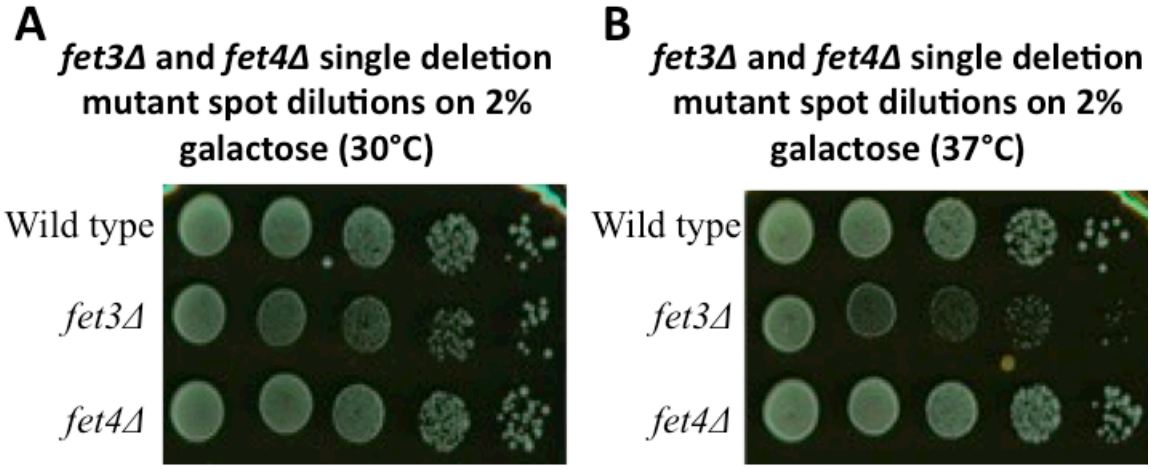

Figure 6: Spot diluitions of *fet3Δ* and *fet4Δ* deletion mutants on galactose.
(A) On galactose at 30°C the *fet3Δ* mutant showed slightly less dense growth than the wild type. The *fet4Δ* mutant showed similar growth to the wild type. (B) On galactose at 37°C the *fet3Δ* mutant showed less growth than the wild type while the *fet4Δ* mutant showed no difference in growth compared to the wild type.

3.2 Spot dilutions of select double deletion metal metabolism mutants highlighted growth defects of *fet4Δ sod1Δ* and *fet3Δ fet4Δ* mutants under certain conditions

In addition to the single mutants described above, spot dilution assays were performed for a subset of double deletion metal metabolism mutants to test the hypothesis that drastic reduction of metal metabolism and metal-related functions affects yeast fitness. These mutants were generated early in the project to test for growth defects that suggest genetic redundancy among family members or genetic interactions between metal metabolism genes. Specifically, these strains were *fet3Δ fet4Δ*, *fet4Δ sod1Δ* and *fet4Δ msc2Δ*. A *fet4 fet5* mutant was also included on the YPD tests at 30°C.

The *fet3Δ fet4Δ* mutant was selected as these are the two major plasma membrane iron importer genes and are likely to be redundant. The *fet4Δ sod1Δ* mutant was selected because Sod1 requires copper and zinc as co-factors, both of which Fet4 is partially responsible for importing into the cell (Cobine et al., 2006; Ellis et al., 2004). This mutant was selected over a *SOD1* and *FET3* double deletion mutant due to mating success of *sod1Δ* with *fet4Δ*. The *fet4Δ msc2Δ* mutant was selected to test if the plasma membrane

zinc import functions of Fet4 (Nicola and Walker, 2009) impaired the ability of Msc2 to import zinc into the ER. A *fet4Δ fet5Δ* mutant was selected to determine whether *FET5* was needed to compensate for a loss of *FET4* transport in high iron, high glucose conditions.

On YPD at 30°C (normal conditions), all of *fet3Δ fet4Δ*, *fet4Δ sod1Δ, fet4Δ msc2Δ* and *fet4Δ fet5Δ* (Figure 7A) showed no impaired growth compared to the wild type.

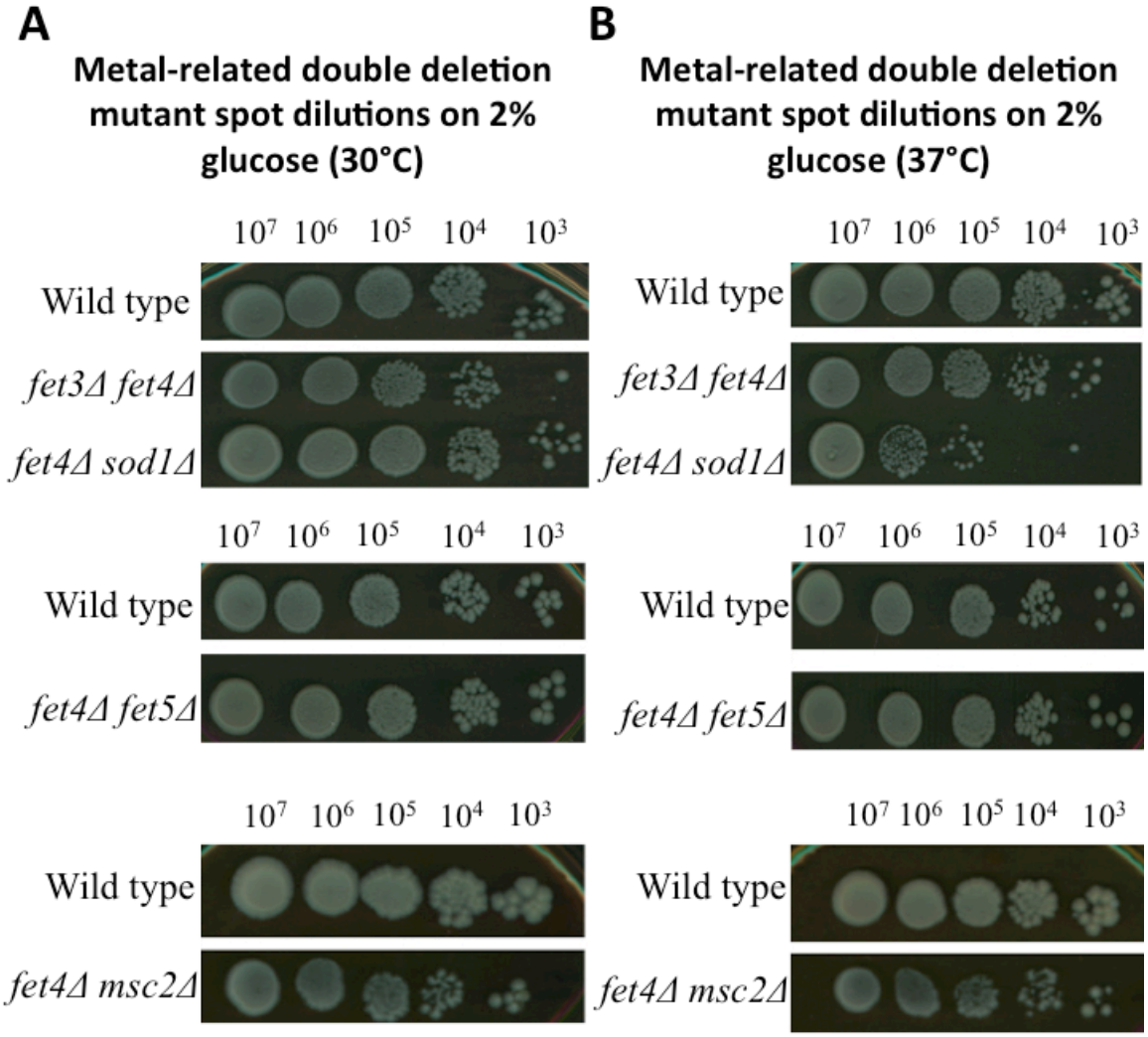

Figure 7: Spot dilutions of *fet3Δ fet4Δ*, *fet4Δ sod1Δ*, *fet4Δ msc2Δ* and *fet4Δ fet5Δ* double deletion mutants on 2% glucose at 30°C and 37°C.
(A) On 2% glucose at 30°C all strains grew normally (B) On 2% glucose at 37°C all strains, except for *fet4Δ sod1Δ* grew normally.

Under conditions of heat stress (YPD at 37°C) the *fet4Δ sod1Δ* (Figure 7B) mutant had hampered growth compared to the wild type. The *fet4Δ msc2Δ*, *fet3Δ fet4Δ* and *fet4Δ fet5Δ* (Figure 7B) growth was no different than that of the wild type despite an elevated growth temperature on YPD.

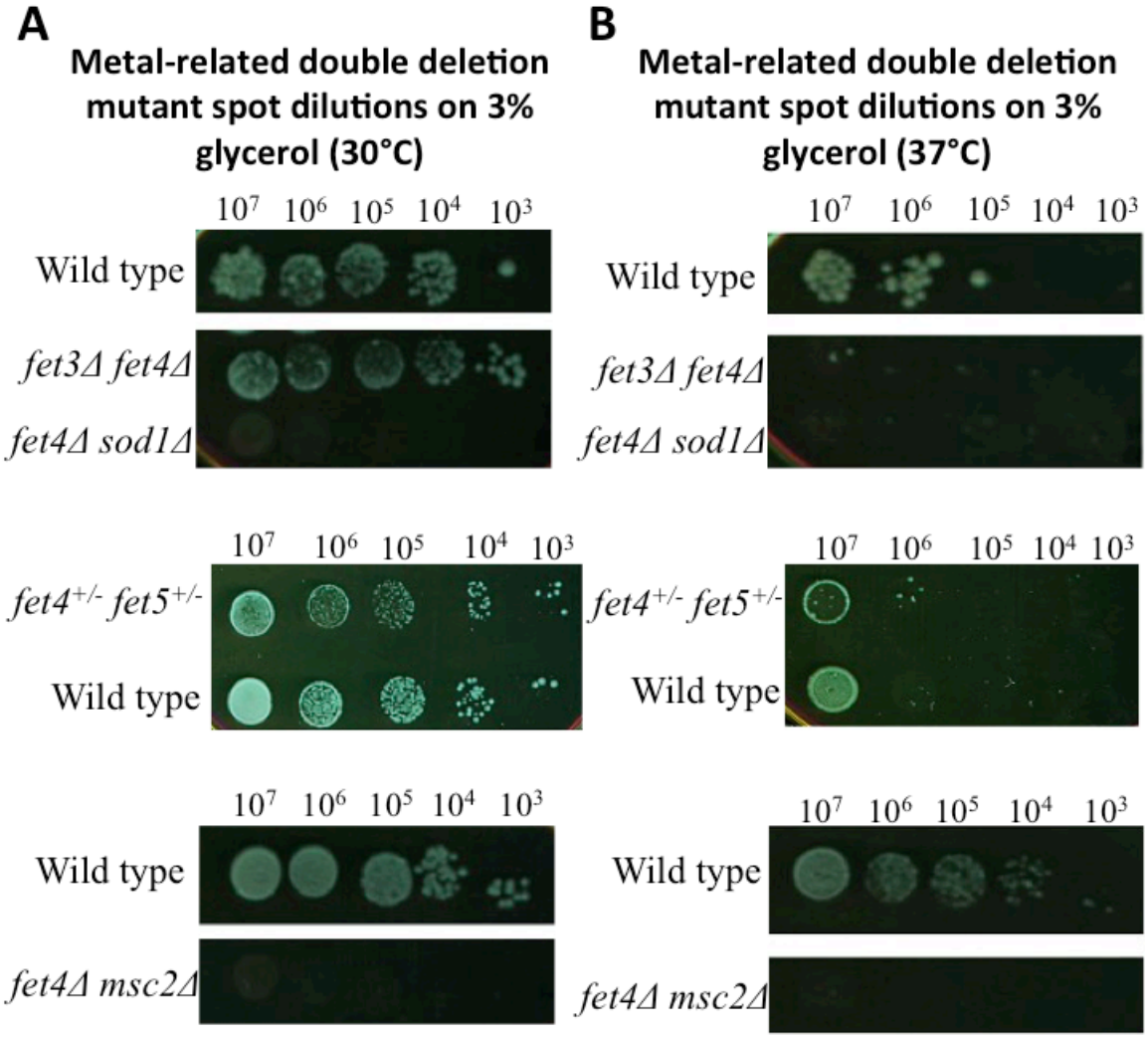

Figure 8: Spot dilutions of metal metabolism-related double deletion mutants on conditions forcing mitochondrial respiration (3% glycerol).
(A) On 3% glycerol at normal temperatures (30°C), the *fet4Δ sod1Δ* and *fet4Δ msc2Δ* double deletion mutants had nearly no growth. The *fet4*$^{+/-}$ *fet5*$^{+/-}$ mutant had slightly less dense growth compared to the wild type. The *fet3Δ fet4Δ* mutant had similar growth as the wild type. (B) On 3% glycerol at heat stress-inducing temperatures (37°C), the *fet3Δ fet4Δ* double deletion mutant also showed no growth compared to the wild type. The *fet4Δ sod1Δ* and *fet4Δ msc2Δ* double mutants continued to show no growth. Growth of the *fet4*$^{+/-}$ *fet5*$^{+/-}$ mutant was further reduced.

Under conditions forcing cellular respiration (YP glycerol at 30°C), again testing the hypothesis that metal metabolism impacts yeast mitochondrial respiration, especially under conditions of heat stress, both *fet4Δ sod1Δ* and *fet4Δ msc2Δ* (Figure 8A) had limited growth on YP glycerol. Additionally the *fet3Δ fet4Δ* mutant (Figure 8A) grew worse than the wild type on YP glycerol at 37°C. The *fet3Δ fet4Δ* mutant had better growth than the *fet4Δ sod1Δ* and *fet4Δ msc2Δ* mutants on YP glycerol at 30°C. Under conditions of heat stress, mitochondrial respiration-based growth of any of these three double deletion mutants was minimal (Figure 8B). This was expected for any of the double deletion mutants lacking a *FET* gene as the *fetΔ* single mutants all had impaired growth under heat stress conditions (Figure 8B).

Data were also collected for the $fet4^{+/-}$ $fet5^{+/-}$ mutant on glycerol and the mutant had a less growth than the wild type at both 30°C and 37°C (Figure 8A,B). These glycerol spot dilutions showed that a functional metal metabolism pathway becomes more important under respiration, especially under heat shock conditions in which HSPs are activated (Daugaard et al., 2007).

3.3 Replicative lifespans of *fetΔ* single deletion mutants were not significantly different from the wild type under fermentative conditions (2% glucose)

To test the hypothesis that the *FET* genes had a significant effect on RLS of *S. cerevisiae* under normal, nutritive growth conditions consisting of 2% glucose, the total numbers of cell divisions for 30 mother cells of each *fetΔ* strain (*fet3Δ*, *fet4Δ*, and *fet5Δ*) were counted using a yeast dissection microscope. A corresponding isogenic wild type plated on the same batch of growth media was also counted and the deletion mutant lifespan curves were statistically compared to the wild type lifespan curves for

differences in RLS trends. Glucose, which is fermentable by *S. cerevisiae*, is its ideal carbon source (at 2%) (Bergman, 2001). Based on the spot dilutions performed above, no significant differences between RLS of the single deletion mutants and the wild type were expected.

The high-affinity iron transporter complex mutant (*fet3Δ*) consistently had a RLS that was not significantly different from the wild type ($p = 0.45$) (Figure 9A). The lack of a statistically significant difference between *fet3Δ* and wild type RLS was reproducible over three trials. A similar trend was observed for the low-iron-affinity divalent metal ion transporter *fet4Δ* in that it had an RLS that was not significantly different than the wild type ($p = 0.58$) (Figure 9B). Finally, the last single deletion *fetΔ* mutant assayed, *fet5Δ*, once again showed a similar RLS trend as the *fet3Δ* and the *fet4Δ* single deletion mutants (Figure 9C). There was no significant difference between the *fet5Δ* mutant and the wild type ($p = 0.43$). These results suggest that individually the *FET* genes do not play a role in RLS under normal fermentative conditions.

3.4 Only *sod1Δ*, and not *msc2Δ* or *mmt1Δ*, had a significantly shorter replicative lifespan than the wild type under fermentative conditions (2% glucose)

To test the hypothesis that these other metal metabolism-related genes were significant to RLS, the RLS of three other metal metabolism deletion strains (*mmt1Δ*, *msc2Δ*, and *sod1Δ*) were assayed under normal nutritive growth condtions (2% glucose). However, based on the spot dilutions which showed no changes in growth of these single mutants compared to the wild type, it was possible that no significant difference in RLS between these strains and the wild type would be observable.

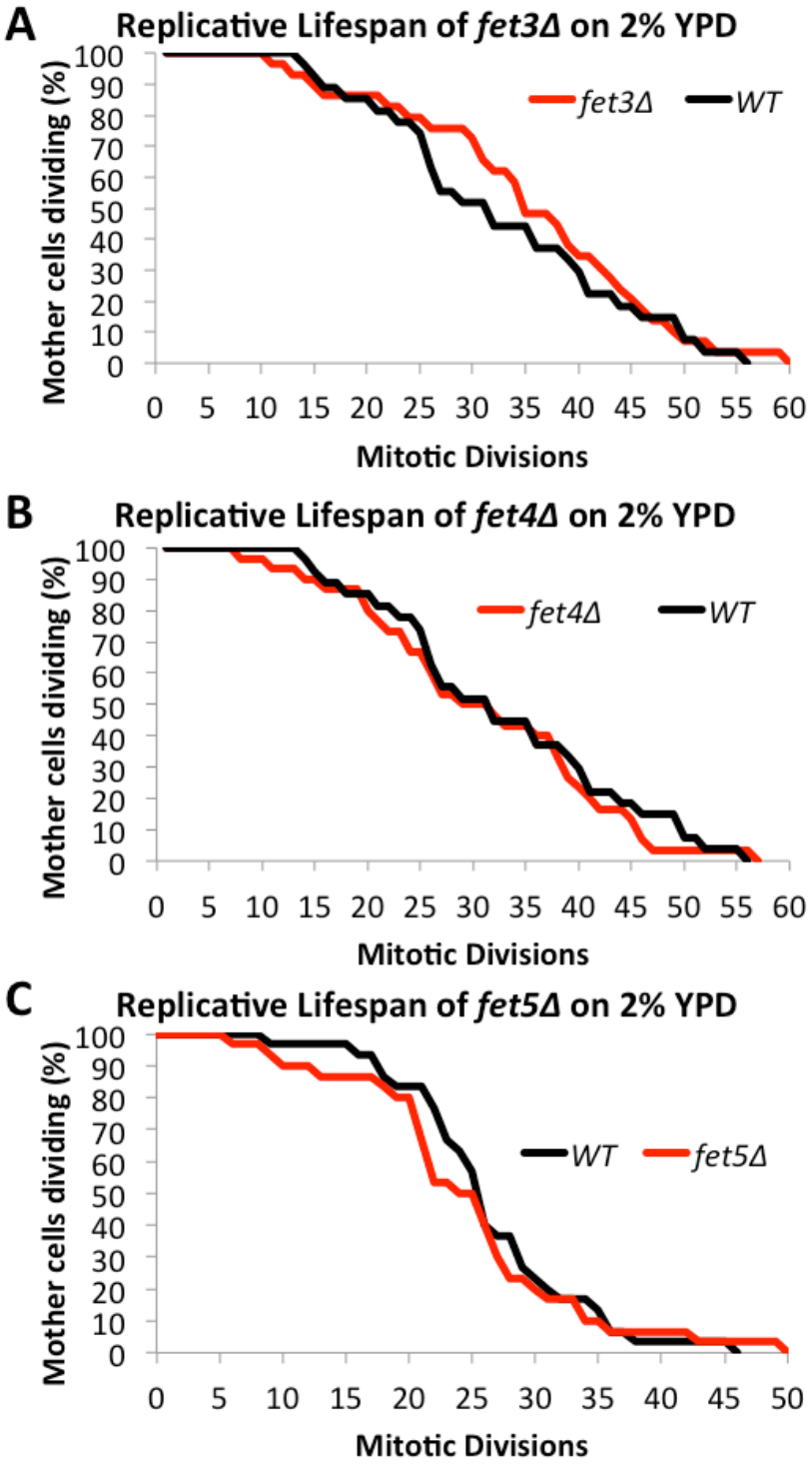

Figure 9: None of the *fetΔ* iron transporter single deletion mutants had an RLS that was different from wild type in energy replete conditions (2% glucose YPD).
The *fet3Δ* (A), *fet4Δ* (B), and *fet5Δ* (C) deletion mutants had no significant difference in number of mitotic divisions compared to the corresponding wild type ($p > 0.05$).

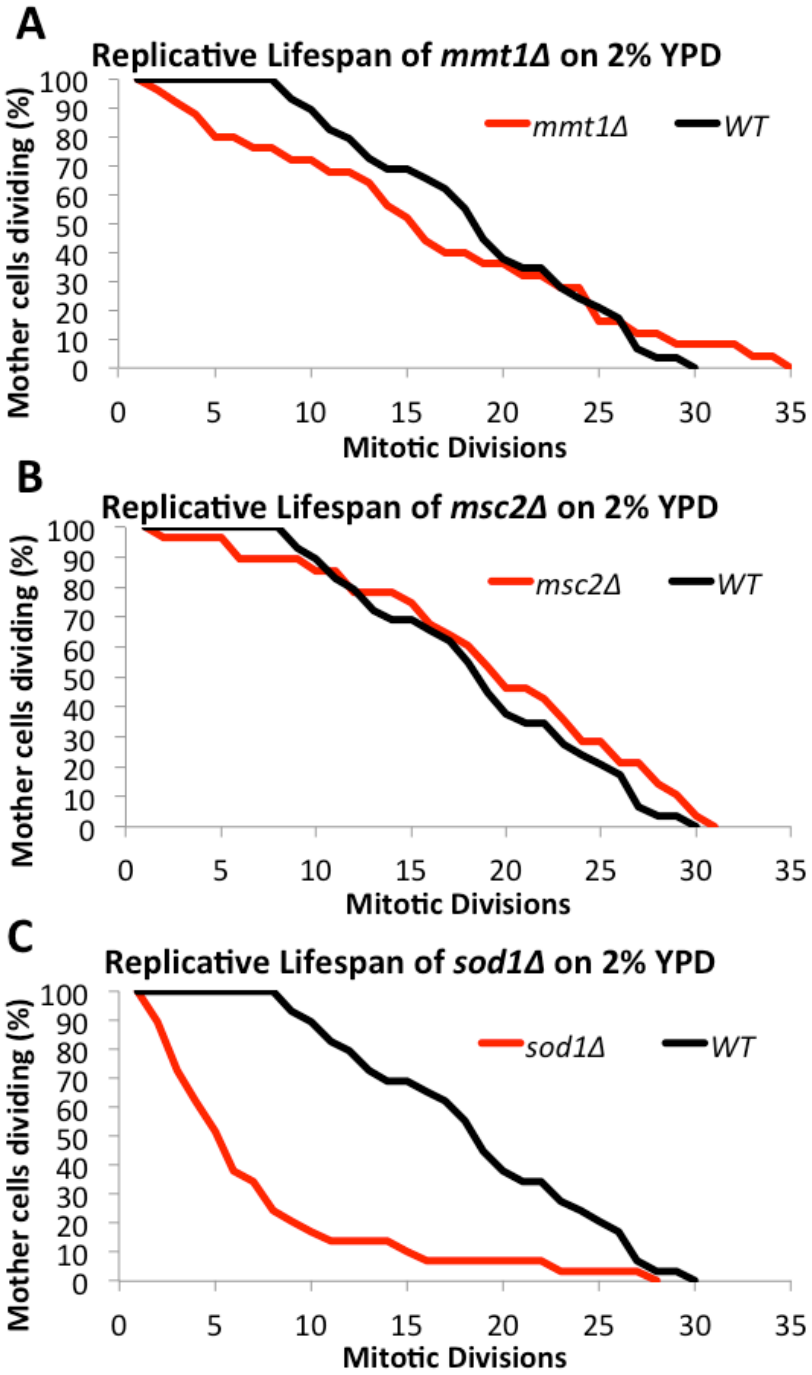

Figure 10: Only *sod1Δ*, not *mmt1Δ* or *msc2Δ*, had a shortened RLS in energy replete conditions (2% glucose YPD).
Both *mmt1Δ* (A) and *msc2Δ* had RLSs that were not significantly different than the wild type ($p > 0.05$). (C) A *sod1Δ* deletion mutant had a RLS that was significantly shorter than the wild type ($p = 3.1 \times 10^{-9}$).

Similar to the *fetΔ* strains, *mmt1Δ* and *msc2Δ* RLS were not significantly different from the wild type (*mmt1Δ*, $p = 0.29$; *msc2Δ*, $p = 0.68$) (Figure 10). The *sod1Δ* strain had an RLS that was significantly shorter than the wild type ($p = 3.1 \times 10^{-9}$; mean lifespan -72%). The mean RLS of *sod1Δ* was 5.125 divisions. The maximum RLS of *sod1Δ* was 15.1 divisions (Figure 10C). The wild type had a mean of 18.5 divisions and a max of 26.7 divisions. This RLS for *sod1Δ* agrees with the published literature (Barker et al., 1999).

3.5 The *fet3Δ fet4Δ* mutant had a significantly shorter replicative lifespan than the wild type on 2% glucose

Since the above-examined *fetΔ* metal metabolism mutants were hypothesized to have an effect on yeast lifespan and yet no lifespan effects were seen under single deletion conditions, combination deletion mutants of these various genes were constructed to test for potential redundancy of the genes. Thus, this aim was to determine whether these putative lifespan genes had genetic redundancies with lifespan implications. The *fet3Δ fet4Δ* mutant was the first examined for RLS effects because this mutant was deemed to be the strain that would best reveal redundancy. The transporter-related proteins removed in this strain reside on the plasma membrane and provide the bulk of iron in the cytoplasm (Philpott, 2012). The experimental RLS data confirmed this prediction, as the *fet3Δ fet4Δ* strain had a mean RLS of 17.75 divisions and a maximum RLS of 28.55 divisions compared to the wild type, which had a mean and maximum lifespan of 31.25 and 49.65 divisions respectively (Figure 11A). This difference in RLS was statistically significant ($p = 1.1 \times 10^{-5}$; mean lifespan -47%). The data suggest that

either FET3 or FET4 must be present for wild type RLS under normal glucose-replete growth conditions.

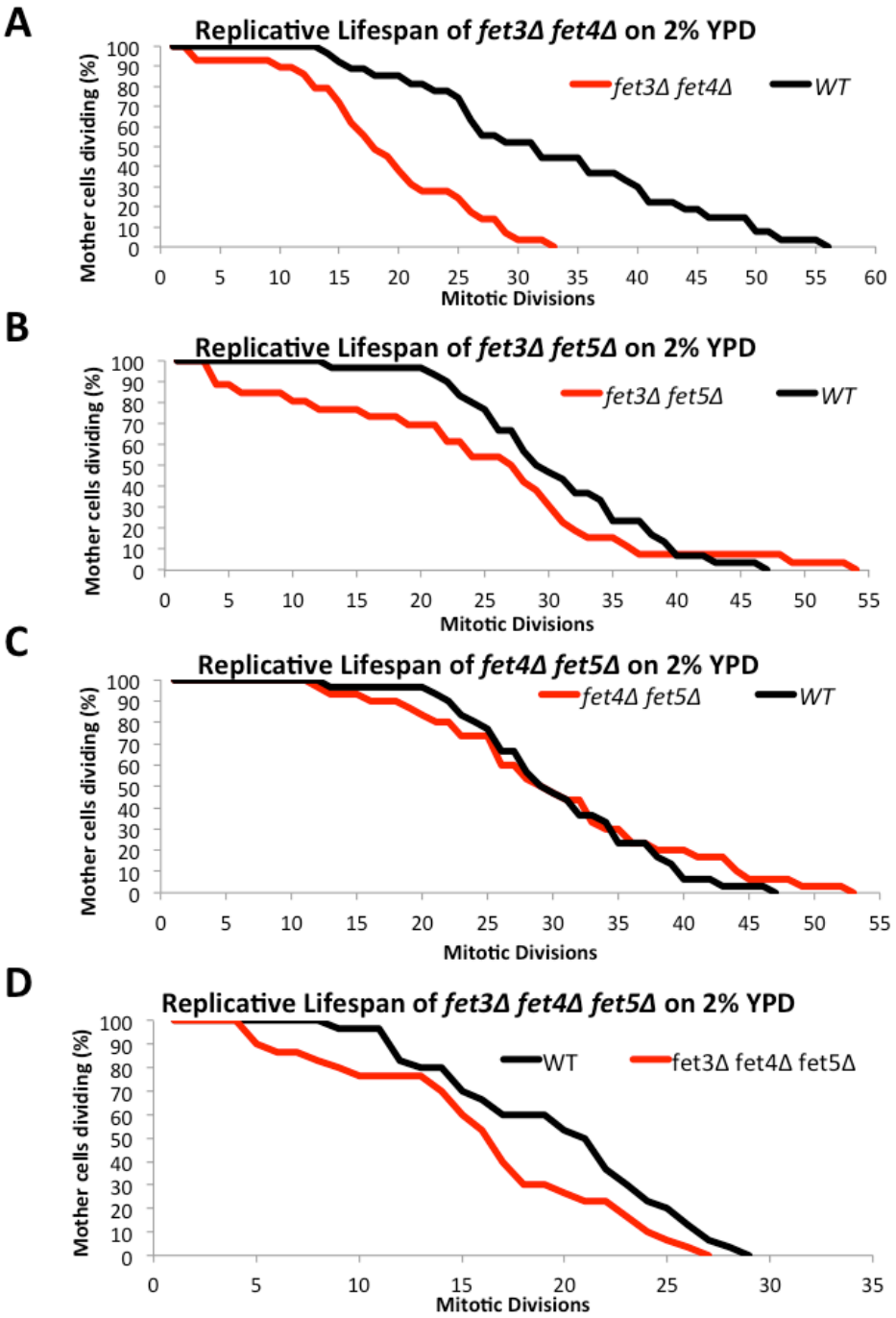

Figure 11: RLS of *fetΔ* double deletion mutants on 2% glucose YPD.
(A) The *fet3Δ fet4Δ* mutant RLS was shorter than the wild type ($p = 1.1\text{x}10^{-5}$). (B) The RLS of *fet3Δ fet5Δ* was shorter than wild type ($p = 0.044$) (C) The RLS of a haploid *fet4Δ fet5Δ* mutant was not significantly different from wild type ($p = 0.94$). (D) The RLS of a haploid *fet3Δ fet4Δ fet5Δ* is significantly shorter than the wild type ($p = 0.026$).

3.6 The *fet3Δ fet5Δ* mutant, but not the *fet4Δ fet5Δ* mutant, had a significantly shorter replicative lifespan than the wild type on 2% glucose

To determine whether loss of Fet3 or Fet4 function, in combination with loss of Fet5 function, was sufficient to maintain a wild type RLS, two double mutants, *fet3Δ fet5Δ* and *fet4Δ fet5Δ*, were constructed through genetic crosses. The *fet3Δ fet5Δ* mutant was deemed more likely to have a negative lifespan effect than the *fet4Δ fet5Δ* mutant given the higher affinity of Fet3 for iron import in comparison to Fet4 (Askwith et al., 1994; Dix et al., 1994). This was the case as the *fet3Δ fet5Δ* lifespan curve was significantly shorter than the wild type (p = 0.044, mean lifespan -7%). The *fet4Δ fet5Δ* double mutant was assayed to determine whether Fet3 alone was sufficient to maintain wild type lifespan in the absence of Fet4 and Fet5. The high-affinity of the Fet3 importer for iron may compensate for the loss of *FET4* and *FET5* and the accompanying lack of vacuolar iron export. This was confirmed by the lack of significant difference between the RLS of the *fet4Δ fet5Δ* mutant and its corresponding wild type (p = 0.94) (Figure 11C). In sum, the results of the double deletion *fetΔ* RLS experiments indicated that Fet3 is the FET protein that plays a dominant role in maintaining wild type RLS levels compared to Fet4 and Fet5. However, the single deletion mutant experiments indicated that in the absence of Fet3, the presence of both Fet4 and Fet5 was sufficient to meet the FET requirements for wild type RLS. This suggests that Fet4 in the absence of both Fet3 and Fet5 was insufficient to maintain wild type RLS levels.

3.7 The *fet3Δ fet4Δ fet5Δ* mutant replicative lifespan was significantly shorter than the wild type on 2% glucose

To confirm the significant role of Fet3 on maintenance of wild type RLS, a *fet3Δ fet4Δ fet5Δ* RLS assay was performed. The removal of *FET3* from the *fet4Δ fet5Δ* mutant should significantly shorten RLS in comparison to the wild type. Indeed, the *fet3Δ fet4Δ fet5Δ* mutant had a significantly shorter RLS compared to the wild type ($p = 0.026$; mean lifespan -23%) with a mean and maximum RLS of 16.25 and 24 divisions (Figure 11D). The corresponding wild type for this experiment had a mean and maximum RLS of 21 and 26.5 divisions. Thus, Fet3 appears to be the primary iron importer required to maintain RLS under normal 2% glucose conditions. Furthermore, the triple mutant is no worse than the *fet3Δ fet4Δ* mutant, indicating *fet3Δ fet4Δ* is epistatic to *fet5Δ* such that deletion of *FET3* and *FET4* renders *FET5* dispensable.

3.8 A *fet4Δ mmt1Δ* mutant had an replicative lifespan that was no different than wild type on 2% glucose

Crosses between the *fetΔ* mutants were the primary focus of this project, but other crosses, such as *fet4Δ mmt1Δ* were made to determine whether metal metabolism as a general pathway, rather than specific genes or one part of metal metabolism, such as iron metabolism, had an influence on RLS (Table 3.1 Materials & Methods). Double mutants with *sod1Δ* were made, but not assayed as they appeared to have drastically reduced doubling time under the dissection microscope and were cold sensitive in that they did not survive the overnight refrigeration portion of the lifespan protocol (data not shown).

Both *FET4* and *MMT1* genes have genetic redundancies. For example, as shown above *FET4* is, to a point, redundant with *FET3* and *FET5*. In addition, *MMT1* is redundant with *MMT2* (Li and Kaplan, 1997; Li et al., 2014). It is therefore possible that

removing both of these redundant genes would not drastically affect RLS. This was experimentally confirmed, as the *fet4Δ mmt1Δ* RLS was not significantly different than the wild type ($p = 0.32$) (Figure 12).

Although there is a 20% difference in mean lifespan of the *fet4Δ mmt1Δ* mutant compared to the wild type at this point on the curve, the trend of the curve for *fet4Δ mmt1Δ* did not differ from the wild type. This discrepancy between the results from comparing two individual data points on the lifespan curve and the overall lifespan trend is why statistical analysis of lifespan curves is a crucial step in data interpretation. A single point, even at the midpoint of the lifespan experiment, does not necessarily give insight into the overall lifespan trends. They are reflective of a single instance in the lifespan and not the whole duration of the lifespan. The *fet4Δ mmt1Δ* double mutant had a maximum lifespan of 45.2 divisions and the wild type had maximum lifespan 44 divisions.

3.9 The *fet5Δ* mutant, but not the *fet4Δ* mutant, had a shorter replicative lifespan than the wild type on 3% glycerol

Since the single deletion mutants had no lifespan effect on 2% glucose media and because iron has a prevalent role in mitochondrial respiration, lifespan effects for single deletion mutants on 3% glycerol were assayed. Media containing 3% glycerol is the standard for testing yeast growth in conditions that force oxidative phosphorylation, which may be indicative of mitochondrial health (Hampsey, 1997). In the literature, the RLS of *fet3Δ* is drastically shortened on 3% gylcerol (Botta et al., 2011), but this was not assessed for *fet4Δ* and *fet5Δ*. The RLS of these two single deletion mutants on 3% glycerol was examined to test whether they showed a similar trend as the *fet3Δ* mutant.

As this experiment was performed peripherally to the primary goal of this thesis, which was simply to elucidate a lifespan response from the *fetΔ* mutants under glucose conditions, *fet3Δ* on glycerol was not studied, in the interest of time and focus, not because it does not merit study at a future time.

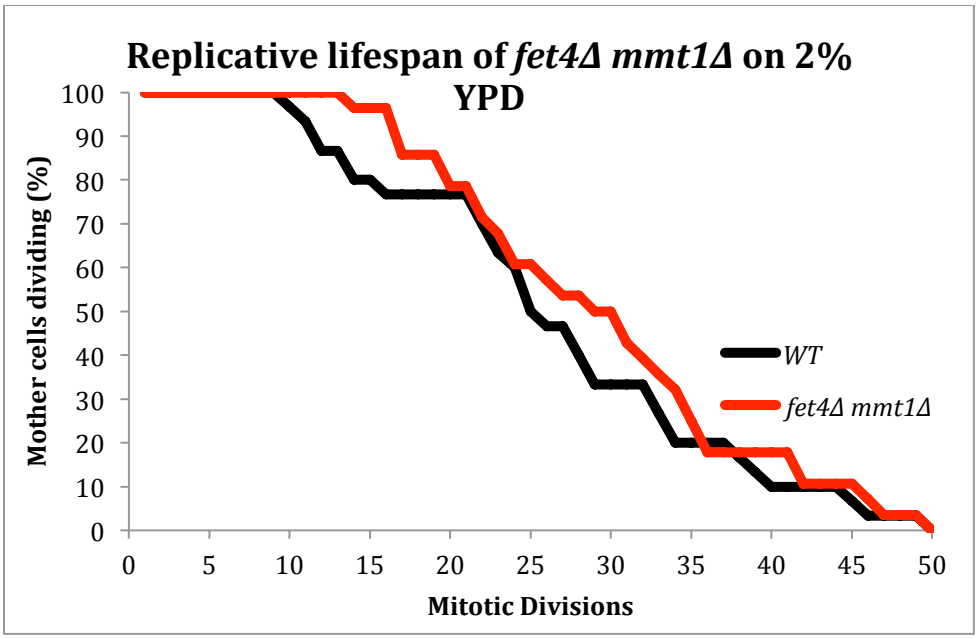

Figure 12: RLS of a *fet4Δ mmt1Δ* double mutant on 2% YPD.
The *fet4Δ mmt1Δ* strain was not significantly different than the wild type ($p = 0.32$).

Under conditions that require high amounts of intracellular iron, such as oxidative phosphorylation, Fet3 is the predominant iron importer in yeast (Askwith et al., 1994). Fet4 plays a more peripheral role in iron transport. In light of these known functions, it makes sense that a strain lacking *FET4* had a RLS that was comparable to wild type on 3% glycerol ($p = 0.78$; Figure 13A). Based on this result, low affinity iron import does not appear significant for RLS of respiring cells.

The vacuole is the major iron storage centre of the yeast cell and contains a Fet3 ferroxidase-like iron transporter-complex protein, Fet5, which contributes to the

movement of iron from the vacuole to the cytoplasm (Spizzo et al., 1997). Considering the high iron requirements of the respiring yeast cell (Philpott, 2012), removing access to this vacuolar iron store had negative implications for RLS on 3% glycerol. When the RLS of *fet5Δ* was assayed on 3% glycerol, the lifespan was significantly shorter than the corresponding wild type (p = 0.021; mean lifespan -24%). The mean RLS of respiring *fet5Δ* was 16.75 divisions, and the maximum lifespan was 23.5 divisons (Figure 13B); while the WT had a mean and maximum lifespan of 22 and 30 divisions. This experiment showed that under conditions requiring oxidative phosphorylation, the yeast cell requires Fet5 to maintain wild type lifespan.

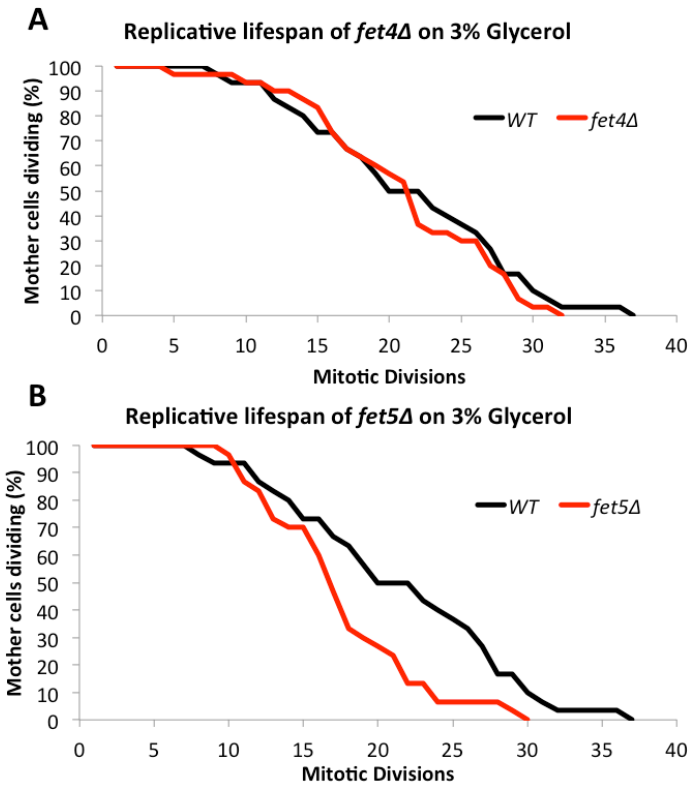

Figure 13: RLS of a *fet4Δ* single mutant and a *fet5Δ* single mutant on conditions requiring oxidative phosphorylation.
(A) The *fet4Δ* mutant, which had a lifespan that was not significantly different than wild type (p = 0.78). (B) The *fet5Δ* mutant had a significantly shorter lifespan than the wild type (p = 0.021).

4. Results II – Growth and replicative lifespans of *fetΔ* mutants under caloric restriction conditions

4.1 Wild type yeast under caloric restriction are responsive to caloric restriction lifespan extension

Considering our results showing that specific effects on RLS were identified for the *FET* genes under fermentative and respirative conditions, determining the specific effects of these genes under CR was a priority. This is because CR is currently the only universal (i.e. functional across organism-types) mechanism of lifespan extension. Since certain combinatorial deletions of *FET* genes demonstrated RLS defects on 2% glucose, we next tested if the double mutants would respond to CR (0.1% glucose). Single *FET* deletion mutants were not tested due to time contraints and the desire to limit possible genetic redundancy. Ideally, cells responding to CR would have a significantly longer lifespan than the same strain under normal glucose conditions (Lin et al., 2000).

To confirm that 0.1% glucose was an appropriate growth medium for CR lifespan assays, the lifespan of the wild type was determined on 2% and 0.1% glucose containing media. The wild type on 2% glucose had a mean and maximum RLS of 23.5 and 33 divisions, while it had a mean and maximum RLS of 32.5 and 46 divisions on 0.1% glucose (Figure 14A). The wild type lifespan on 0.1% glucose was significantly higher than the wild type lifespan on 2% glucose ($p = 0.0012$; mean lifespan +28%). This is the standard CR response for the wild type, published by other labs (Jiang et al., 2000; Kaeberlein et al., 2005a; Lin et al., 2000; Postnikoff et al., 2012). With the expected response confirmed, the CR response of *fetΔ* double mutants was tested next.

4.2 Both *fet3Δ fet5Δ* and *fet4Δ fet5Δ* mutants were unresponsive to replicative lifespan extension by caloric restriction

The *fet3Δ fet5Δ* and *fet4Δ fet5Δ* each had an RLS on 0.1% glucose that was not significantly different than the same strain on 2% glucose ($p > 0.05$). For the *fet3Δ fet5Δ* double mutant, the mean lifespans on 0.1% glucose and 2% glucose were 29 and 26 divisions, respectively (Figure 14B). The maximum lifespans for *fet3Δ fet5Δ* on 0.1% glucose and 2% glucose were 41 and 35 divisions. There was no significant difference in RLS ($p = 0.24$). For the *fet4Δ fet5Δ* double mutant, the mean lifespans on 0.1% glucose and 2% glucose were 27 and 25 divisions (Figure 14C). The maximum lifespans were 40 and 33 divisions. Again, there was no significant difference in RLS ($p = 0.082$).

4.3 The *fet3Δ fet4Δ* mutant responded to caloric restriction

To confirm that *FET5* in the absence of *FET3* and *FET4* was sufficient for the CR response, the *fet3Δ fet4Δ* mutant was assayed on 0.1% glucose. The *fet3Δ fet4Δ* mutant had a characteristic lifespan extension on 0.1% glucose compared to 2% glucose-containing media that was significant ($p = 0.018$; mean lifespan +30%). The mean and maximum lifespan for *fet3Δ fet4Δ* on 2% glucose was 22.3 and 35 divisions (Figure 14D). On 0.1% glucose *fet3Δ fet4Δ* had a mean RLS of 32 divisions and a maximum RLS of 45.5 divisions. These results suggest that *FET5* alone, in the absence of *FET3* or *FET4* is capable of responding to CR in yeast. The yeast cell is still responsive to caloric CR when both plasma membrane FET transporter-related proteins are removed.

4.4 The heterozygous diploid *fet4*$^{+/-}$ *fet5*$^{+/-}$ mutant did not respond to caloric restriction

In the process of producing a *fet4Δ fet5Δ* haploid mutant, a heterozygous diploid *fet4*$^{+/-}$ *fet5*$^{+/-}$ mutant was made. This heterozygous diploid allows for an examination of the effects of reduced *FET4* and *FET5* expression rather than a complete loss of expression. While a wild type diploid strain responded to CR (Figure 14E) in that it showed the expected increase in RLS (p = 0.0068; mean lifespan +36%), the diploid *fet4*$^{+/-}$ *fet5*$^{+/-}$ heterozygote did not show a lifespan increase on 0.1% glucose in response to CR when compared to 2% glucose (p = 0.99) (Figure 14F). These effects could be due to the heterozygosity of *FET4* or the heterozygosity of *FET5.* The mean lifespan of the wild type on 2% glucose was 31.5 divisions, and this was extended to 49 divisions on 0.1% glucose. In contrast, the *fet4*$^{+/-}$ *fet5*$^{+/-}$ heterozygote mutant had a mean RLS of 36 divisions on 2% glucose and a mean lifespan of 30.5 divisions on 0.1% glucose. Thus reducing the expression of both *FET4* and *FET5* abolished the cell's response to CR.

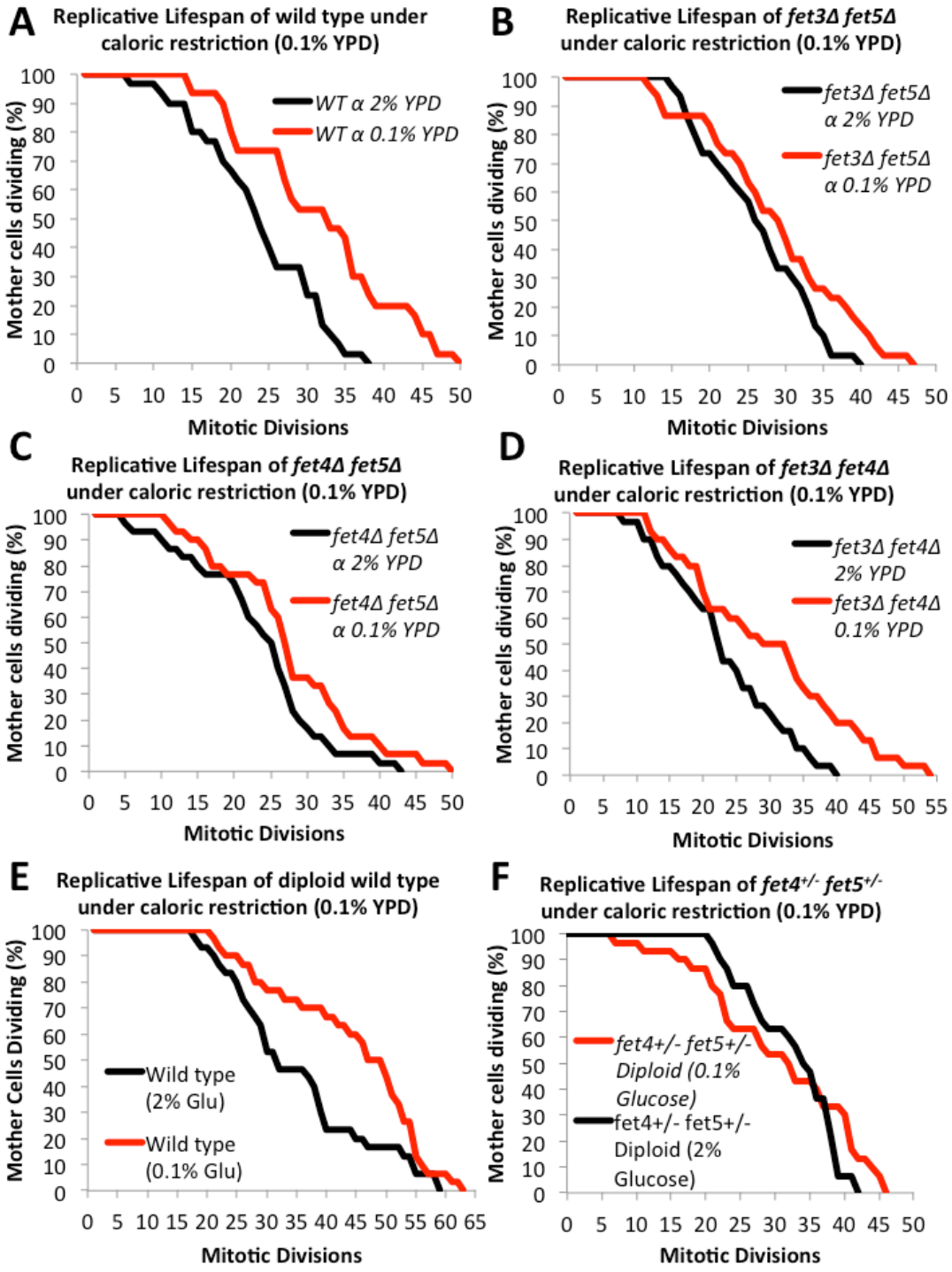

Figure 14: RLSs of *fetΔ* double deletion mutants under CR (0.1% glucose YPD). The RLS of a haploid wild type under CR is longer than the wild type under 2% glucose conditions (p = 0.0012). (B) The calorically restricted *fet3Δ fet4Δ* mutant had a longer lifespan than the wild type under normal conditions (p = 0.018). (C) The *fet3Δ fet5Δ* (C) and the *fet4Δ fet5Δ* (D) double mutants were unresponsive to CR (p > 0.05). (E) The diploid wild type was responsive to CR (p = 0.0068). (F) The heterozygous diploid *fet4*$^{+/-}$ *fet5*$^{+/-}$ had a RLS that was unresponsive to CR (p = 0.99).

5. Results III – Growth and RLSs of *ssaΔ* mutants on various carbon sources

5.1 Spot dilutions showed that heat shock protein mutants *ssa1Δ* and *fet4Δ ssa2Δ* were resistant to heat stress

Spotting assays were performed to characterize the *ssaΔ* single mutants and select double deletion mutants, notably *fet4Δ ssa1Δ* and *fet4Δ ssa2Δ* to begin testing the hypothesis that metal metabolism and HSPs interact to positively regulate yeast lifespan. Mutants were spotted along with the corresponding single mutants on YPD and YP glycerol. Plates were incubated at 30°C and 37°C to contrast normal and stress growth conditions. None of the strains showed any drastic difference from one another on 2% YPD at either 30°C or 37°C (Figure 15A,B). However, on 3% YP glycerol *ssa1Δ* appeared to grow better than the wild type on YP glycerol at heat stress temperatures (Figure 15C,D). Most surprisingly, the *fet4Δ ssa2Δ* double mutant grew consistently better than the wild type on YP glycerol at heat stress temperatures (Figure 15C,D). The *ssa1Δ* and *fet4Δ ssa2Δ* mutants grew similarly to the wild type on 3% glycerol at normal temperatures (30°C). The other strains spotted on 3% glycerol, which were *fet4Δ, ssa2Δ*, and *fet4Δ ssa1Δ*, grew similar to the wild type at 30°C, but worse than the wild type at 37°C.

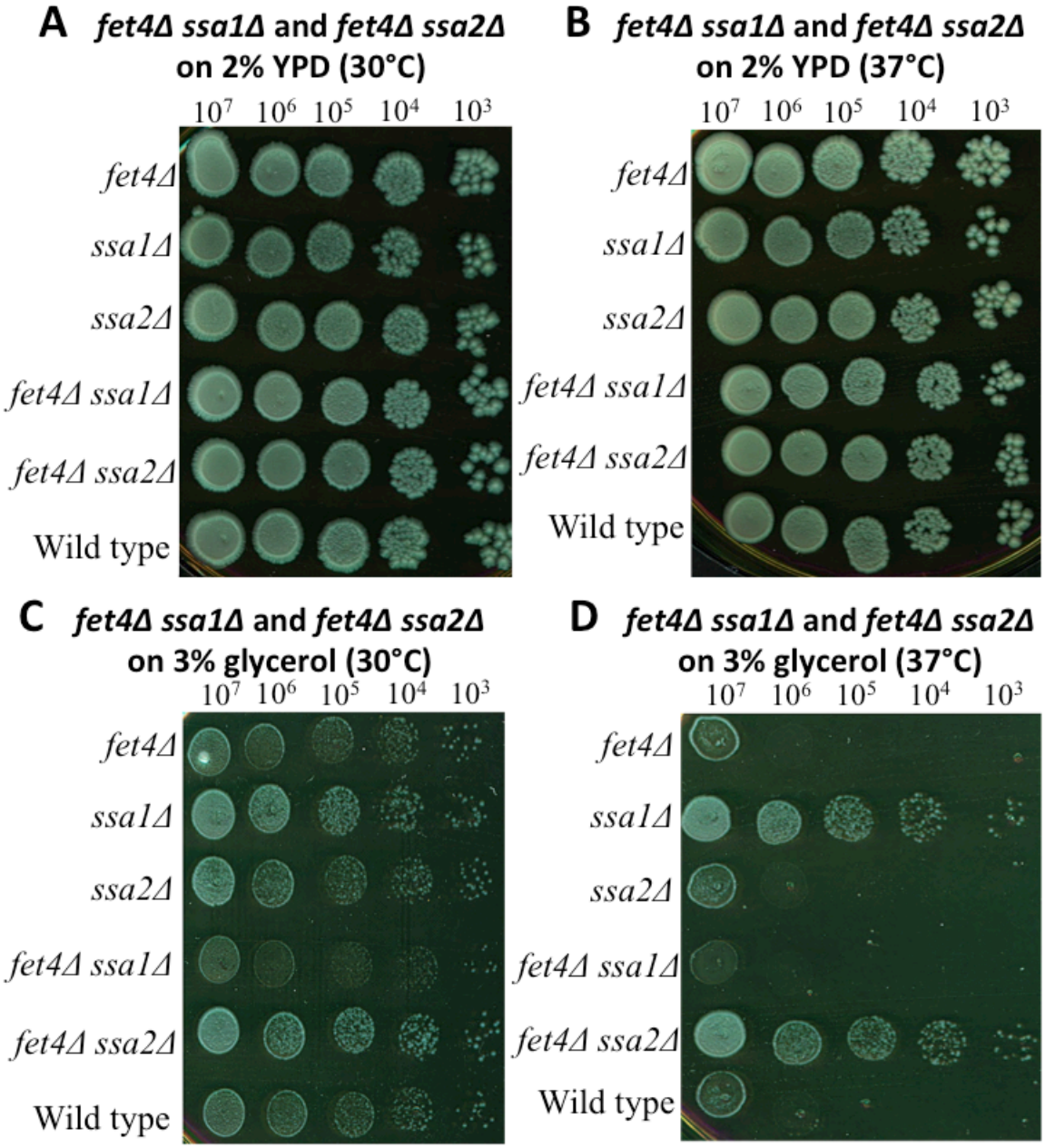

Figure 15: Spot dilutions for *fet4 ssa1* and *fet4 ssa2* double deletion mutants on 2% glucose and 3% glycerol at 30°C and 37°C.

(A) There were no noticeable differences between *fet4Δ ssa1Δ*, *fet4Δ ssa2Δ* and the wild type on 2% glucose at 30°C. (B) The lack of any noticeable differences between *fet4Δ ssa1Δ*, *fet4Δ ssa2Δ* and the wild type also occurred on 2% glucose at 37°C. (C) On 3% glycerol media at 30°C all tested strains grew similarly to the wild type. (D) On 3% glycerol at 37°C, the *fet4Δ* and *ssa2Δ* single mutants appeared to grow the same as the wild type. The *ssa1Δ* single mutant and the *fet4Δ ssa2Δ* double mutant grew better than the wild type.

5.2 The RLS of *ssaΔ* single deletion mutants on 2% glucose was similar to wild type, but *sse2Δ* RLS was significantly shorter.

The array of *ssaΔ* single deletion mutants did not have RLSs on 2% glucose that were significantly different than the wild type ($p > 0.05$) (Figure 16). The mean and maximum lifespan values for these *SSA* single deletion mutants and all other mutants discussed in this section are given in Table 6.1.

The *SSE2* gene has only 75% similarity to the *SSA* gene family, in comparison to the 96% similarity that the *SSA* gene family members have to one another (Hideyuki et al., 1993). It also had a RLS that is significantly shorter than the wild type ($p = 0.002016$; mean lifespan -26%) (Figure 16C). Note that data for this experiment was collected at the same time as the data for *ssa3Δ* and *ssa4Δ*. These mutants have the same corresponding wild type.

5.3 The *ssa1Δ ssa2Δ* and *fet4Δ ssa1Δ* mutants had a replicative lifespan that was not significantly different than the WT, while the *fet4Δ ssa2Δ* mutant replicative lifespan was shorter

The four *SSA* family members that exist in yeast are likely redundant (Hasin et al., 2014). To test this hypothesis, an RLS assay on an *ssa1Δ ssa2Δ* double mutant was performed. The *ssa1Δ ssa2Δ* mutant had a RLS that was not significantly different than the wild type ($p = 0.3488$) (Figure 17A).

To test the hypothesis that Ssa1 and Ssa2 would respond differently in the absence of *FET4*, due to the variation in expression and function of these two proteins noted in the literature (Hasin et al., 2014), the double mutants, *fet4Δ ssa1Δ* and *fet4Δ ssa2Δ,* were tested for RLS. The *fet4Δ ssa2Δ* double mutant has an RLS that was significantly shorter than the wild type ($p = 0.02309$; mean lifespan -20%) (Figure 17B).

In contrast the *fet4Δ ssa1Δ* double mutant had an RLS that was statistically similar to WT ($p = 0.09201$) (Figure 17C), but nearly all points along the curve were shifted to the right compared to the wild type.

To determine whether the shortened lifespan of *fet4Δ ssa2Δ* was independent of mitochondrial respiration, the RLS of this mutant on glycerol was tested. In this experiment, the *fet4Δ ssa2Δ* double mutant again had a RLS that was significantly shorter than the wild type ($p = 0.03683$; mean lifespan -30%) (Figure 17D).

Table 5.1: Mean and maximum RLSs for *ssaΔ* mutant strains
The corresponding mean and maximum RLS for the wild type is given in brackets next to the mutant strain value. The *p*-value significance between the mutant curve and wild type curve is also shown. A *p*-value greater than 0.05 indicates no significant difference between wild type and mutant strains. A *p*-value less than 0.05 indicates a difference between the wild type and mutant. Data for all strains collected on 2% YPD at 30°C unless otherwise specified. A * indicates data for these strains was collected in the same experiment with the same wild type. The same number of * symbols indicates the same experiment.

Strain	**Mean RLS (Mitotic Divisions)**	**Max RLS (Mitotic Divisions)**	***P*- value compared to Wild type (Entire RLS curve comparison)**
wt*	21.2	31.7	N/A
wt**	25	39	N/A
wt***	18	36.8	N/A
*ssa1Δ**	19.25	25	0.1236
*ssa2Δ***	25.7	45	1
*ssa3Δ****	18.75	29.35	0.6187
*ssa4Δ****	24.25	33.9	0.1819
*sse2Δ****	13.25	18.05	0.002016
*ssa1Δ ssa2Δ****	18.5	22.8	0.3488
*fet4Δ ssa2Δ***	20	36	0.02309
*fet4Δ ssa1Δ**	25.5	38	0.09201
wt (on 3% glycerol at 30°C)	21	24.8	N/A
fet4Δ ssa2Δ (on 3% glycerol at 30°C)	14.7	18.5	0.03683

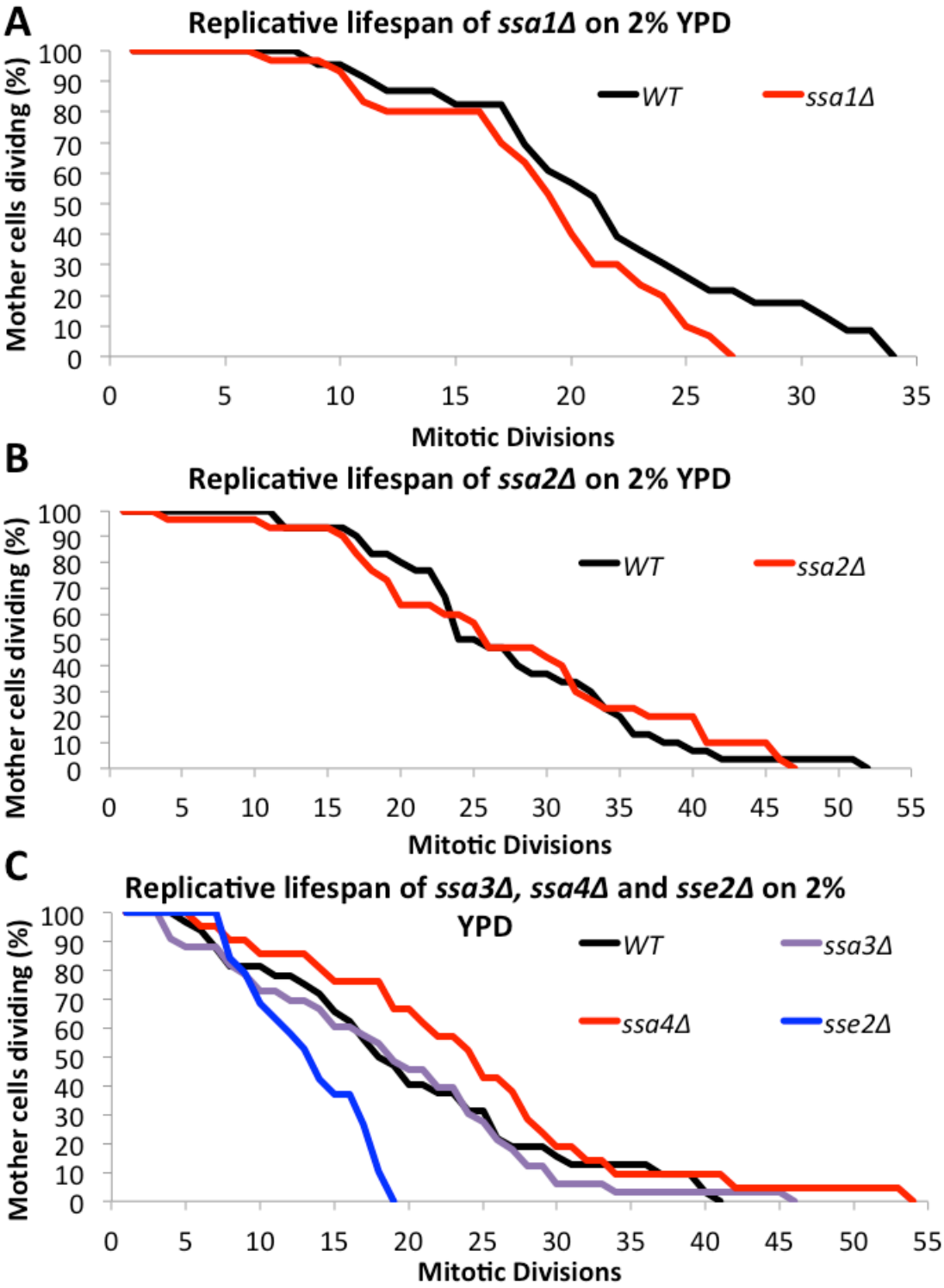

Figure 16: RLS for *ssaΔ* single deletion mutants on 2% YPD.
(A) The *ssa1Δ,* (B) *ssa2Δ* (C) *ssa3Δ* and *ssa4Δ* mutants had RLSs that were not significantly different than the wild type ($p > 0.05$). The RLS of an *sse2Δ* mutant was significantly shorter than the wild type ($p = 0.002016$).

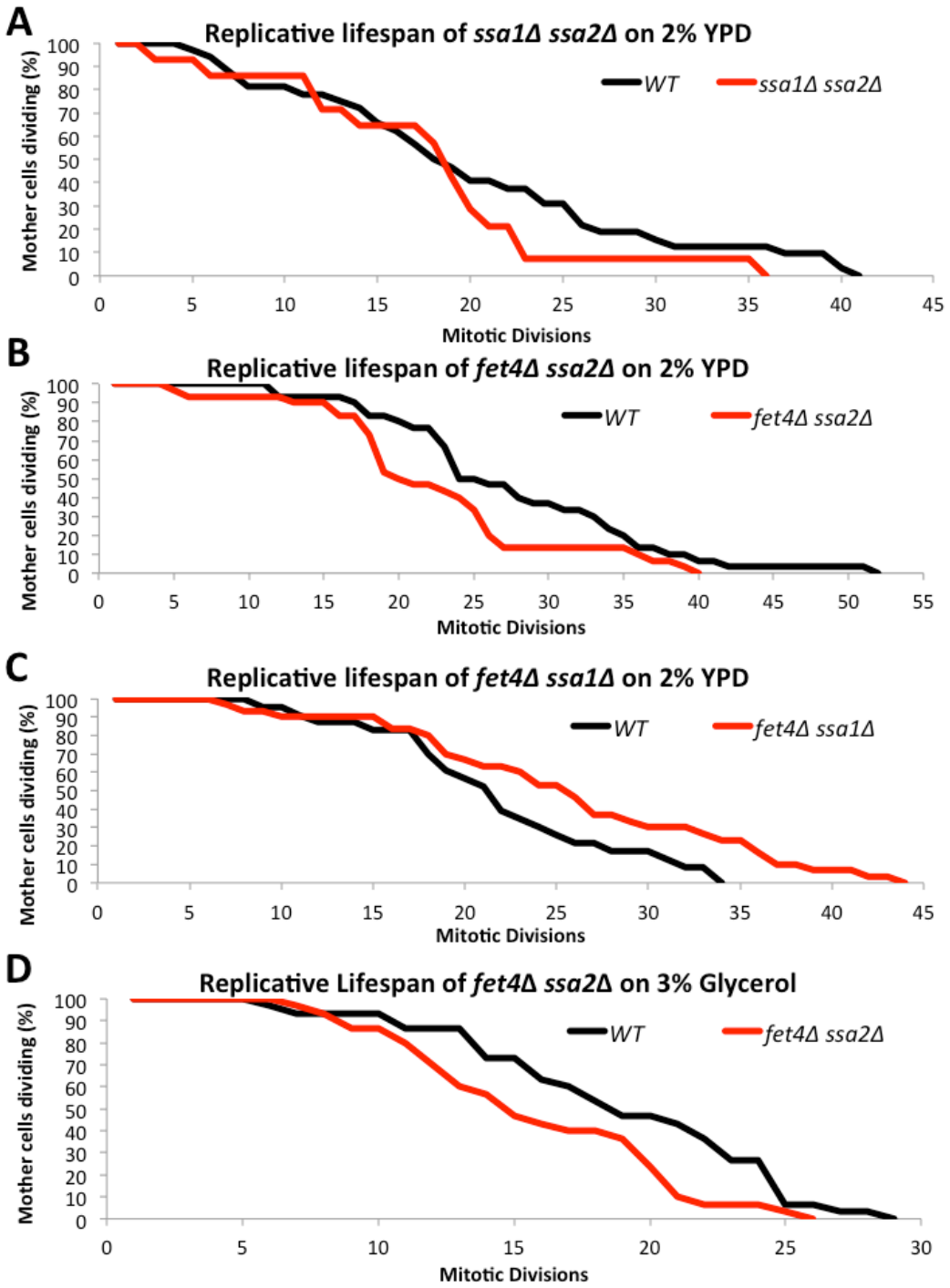

Figure 17: RLSs for select *ssaΔ* double deletion mutants.
The (A) *ssa1Δ ssa2Δ* double deletion mutant had an RLS that was not different than the wild type (p = 0.3488). (B) The *fet4Δ ssa2Δ* double deletion mutant had a RLS that was shorter than the wild type (p = 0.02309) on 2% glucose. (C) The *fet4Δ ssa1Δ* double deletion mutant had a RLS that did not differ from the wild type (p = 0.09201) on 2% glucose. However, a trend towards an extended lifespan in this mutant may be noted. (D) On glycerol the *fet4Δ ssa2Δ* double deletion mutant had shorter lifespan than the wild type (p = 0.03683).

6. Discussion and Future Work

6.1 *FET3* contributes the most to wild type length replicative lifespan in comparison to *FET4* and *FET5*

The purpose of this project was to determine whether a set of metal-related genes or HSP-encoding genes identified in a recent screen for aging-related genes (Ghavidel et al., 2015) had an effect on the RLS of yeast cells. The screen was performed using a growth "barcode" assay. A selectable marker was misregulated when an aging controlled locus was de-repressed as cells reached the end of their replicative capability. The screen did not produce concrete RLS values, rather it assayed, as stated, the de-repression of an aging controlled locus, specifically the mating type locus. Growth of the cells in a liquid media during the screen varied from the solid-media conditions found in a formal RLS assay. The high-density of yeast cells that occurs during growth in liquid media and the depletion of glucose in liquid media with culture time (DeRisi et al., 1997) would be confounding factors for cellular aging, as would be the lack of quantifiable replicative age for individual cells. In this thesis project, a selection of novel, and possibly interacting, screen-identified genes was examined under varying genetic and carbon-source conditions. These genetic conditions included single deletions of the identified genes and various combinations of double gene deletions. The carbon conditions included glucose (a fermentative carbon-source), at both normal and calorically restricted concentrations, and glycerol (a non-fermentative carbon source). Many of the aging effects identified in this study were genotype or context specific. This was not apparent from the screen alone since the screen was performed on single deletion mutants over a long period of time in liquid media without following individual cells.

To test the central hypothesis of this thesis that cellular replicative aging is caused by misregulated iron transport, which leads to a reliance on HSPs for lifespan maintenance, we tested the RLS of various metal metabolism and HSP mutants both individually and in combination on various carbon-sources, which included fermentation-encouraging 2% glucose, calorically restricted 0.1% glucose and mitochondrial respiration-inducing 3% glycerol. The major finding of this thesis project regarding the relationship between yeast metal metabolism and RLS is that there is interplay between the *FET* genes required for 1) maintenance of RLS on normal 2% glucose conditions and 2) the lifespan extension response due to CR. Under normal conditions, which encouraged robust growth of yeast cells, *FET3* was identified to contribute the most to lifespan maintenance. This was examined by measuring RLS of the *fetΔ* single mutants and a combination of double and triple *fetΔ* deletion mutants using a yeast dissection microscope. All of the *fetΔ* single deletion mutants had RLSs that were no different than those of the wild type controls. When pairs of the *FET* genes were deleted, only the *fet4Δ fet5Δ* double mutant, which still contained *FET3,* maintained wild type RLS. This suggested that *FET3* had a more prominent role in lifespan maintenance under normal conditions than the other two *FET* genes. In other words, a shortening of RLS on 2% glucose for the tested *FET* mutants occurred when either *FET3* and *FET5* or *FET3* and *FET4* were deleted. However, maintenance of wild type lifespan was still possible in the absence of *FET3* but the presence of both *FET4* and *FET5*, since the *fet3Δ* single deletion mutant maintained a wild type lifespan. In a triple mutant consisting of *fet3Δ fet4Δ fet5Δ* deletions, the mutant RLS was significantly shorter than the wild type, which would be expected if the presence of *FET3* in a *fet4Δ fet5Δ* double mutant were the only gene

maintaining wild type lifespan length. That the relative decrease in RLS between the *fet3Δ fet4Δ fet5Δ* triple mutant and the wild type was no worse than the decrease in the RLS of the *fet3Δ fet4Δ* mutant when compared to wild type may imply that Fet5, and the vacuolar iron stores, are not used extensively under normal (2% glucose) conditions, even when *FET3* and *FET4* are deleted.

Comparing the double and triple mutant *fetΔ* strains to one another instead of the wild type could further tease out the hierarchy of *FET* function. Most notably future experiments could include: 1) a direct comparison (i.e. in the same assay) of the *fet3Δ fet4Δ fet5Δ* triple mutant to the *fet4Δ fet5Δ* mutant, which would further confirm whether *FET3* function does ensure a longer lifespan in the *fet4Δ fet5Δ* mutant on 2% glucose. 2) A direct comparison (i.e. on the same assay) of the *fet3Δ fet5Δ* mutant to the *fet3Δ fet4Δ fet5Δ* triple mutant would determine whether *FET4* has any significant role in lifespan, as the current results presented in this thesis indicated that *FET4* was not significant. Although the *fet3Δ fet5Δ* mutant had a shorter lifespan than the wild type, as did the *fet3Δ fet4Δ fet5Δ* triple mutant, if the *fet3Δ fet5Δ* mutant had a lifespan longer than the *fet3Δ fet4Δ fet5Δ* triple mutant, then it would be possible to conclude that *FET4* does have a marginal influence on RLS of the yeast cell. Another experiment could be 3) a direct comparison of the *fet3Δ fet4Δ fet5Δ* mutant to a *fet3Δ fet4Δ* mutant. This would establish whether there is an epistatic or masking effect of the additional *FET5* deletion in a *fet3Δ fet4Δ* background.

6.2 *FET5* renders cells responsive to caloric restriction

An array of double deletion mutants: *fet3Δ fet4Δ, fet4Δ fet5Δ* and *fet3Δ fet5Δ* were tested under CR since the double deletion mutants were the only strains to show a RLS

effect on 2% glucose. Admittedly, that the RLS of single deletion mutants were not assayed under CR conditions is a flaw of this study. Each double mutant contained one screen-identified *FET* gene. Note that the genes *FET1* and *FET2* are not related to iron transport or iron metabolism (Raymond et al., 1992). If a double mutant was not responsive to CR, then it could be concluded that the third *FET* remaining in the mutant was insufficient for the CR response. However, if the strain remained responsive to CR, then it could be concluded that the remaining *FET* gene had a role in the CR lifespan extension response.

Under conditions of CR (0.1% glucose in this study), only the *fet3Δ fet4Δ* double mutant, which contained *FET5*, was responsive to CR. It showed the characteristic lifespan extension shift. When *FET3* and *FET5* were deleted (leaving functional *FET4*) or *FET4* and *FET5* were deleted (leaving functional *FET3*) the yeast cell became unresponsive to CR conditions. We interpret this to mean that *FET5*, in the absence of *FET3* and *FET4*, is sufficient for the CR response in yeast. That *FET5* encodes a vacuolar iron transporter component (Urbanowski and Piper, 1999) suggests that vacuolar iron stores have a significant role in CR lifespan extension of yeast cells. The cell relies on stored iron in the vacuole under CR conditions (De Freitas et al., 2003). Testing the response of a *fet5Δ* single deletion strain to CR is an important topic for future research related to this project. The relevance of the *FET* genes to CR was examined because CR is the only anti-aging intervention that functions universally across all organisms (Fontana et al., 2010). The impinging of *FET* genes on this intervention points towards these genes functioning in a major anti-aging pathway that is a promising target of future therapies. We interpret our findings to indicate that Fet3 and Fet4 are required for iron

influx into the cell from external sources under normal conditions, whereas under stress conditions, such as CR or even galactose, Fet5 becomes the primary player, indicating that mobilization of iron form the vacuole is important under these conditions.

In addition, spot dilution growth assay data revealed that the *fet3Δ*, *fet4Δ*, *fet5Δ* and *sod1Δ* single mutants, along with the *fet3Δ fet4Δ* double mutant could not meet the increased iron requirements of the cell under mitochondrial respiration conditions (Philpott, 2012). The *fet3Δ fet4Δ* double mutant consistently grew worse than the wild type on 3% glycerol. The *fet3Δ*, *fet4Δ*, and *fet5Δ* single mutants grew marginally worse than the wild type on 3% glycerol at 30°C, but drastically worse than the wild type at 37°C. The 3% glycerol growth media forces the cell to switch to mitochondrial respiration as its main energy source (Hampsey, 1997). During this switch, genes encoding iron transporters, especially the Fet3 iron transport complex, are upregulated (Philpott, 2012). The increased iron needed by the cell during respiration is primarily used for iron-containing structures in mitochondrial enzymes, such as iron sulfur clusters and heme (Philpott, 2012). Some iron-containing mitochondrial enzymes contribute to respiration itself (Philpott, 2012). Other iron-containing mitochondrial enzymes cope with the toxic ROS produced by respiration (Kathiresan et al., 2014). This reliance on iron for respiration and handling ROS toxicity can explain the reduced growth of *fet3Δ*, *fet4Δ*, and *fet5Δ* mutants on glycerol at both 30°C and 37°C. The *fet3Δ fet4Δ* mutant had impaired mitochondrial respiration at 37°C, but unimpaired respiration at 30°C, which suggests that *fet3Δ fet4Δ* had enough mitochondrial respiration-function to be responsive to CR, which can upregulate respiration in CR responsive cells (Lin et al., 2002), although this upregulation of respiration for the CR response is not always required

(Kaeberlein et al., 2005a). Future work could examine whether the *fet4Δ fet5Δ* and *fet3Δ fet5Δ* mutants are mitochondrial respiration-deficient and correlate this with the lack of CR response in these two strains.

That *FET* iron transport-related genes have effects on RLS pathways of yeast cells suggests that it may be the whole iron metabolic pathway that affects yeast lifespan. Future work could modify the iron content in the yeast media and determine whether differing levels of iron are sufficient to change the lifespan of yeast cells under normal conditions of 2% glucose, or alter the yeast response to CR conditions of 0.1% glucose. New beamline facilities at the University of Saskatchewan Canadian Light Source would be able to quantify iron content and species within yeast cells (Roudeau et al., 2014). This level of detail regarding cellular iron content could indicate whether intracellular iron levels play a role in lifespan maintenance or extension and whether the species of intracellular iron is significant. Knowledge of both content levels and species type could have implications for human iron control and cellular lifespan regulation, either through diet, pharmacological supplementation or chelation (Arruda et al., 2013).

Future work with genes alterations that mimic CR, such as *tor1Δ* or *gpr1Δ* could indicate whether CR insensitivity of the *fet4Δ fet5Δ* mutant, or a *fet5Δ* mutant if it proves to be insensitive to CR, intersects with traditional CR-responsive pathways. For example, work withon a *tor1Δ fet4Δ fet5Δ* triple mutant, or a *tor1Δ fet5Δ* double mutant, could be used to examine the CR pathway interaction. These mutants are significant because the *tor1Δ* mutant, in which the TOR complex is non-functional, has an extended RLS (Kaeberlein et al., 2005c). The *tor1Δ* mutant is also insensitive to further lifespan extension by CR. In other words, *tor1Δ* impinges on a lifespan extension pathway that is

a CR mimic. If the *tor1Δ fet4Δ fet5Δ* triple mutant does not have the same extended lifespan of the *tor1Δ* mutant under normal conditions, then the lack of response to CR-resembling lifespan extending interventions charactersistic of the *fet4Δ fet5Δ* mutant would allow us to conclude that *FET4* and *FET5* function in same pathway as *tor1Δ*. This could be concluded because the lifespan extension that occurs in the *tor1Δ* mutant would be masked by the *fet4Δ fet5Δ* mutant, meaning that *TOR1* is likely a downstream target of aging pathways activated by proper functiong of Fet4 and Fet5. This would provide further evidence that iron metabolism could regulate lifespan extension responses in yeast. However, multiple gene deletions lead to yeast mutants that are CR mimics (Kaeberlein et al., 2005b; Lin et al., 2000). To determine where in the nutrient sensing pathway the *fet4Δ fet5Δ* mutant could affect the CR response, additional deletions of *HXK2, GPR1* or *GPA2* in the *fet4Δ fet5Δ* background could be used. If a triple mutant consisting of *fet4Δ fet5Δ* with a deletion of any of the aforementioned CR genes does not show a lifespan extension compared to the wild type on 2% glucose, then it could be concluded that *FET4* and/or *FET5* functions upstream of these nutrient sensing genes to enact CR sensitivity. In addition it would be useful to determine whether any CR effects seen in the BY4741 *fetΔ* mutants are conserved in other wild type backgrounds as lifespan effects of gene deletions can be strain specific (Kaeberlein et al., 2005b). Future RLS work with these *FET* mutants under stress conditions, such as heat shock, may reveal a role of these genes above the heat stress growth-sensitivity on 3% glycerol that the *FET* mutants showed in this thesis.

6.3 Cells become sensitive to genetic perturbation and stress in the absence of *SOD1*

In addition, this work showed that the multiple divalent metal substrates for the FET4 transporter might have implications for metal metabolism beyond iron metabolism. For example, this work has shown that deletion of *FET4* in addition to *SOD1* exacerbates growth defects of *sod1Δ* on glycerol, perhaps due to insufficient iron-sulfur cluster replacement (De Freitas et al., 2000) in a high ROS environment. Under conditions of heat stress (YPD at 37°C) the *fet4Δ sod1Δ* (Figure 4B) mutant had hampered growth compared to the wild type. This could be because cells lacking *SOD1* have higher iron requirements (De Freitas et al., 2000) than wild type cells. It is likely that reducing iron transport by deleting *FET4* caused the cell to fail to meet its higher iron requirements under stress conditions. This failure results in higher levels of ROS, which then inactivate iron-sulfur clusters which are found in proteins responsible for mitochondrial respiration or damage proteins and lipids in the mitochondrial inner membrane (De Freitas et al., 2000; Kowaltowski and Vercesi, 1999). In short, the *fet4Δ sod1Δ* mutant may be unable to handle the increased ROS production that occurs under respiration without functioning Sod1 or overcome the higher iron requirements to compensate for excess ROS interactions with iron sulfur clusters.

6.4 *FET4* and *MMT1* do not interact

Mmt1 is likely dispensable for RLS maintenance under normal conditions since Mmt1 is redundant with Mmt2, a protein with similar functions (Li et al., 2014). The *fet4Δ mmt1Δ* RLS experiment showed that the redundancies of the *FET4* and *MMT1* genes could be sufficiently compensated since no shortening of lifespan occurred when both genes were deleted. It is also possible that the lack of change in RLS indicates that

these genes are involved in separate pathways or biological processes. Since it is possible for these proteins to have other unique targets, rather than being simply redundant, a further study of other metal metabolism mutant combinations between genes more distantly related could be an avenue of a future project. In addition future work utilizing *mmt2*Δ, and *mmt1*Δ *mmt2*Δ mutants would show whether the *MMT* gene family has any role to play in RLS.

6.5 *FET4* and *MSC2* interact under conditions requiring mitochondrial respiration

Deletion of *FET4* and *MSC2* in a glycerol-based environment, regardless of heat-stress, creates a growth defect that may be due to a dysfunctional ER unfolded protein response (ER UPR) in combination with a divalent metal ion deficiency (Ellis et al., 2004). The non-functioning ER UPR is due to the absence of Msc2, which is activated by higher levels of ROS, such as those that may accompany mitochondrial respiration or heat stress (Gardner et al., 2013). When combined with reduced iron transport due to the absence of Fet4, the lack of ER UPR and the resulting high levels of ROS may lead to the impairment of normal functioning of Sod1, as discussed above, rendering the cell further incapable of coping with the increased oxidative stress caused by mitochondrial respiration. A *fet4Δ msc2Δ sod1Δ* triple mutant would likely give new insight into whether *SOD1* is indeed negatively affected by a deletion of *FET4* and *MSC2*.

Under normal temperature conditions on 2% YPD, growth of the *fet4Δ msc2Δ* mutant resembled the wild type because the cells were neither stressed or in conditions requiring mitochondrial respiration. Most proteins would be in their native conformations, meaning the ER UPR (Gardner et al., 2013) which requires Msc2 (Ellis et al., 2004) would not be activated. Growth of *fet4Δ msc2Δ* was no different than that of

the wild type on 2% glucose at 37°C despite an elevated growth temperature, perhaps because UPR activity of the ER was not needed on this growth media.

Currently it appears *MSC2* is not required for RLS under normal conditions since genetic redundancies with vacuolar zinc importers *ZRC1* and *COT1* may mask the effects of *MSC2* deletions (Ellis et al., 2004). Examining how *ZRC1* and *COT1* interactions with *MSC2* affect RLS or examining whether lifespan effects of these mutants may be exacerbated under stress conditions could be other avenues for future work.

6.6 *SSE2* may promote lifespan maintenance in aged cells

The shortened RLS on 2% glucose observed for the *sse2Δ* single deletion mutant could indicate that *SSE2* is functionally distinct from the *SSA* family. Future work overexpressing *SSE2* may give further insight as to whether this gene has a lifespan-promoting role. Sse2 is consistently found to be upregulated in older cells, perhaps playing a role in handling increasing levels of damaged proteins in aging cells when the primary HSPs (e.g. SSA family) become overwhelmed (Laun et al., 2005; Soti and Csermely, 2007; Wanichthanarak et al., 2015).

6.7 The inducible Ssa3 and Ssa4 heat shock proteins may compensate for an absence of constitutive Ssa1 and Ssa2 proteins

SSA HSP genes have been identified to have a role in lifespan (Hasin et al., 2014; Morimoto, 2011). The SSA HSPs are related to the mammalian HSP70 family (Daugaard et al., 2007). These HSPs are responsible for the proper folding of nascent proteins and, under stress conditions, re-folding or sorting of damaged and misfolded proteins (Malyshev, 2013). As proteins are more prone to misfolding as cells age, it is easy to

imagine how HSPs are significant for lifespan maintenance. This project found that when *SSA* family member genes are individually deleted, the effects on yeast RLS are minimal, likely due to the high degree of similarity between the various HSP family members. It is possible that the *ssa4Δ* mutant RLS was trending towards an extension in comparison to the wild type, but this requires further investigation.

When two *SSA* genes, *SSA1* and *SSA2* were deleted in combination, there was no change in RLS on 2% glucose compared to the wild type. This could indicate that there may be greater functional overlap between the *SSA* genes, in this case *SSA3* and *SSA4,* which were still present, in regards to lifespan. In other words, the presence of *SSA3* and/or *SSA4* may be sufficient to compensate for the loss of *SSA1* and *SSA2*. Alternatively, *SSA1* and *SSA2* may not be involved in RLS. Future experiments will require the construction of additional mutant combinations to test this further. However, as will be discussed below, functional uniqueness was observed when *SSA1* and *SSA2* were separately deleted in combination with *FET4*. This agrees with the literature which states that despite much overlap, there are unique functions of *SSA* family members as examined in-depth by a high throughput study in which the genomic profile of yeast expressing only one variant of *SSA1-4* at a time was determined (Hasin et al., 2014).

6.8 The Fet4 low-affinity iron transporter interacts with Ssa1 and Ssa2 in opposing ways

The *fet4Δ ssa1Δ* mutant RLS could eventually resolve to a longer lifespan than the wild type, but the statistics indicate that there was no significant difference between this strain and the wild type. Further experimentation on this strain, perhaps by increasing the number of cells tested for each strain from 30 to 60 cells, could determine whether

there is a significant difference between the wild type and *fet4Δ ssa1Δ*. If further experimentation does resolve a significantly extended lifespan for the *fet4Δ ssa1Δ* mutant, then perhaps the altered iron transport of this mutant in conjunction with the subset of genes upregulated by the absence of *SSA1* (Hasin et al., 2014) contributes to a lifespan extending effect. Future work can determine whether *fet4Δ ssa1Δ* has altered iron levels or expression when compared to the wild type.

The *fet4Δ ssa2Δ* double deletion mutant had a significantly shorter lifespan than the wild type on 2% glucose, which is essentially the opposite of the trend observed for the *fet4Δ ssa1Δ* double deletion mutant. These two different double mutant lifespans suggest that Ssa1 and Ssa2 have different functions in regards to Fet4. Not only do these two lifespan experiments give insight into the interactions between *FET4* and *SSA* genes, they also show that individual *SSA* genes are functionally distinct from one another. This corresponds to studies on protein interactions and gene expression of the different HSP found in yeast (Brownridge et al., 2013; Hasin et al., 2014).

For example, when three SSA family members are deleted in combination, leaving only one functional SSA protein, gene expression shows changes in cellular ability to handle heat stress or deal with protein aggregation (Hasin et al., 2014). High throughput studies show that the SSA HSPs are shown to have many overlapping protein targets, but at the same time many distinct protein targets that are unique to each SSA protein (Brownridge et al., 2013; Hasin et al., 2014). The SSA proteins may assist in the proper folding of these protein targets. Perhaps in the absence of *FET4*, the activity of Ssa2 is enhanced to maintain longevity, which is why a *fet4Δ ssa2Δ* double mutant has a shortened lifespan. It is also possible that Ssa1 may limit cellular lifespan in the absence

of *FET4,* which is why there could be lifespan extension in the *fet4Δ ssa1Δ* double mutant.

The lifespan limitation caused by Ssa1 in the absence of *FET4* may occur through the following mechanism (Figure 18): 1) The absence of *FET4* leads to an increase in iron-uptake by Fet3 (Dix et al., 1994). 2) An increase in cellular iron leads to increased production of ROS and protein aggregates (Nyström, 2005). 3) Increased protein aggregation over-activates SSA1 (Sanchez de Groot et al., 2015). 4) Ssa1 potentiates aggregate formation and limits cellular lifespan (Chernova et al., 2014). In contrast, Ssa2 eliminates certain protein aggregates more effectively than Ssa1 (Chernova et al., 2014), which could explain why the *fet4Δ ssa2Δ* mutant has a drastically shortened lifespan. These results show the power of the RLS assay in finding potential tangible and physiologically relevant genetic interactions.

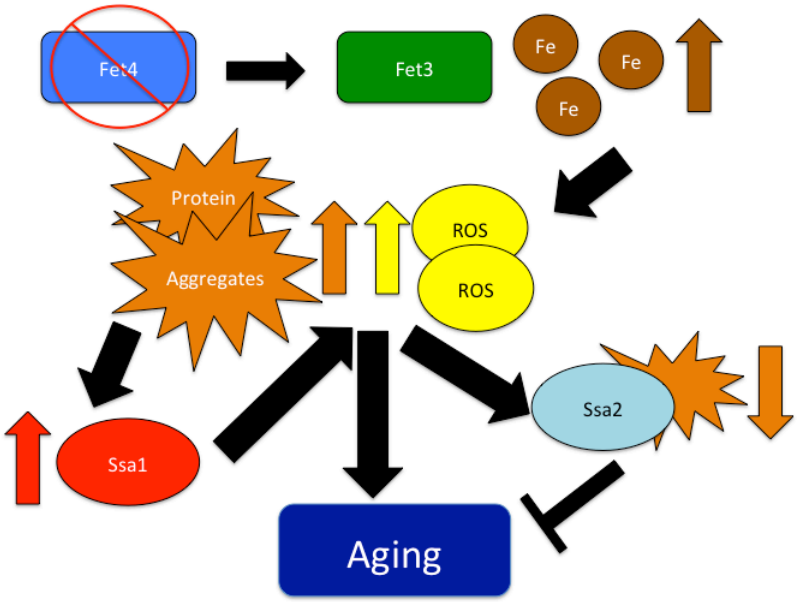

Figure 18: Model of Fet4 and Fet3 interaction with Ssa1 and Ssa2.
In the absence of Fet4, Fet3 contributes to increased intracellular iron. This potentiates protein aggregate and ROS formation. Although Ssa1 is recruited to minimize the effects of protein aggregation, it may end up potentiating their formation, while Ssa2 efficiently diminishes aggregates size. Effective aggregate curing may slow aging.

In regards to the spot dilution growth assays for these strains, that the *fet4Δ ssa2Δ* double mutant grew better than the wild type on glycerol under normal and heat stress temperatures indicates that *FET4* and *SSA2* may interact in a growth limiting way in conditions requiring mitochondrial respiration since when both genes are absent, the mutant flourishes. *FET4* and *SSA2* may interact only in conditions requiring mitochondrial respiration since no difference from the wild type was observed at both normal and stress temperatures on 2% YPD.

The impaired RLS of the *fet4Δ ssa2Δ* double mutant on glycerol, in conjunction with the enhanced growth on glycerol compared to the wild type, may indicate that although short-lived, the strain may be more stress resistant or faster growing. Perhaps the *fet4Δ ssa2Δ* mutant mimics hormesis, which is the exposure of an organism to a stressor at non-toxic levels that may yield benefits to the growth of an organism, but potentially with a cost, such as a shorter lifespan when toxically stressed (Blagosklonny, 2011) or, as may be the case in more complex organisms, impaired immunity (McClure et al., 2014).

Interestingly, the *ssa1Δ* mutant grew better than the wild type on glycerol at both regular and heat stress temperatures while the *fet4Δ* single mutant grew worse than the wild type. In addition, the *fet4Δ ssa1Δ* double mutant grew worse than either the *fet4Δ* or *ssa1Δ* single mutants. This suggests that the interaction between *FET4* and *SSA1* may be epistatic in that the double deletion mutant growth resembles that of the *fet4Δ* single mutant. Perhaps Fet4 provides iron or another divalent metal ion to a protein that is required to compensate for the loss of the *SSA1* gene for growth on glycerol.

The overarching hypothesis of this thesis was that cellular aging occurred when iron transport was misregulated, which led to a reliance on HSPs for lifespan maintenance. Cellular aging was assayed using the RLS assay on both metal metabolism and heat shock mutants, and the last set of experiments regarding *fet4Δ ssa1Δ* and *fet4Δ ssa2Δ* mutants discussed above provide evidence that this hypothesis is correct. The first portion of this thesis showed that as an isolated category, metal metabolism-related genes exhibited lifespan effects, such as lifespan maintenance and CR response while HSP-related genes exhibited less discernable lifespan effects. However, when mutations in metal metabolism and HSP-genes were combined, further defects in lifespan maintenance occurred. It is reasonable to suppose that HSPs and metal metabolism genes interact in a similar genetic pathway. Both sets of genes contribute to processes responsible for cellular aging. These include the formation of toxic levels of ROS that ultimately lead to the formation of protein aggregates. Protein aggregate formation can occur either indirectly due to the presence of the ROS (as is the case with metal metabolism genes) or directly due to protein misfolding (as is the case with the *SSA* family of genes) (Morimoto, 2011). However, *SSA* family members are distinct, and certain *SSA* genes may be enhanced by the presence or absence of another metal metabolism gene.

Future work with HSP family members may include an in-depth examination of the response of *ssaΔ* mutants to CR. In addition, techniques used in a preliminary manner in this project, but not discussed in this thesis, such as the characterization of protein aggregate formation and clearance using aggregate forming plasmids, may help further show a relationship between HSPs, ROS quenching by Sod1, metal metabolism

(especially the *sod1Δ* phenotype exacerbation in the absence of *FET4*) and protein aggregation.

6.9 Summary of findings

The following is a summary of the main findings for each of the 11 putative lifespan affecting genes.

1) *FET4*: Deletion of *FET4* alone did not produce a significant lifespan effect. When *FET4* was deleted in combination with *FET3* a shortening of lifespan occurred on 2% glucose. The *fet3Δ fet4Δ* double mutant was also responsive to CR. When deletion of *FET4* was combined with deletion of either the *SSA1* or *SSA2* HSPs, an effect on lifespan (a possible extension and shortening respectively) was observed. In addition, deletion of *FET4* led to reduced growth on glycerol, especially under conditions of heat stress. However, this reduced growth on glycerol did not translate to a shortened lifespan at 30°C. Deletion of *FET4* and *FET5* in combination did not shorten lifespan on 2% glucose, but the *fet4Δ fet5Δ* mutant was not responsive to CR. It appears *FET4* modulates yeast lifespan in cooperation with other iron transport-related proteins and HSPs in fermentative, respiratory and CR conditions.
2) *FET3*: While *FET3* deletion alone did not affect RLS on 2% glucose, growth on 3% glycerol was drastically reduced. In addition, *FET3* appeared to compensate for the absence of other *FET* genes since both the *fet3Δ fet5Δ* and *fet3Δ fet4Δ* mutants had shortened RLS lengths. The *fet4Δ fet5Δ* mutant, in which *FET3* was present, was unaffected. Only the *fet3Δ fet4Δ* mutant was responsive to CR, which suggests that *FET3* does not have a significant role in this process. *FET3* appears

to be most significant for cellular aging in fermentative and respiratory conditions.

3) *FET5*: *FET5* did appear to be most significant under CR conditions, as double mutants lacking *FET5,* the *fet3Δ fet5Δ* and *fet4Δ fet5Δ* double deletion mutants, were unresponsive to CR. In addition, growth on glycerol was reduced when *FET5* was absent, as was RLS on glycerol. Under fermentative conditions, when both *FET3* and *FET5* were absent did yeast have a shortened RLS. This suggests that *FET5* does have a more important role in lifespan maintenance under fermentative conditions than *FET4*. *FET5* appears to be significant for aging in fermentative, respiratory and CR conditions.
4) *SOD1:* On fermentative conditions (2% glucose), a mutant lacking *SOD1* had a significantly shorter lifespan than the wild type. This agreed with published literature on the mutant (Barker et al., 1999). A *sod1Δ* single mutant and a *fet4Δ sod1Δ* double mutant were extremely sensitive to heat stress under fermentative conditions and could not grow on glycerol. This could be due to increased cellular demand for ROS removal under the altered iron conditions that accompany a *FET4* deletion. *SOD1* plays a role in cellular aging in fermentative and respiratory conditions, especially during heat stress.
5) *MMT1*: *MMT1* does not appear to play a role in regulating lifespan when it is deleted single or in combination with another iron transporter, *FET4.* This is likely due to the presence of *MMT2.*
6) *MSC2:* Although an *msc2Δ* deletion mutant did not have RLS that was any different than the wild type, a *fet4Δ msc2Δ* double deletion mutant was unable to

grow on glycerol at both normal and heat stress temperatures. This suggests that *MSC2* and *FET4* interact to encourage RLS maintenance, or at least growth, under respiratory conditions. Perhaps impaired copper and zinc transport affects the functioning of SOD1, which contains both metal ions as a co-factor, and removes ROS.

7) *SSA1:* RLS of an *ssa1Δ* mutant and an *ssa1Δ ssa2Δ* double mutant was not significantly different than the wild type on 2% glucose. This partially confirms the above hypothesis as clearly *SSA1* deficiency is being compensated when it alone is removed, or even in combination with *SSA2*. However, *SSA1* may limit lifespan in the absence of *FET4* as an *ssa1Δ fet4Δ* double deletion mutant has a longer lifespan than any of the wild type, *ssa1Δ* mutant or *fet4Δ* mutant. This shows that metal metabolism and HSPs interact, perhaps through an aging factor, such as protein aggregates or ROS. Interestingly, an *ssa1Δ* mutant grows better than the wild type on glycerol, especially under heat shock conditions, perhaps due to compensation by the other SSA family members. In terms of cellular aging, *SSA1* appears to play a role in fermentative conditions when iron transport is modified. It may play a role in aging on glycerol. In both cases, *SSA1* may actually limit lifespan length rather than promote longevity.
8) *SSA2:* Single deletion of *SSA2* does not alter RLS on 2% glucose and the gene appears to be redundant with other *SSA* family members as the RLS on 2% glucose does not differ from wild type when both *SSA1* and *SSA2* are removed. However, RLS does shorten when *SSA2* is removed in combination with *FET4*. This indicates that removal of *FET4* may require *SSA2* to compensate for its loss.

The toxic by-products of metal metabolism could be the source of *FET4* and *SSA2* interaction. Interestingly, the *fet4Δ ssa2Δ* mutant showed more growth on glycerol at both normal and heat stress temperatures than the wild type. A compensatory stress response to the loss of these two genes could promote growth, but shortens lifespan.

9) *SSA3:* This hypothesis is confirmed for RLS on 2% glucose at normal temperatures, as the RLS of the *ssa3Δ* mutant was no different than the wild type.
10) *SSA4:* Like *ssa3Δ*, *ssa4Δ* did not have a RLS that differed from the wild type on 2% glucose under normal conditions. This indicates that the other *SSA* family members can compensate for the loss of *SSA4* and that *SSA4* is not important to fermentative growth at permissive temperatures.
11) *SSE2:* As expected, RLS is negatively affected when *SSE2* is removed. This is likely because *SSE2* is required to regulate the later stages of replicative aging.

An amalgamated network constructed from the findings of this thesis is given in Figure 19. A multi-coloured line indicates multiple processes affected. The figure is read from top to bottom. For example, each of *SSA1*, *SSA2* and *FET3* contain a green portion in the lines connecting them to *FET4.* This means each of these genes interact with *FET3* to influence fermentative RLS. Following the green line from *FET4* we see that heat stress is not required for this response. If a gene does not connect to a gene higher-up on the figure with the same coloured line, then that gene itself is the starting point for the effect. For example, *FET5* has an orange line, indicating an effect on respiratory RLS that is reliant on *FET5* alone. Conversely, *FET4* requires an interaction with *SSA2* to

influence respiratory RLS. Only one effect could not be accurately mapped: *SOD1* is capable of influencing respiratory growth in the absence of heat stress in combination with *FET4*. This may not be immediately apparent from Figure 19. This interaction network can also serve as a guide for future work determining interactions between HSP-encoding genes and metal metabolism genes.

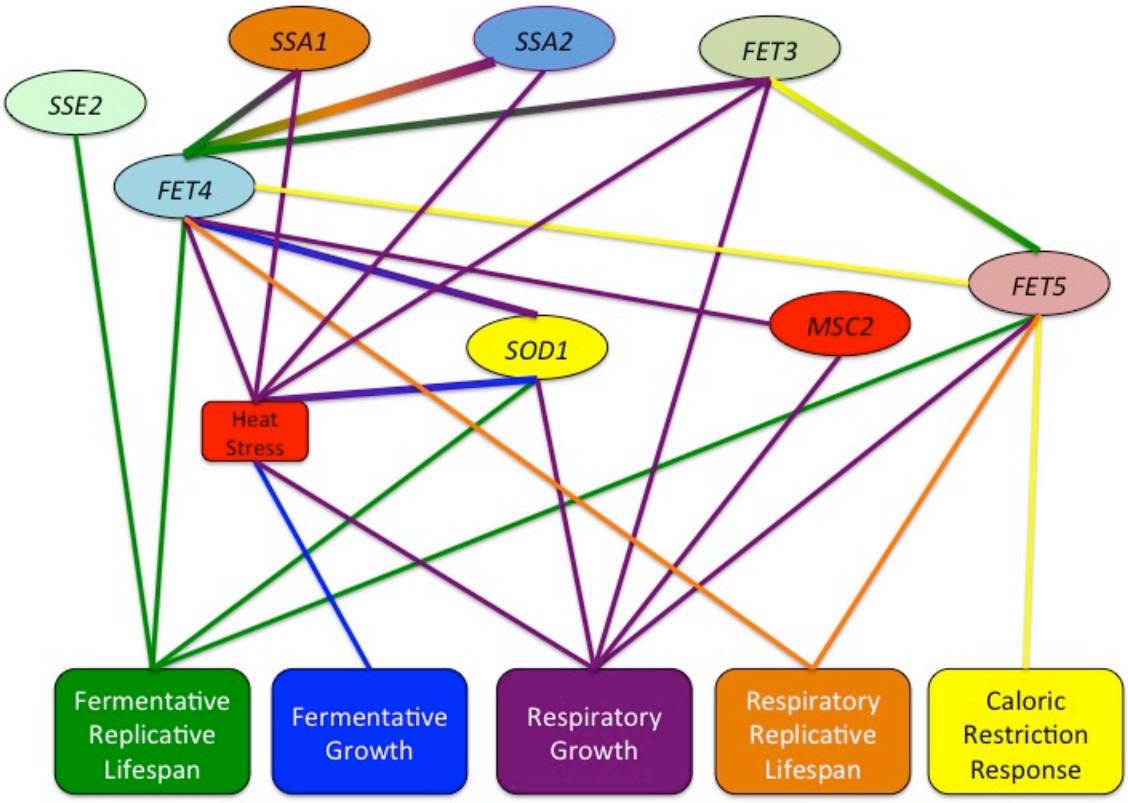

Figure 19: Proposed interaction network for genes examined in this thesis.
Figure is read from top to bottom. Multi-coloured lines indicate involvement in multiple pathways. For example, *FET5* has a single orange line extending to it from the Respiratory Replicative Lifespan box. This means that *FET5* alone can affect this process. However, the yellow line corresponding to the Caloric Restriction Response box extends to *FET5* and then onwards to *FET4* and *FET3*. This means that *FET5* in combination with either *FET4* or *FET3* is required to affect the CR response. Note that the line connecting *FET5* and *FET3* is both yellow and green as an interaction between *FET3* and *FET5* can also affect RLS under fermentative conditions.

7. References

Aguilaniu, H., Gustafsson, L., Rigoulet, M., and Nyström, T. (2003). Asymmetric Inheritance of Oxidatively Damaged Proteins During Cytokinesis. Science *299*, 1751-1753.

Ahuatzi, D., Herrero, P., de la Cera, T., and Moreno, F. (2004). The Glucose-regulated Nuclear Localization of Hexokinase 2 in Saccharomyces cerevisiae Is Mig1-dependent. Journal of Biological Chemistry *279*, 14440-14446.

Apfeld, J., O'Connor, G., McDonagh, T., DiStefano, P.S., and Curtis, R. (2004). The AMP-activated protein kinase AAK-2 links energy levels and insulin-like signals to lifespan in C. elegans. Genes Dev *18*, 3004-3009.

Arruda, L.F., Arruda, S.F., Campos, N.A., de Valencia, F.F., and Siqueira, E.M. (2013). Dietary iron concentration may influence aging process by altering oxidative stress in tissues of adult rats. PLoS One *8*, e61058.

Ashrafi, K., Lin, S.S., Manchester, J.K., and Gordon, J.I. (2000). Sip2p and its partner Snf1p kinase affect aging in S. cerevisiae. Genes & Development *14*, 1872-1885.

Askwith, C., Eide, D., Van Ho, A., Bernard, P.S., Li, L., Davis-Kaplan, S., Sipe, D.M., and Kaplan, J. (1994). The FET3 gene of S. cerevisiae encodes a multicopper oxidase required for ferrous iron uptake. Cell *76*, 403-410.

Austriaco, N.R. (1996). Review: To bud until death: The genetics of ageing in the yeast, Saccharomyces. Yeast *12*, 623-630.

Banasik, K., Ribel-Madsen, R., Gjesing, A.P., Wegner, L., Andersson, A., Poulsen, P., Borglykke, A., Witte, D.R., Pedersen, O., Hansen, T.*, et al.* (2011). The FOXO3A rs2802292 G-allele associates with improved peripheral and hepatic insulin sensitivity and increased skeletal muscle-FOXO3A mRNA expression in twins. J Clin Endocrinol Metab *96*, E119-124.

Barker, M.G., Brimage, L.J.E., and Smart, K.A. (1999). Effect of Cu,Zn superoxide dismutase disruption mutation on replicative senescence in Saccharomyces cerevisiae. FEMS Microbiology Letters *177*, 199-204.

Batista-Nascimento, L., Pimentel, C., Menezes, R.A., and Rodrigues-Pousada, C. (2012). Iron and neurodegeneration: from cellular homeostasis to disease. Oxid Med Cell Longev *2012*, 128647.

Baur, J.A., Pearson, K.J., Price, N.L., Jamieson, H.A., Lerin, C., Kalra, A., Prabhu, V.V., Allard, J.S., Lopez-Lluch, G., Lewis, K.*, et al.* (2006). Resveratrol improves health and survival of mice on a high-calorie diet. Nature *444*, 337-342.

Bellizzi, D., Rose, G., Cavalcante, P., Covello, G., Dato, S., De Rango, F., Greco, V., Maggiolini, M., Feraco, E., Mari, V.*, et al.* (2005). A novel VNTR enhancer within the SIRT3 gene, a human homologue of SIR2, is associated with survival at oldest ages. Genomics *85*, 258-263.

Bergman, L. (2001). Growth and Maintenance of Yeast. In Two-Hybrid Systems, P. MacDonald, ed. (Humana Press), pp. 9-14.

Bishop, N.A., and Guarente, L. (2007). Genetic links between diet and lifespan: shared mechanisms from yeast to humans. Nat Rev Genet *8*, 835-844.

Blagosklonny, M.V. (2011). Hormesis does not make sense except in the light of TOR-driven aging. Aging (Albany NY) *3*, 1051.

Blagosklonny, M.V. (2014). Aging: ROS or TOR. Cell Cycle *7*, 3344-3354.

Botstein, D., Chervitz, S.A., and Cherry, J.M. (1997). Yeast as a Model Organism. Science (New York, NY) *277*, 1259-1260.

Botta, G., Turn, C.S., Quintyne, N.J., and Kirchman, P.A. (2011). Increased iron supplied through Fet3p results in replicative life span extension of Saccharomyces cerevisiae under conditions requiring respiratory metabolism. Exp Gerontol *46*, 827-832.

Brachmann, C.B., Davies, A., Cost, G.J., Caputo, E., Li, J., Hieter, P., and Boeke, J.D. (1998). Designer deletion strains derived from Saccharomyces cerevisiae S288C: a useful set of strains and plasmids for PCR-mediated gene disruption and other applications. YEAST-CHICHESTER- *14*, 115-132.

Briat, J.F., Ravet, K., Arnaud, N., Duc, C., Boucherez, J., Touraine, B., Cellier, F., and Gaymard, F. (2010). New insights into ferritin synthesis and function highlight a link between iron homeostasis and oxidative stress in plants. Ann Bot *105*, 811-822.

Brownridge, P., Lawless, C., Payapilly, A.B., Lanthaler, K., Holman, S.W., Harman, V.M., Grant, C.M., Beynon, R.J., and Hubbard, S.J. (2013). Quantitative analysis of chaperone network throughput in budding yeast. Proteomics *13*, 1276-1291.

Brundin, P., Melki, R., and Kopito, R. (2010). Prion-like transmission of protein aggregates in neurodegenerative diseases. Nat Rev Mol Cell Biol *11*, 301-307.

Bufalino, M.R., DeVeale, B., and van der Kooy, D. (2013). The asymmetric segregation of damaged proteins is stem cell-type dependent. J Cell Biol *201*, 523-530.

Burhans, W., and Weinberger, M. (2012). DNA damage and DNA replication stress in yeast models of aging. In Aging Research in Yeast, M. Breitenbach, S.M. Jazwinski, and P. Laun, eds. (Springer Netherlands), pp. 187-206.

Cabiscol, E., Tamarit, J., and Ros, J. (2014). Protein carbonylation: proteomics, specificity and relevance to aging. Mass Spectrom Rev *33*, 21-48.

Canto, C., and Auwerx, J. (2009). Caloric restriction, SIRT1 and longevity. Trends Endocrinol Metab *20*, 325-331.

Canto, C., Gerhart-Hines, Z., Feige, J.N., Lagouge, M., Noriega, L., Milne, J.C., Elliott, P.J., Puigserver, P., and Auwerx, J. (2009). AMPK regulates energy expenditure by modulating NAD+ metabolism and SIRT1 activity. Nature *458*, 1056-1060.

Chernova, T.A., Wilkinson, K.D., and Chernoff, Y.O. (2014). Physiological and environmental control of yeast prions. FEMS Microbiol Rev *38*, 326-344.

Cherry, J.M., Hong, E.L., Amundsen, C., Balakrishnan, R., Binkley, G., Chan, E.T., Christie, K.R., Costanzo, M.C., Dwight, S.S., Engel, S.R.*, et al.* (2012). Saccharomyces Genome Database: the genomics resource of budding yeast. Nucleic Acids Res *40*, D700-705.

Chichester, L., Wylie, A.T., Craft, S., and Kavanagh, K. (2015). Muscle heat shock protein 70 predicts insulin resistance with aging. J Gerontol A Biol Sci Med Sci *70*, 155-162.

Cobine, P.A., Pierrel, F., and Winge, D.R. (2006). Copper trafficking to the mitochondrion and assembly of copper metalloenzymes. Biochim Biophys Acta *1763*, 759-772.

Curtis, J.M., Hahn, W.S., Long, E.K., Burrill, J.S., Arriaga, E.A., and Bernlohr, D.A. (2012). Protein carbonylation and metabolic control systems. Trends Endocrinol Metab *23*, 399-406.

D'Autreaux, B., and Toledano, M.B. (2007). ROS as signalling molecules: mechanisms that generate specificity in ROS homeostasis. Nat Rev Mol Cell Biol *8*, 813-824.

D'Mello, N.P., and Jazwinski, S.M. (1991). Telomere length constancy during aging of Saccharomyces cerevisiae. Journal of Bacteriology *173*, 6709-6713.

Daugaard, M., Rohde, M., and Jaattela, M. (2007). The heat shock protein 70 family: Highly homologous proteins with overlapping and distinct functions. FEBS Lett *581*, 3702-3710.

de Cabo, R., Carmona-Gutierrez, D., Bernier, M., Hall, M.N., and Madeo, F. (2014). The Search for Antiaging Interventions: From Elixirs to Fasting Regimens. Cell *157*, 1515-1526.

De Freitas, J., Wintz, H., Hyoun Kim, J., Poynton, H., Fox, T., and Vulpe, C. (2003). Yeast, a model organism for iron and copper metabolism studies. Biometals *16*, 185-197.

De Freitas, J.M., Liba, A., Meneghini, R., Valentine, J.S., and Gralla, E.B. (2000). Yeast Lacking Cu-Zn Superoxide Dismutase Show Altered Iron Homeostasis: ROLE OF OXIDATIVE STRESS IN IRON METABOLISM. Journal of Biological Chemistry *275*, 11645-11649.

de Silva, D., Davis-Kaplan, S., Fergestad, J., and Kaplan, J. (1997). Purification and Characterization of Fet3 Protein, a Yeast Homologue of Ceruloplasmin. Journal of Biological Chemistry *272*, 14208-14213.

DeRisi, J.L., Iyer, V.R., and Brown, P.O. (1997). Exploring the Metabolic and Genetic Control of Gene Expression on a Genomic Scale. Science *278*, 680-686.

Diaz de la Loza Mdel, C., Gallardo, M., Garcia-Rubio, M.L., Izquierdo, A., Herrero, E., Aguilera, A., and Wellinger, R.E. (2011). Zim17/Tim15 links mitochondrial iron-sulfur cluster biosynthesis to nuclear genome stability. Nucleic Acids Res *39*, 6002-6015.

Dix, D.R., Bridgham, J.T., Broderius, M.A., Byersdorfer, C.A., and Eide, D.J. (1994). The FET4 gene encodes the low affinity Fe(II) transport protein of Saccharomyces cerevisiae. Journal of Biological Chemistry *269*, 26092-26099.

Duce, J.A., Tsatsanis, A., Cater, M.A., James, S.A., Robb, E., Wikhe, K., Leong, S.L., Perez, K., Johanssen, T., Greenough, M.A*., et al.* (2010). Iron-export ferroxidase activity of beta-amyloid precursor protein is inhibited by zinc in Alzheimer's disease. Cell *142*, 857-867.

Egilmez, N.K., and Jazwinski, S.M. (1989). Evidence for the involvement of a cytoplasmic factor in the aging of the yeast Saccharomyces cerevisiae. Journal of Bacteriology *171*, 37-42.

Ellis, C.D., Wang, F., MacDiarmid, C.W., Clark, S., Lyons, T., and Eide, D.J. (2004). Zinc and the Msc2 zinc transporter protein are required for endoplasmic reticulum function. J Cell Biol *166*, 325-335.

Flachsbart, F., Caliebe, A., Kleindorp, R., Blanche, H., von Eller-Eberstein, H., Nikolaus, S., Schreiber, S., and Nebel, A. (2009). Association of FOXO3A variation with human longevity confirmed in German centenarians. Proceedings of the National Academy of Sciences of the United States of America *106*, 2700-2705.

Fontana, L., Partridge, L., and Longo, V.D. (2010). Extending Healthy Life Span—From Yeast to Humans. Science *328*, 321-326.

Fröhlich, K.-U., and Madeo, F. (2000). Apoptosis in yeast – a monocellular organism exhibits altruistic behaviour. FEBS Letters *473*, 6-9.

Funakoshi, M., Tsuda, M., Muramatsu, K., Hatsuda, H., Morishita, S., and Aigaki, T. (2011). A gain-of-function screen identifies wdb and lkb1 as lifespan-extending genes in Drosophila. Biochem Biophys Res Commun *405*, 667-672.

Gagnon-Kugler, T., Langlois, F., Stefanovsky, V., Lessard, F., and Moss, T. (2009). Loss of human ribosomal gene CpG methylation enhances cryptic RNA polymerase II transcription and disrupts ribosomal RNA processing. Mol Cell *35*, 414-425.

Gami, M.S., and Wolkow, C.A. (2006). Studies of Caenorhabditis elegans DAF-2/insulin signaling reveal targets for pharmacological manipulation of lifespan. Aging Cell *5*, 31-37.

Ganley, A.R., and Kobayashi, T. (2014). Ribosomal DNA and cellular senescence: new evidence supporting the connection between rDNA and aging. FEMS Yeast Res *14*, 49-59.

Garay, E., Campos, S.E., Gonzalez de la Cruz, J., Gaspar, A.P., Jinich, A., and Deluna, A. (2014). High-resolution profiling of stationary-phase survival reveals yeast longevity factors and their genetic interactions. PLoS Genet *10*, e1004168.

Gardner, B.M., Pincus, D., Gotthardt, K., Gallagher, C.M., and Walter, P. (2013). Endoplasmic reticulum stress sensing in the unfolded protein response. Cold Spring Harb Perspect Biol *5*, a013169.

Garrick, M., Dolan, K., Horbinski, C., Ghio, A., Higgins, D., Porubcin, M., Moore, E., Hainsworth, L., Umbreit, J., Conrad, M.*, et al.* (2003). DMT1: A mammalian transporter for multiple metals. Biometals *16*, 41-54.

Gershon, H., and Gershon, D. (2000). The budding yeast, Saccharomyces cerevisiae, as a model for aging research: a critical review. Mechanisms of Ageing and Development *120*, 1-22.

Ghavidel, A., Baxi, K., Ignatchenko, V., Prusinkiewicz, M., Arnason, T.G., Kislinger, T., Carvalho, C.E., and Harkness, T.A. (2015). A Genome Scale Screen for Mutants with Delayed Exit from Mitosis: Ire1-Independent Induction of Autophagy Integrates ER Homeostasis into Mitotic Lifespan. PLoS Genet *11*, e1005429.

Greer, E.L., and Brunet, A. (2009). Different dietary restriction regimens extend lifespan by both independent and overlapping genetic pathways in C. elegans. Aging Cell *8*, 113-127.

Greer, E.L., Oskoui, P.R., Banko, M.R., Maniar, J.M., Gygi, M.P., Gygi, S.P., and Brunet, A. (2007). The energy sensor AMP-activated protein kinase directly regulates the mammalian FOXO3 transcription factor. J Biol Chem *282*, 30107-30119.

Groeger, G., Quiney, C., and Cotter, T.G. (2009). Hydrogen Peroxide as a Cell-Survival Signaling Molecule. Antioxidants & Redox Signaling *11*, 2655-2671.

Grune, T., Jung, T., Merker, K., and Davies, K.J. (2004). Decreased proteolysis caused by protein aggregates, inclusion bodies, plaques, lipofuscin, ceroid, and 'aggresomes' during oxidative stress, aging, and disease. Int J Biochem Cell Biol *36*, 2519-2530.

Guarente, L. (2007). Sirtuins in Aging and Disease. Cold Spring Harbor Symposia on Quantitative Biology *72*, 483-488.

Gwinn, D.M., Shackelford, D.B., Egan, D.F., Mihaylova, M.M., Mery, A., Vasquez, D.S., Turk, B.E., and Shaw, R.J. (2008). AMPK phosphorylation of raptor mediates a metabolic checkpoint. Mol Cell *30*, 214-226.

Ha, C.W., and Huh, W.-K. (2011). The implication of Sir2 in replicative aging and senescence in Saccharomyces cerevisiae. Aging (Albany NY) *3*, 319-324.

Hampsey, M. (1997). A Review of Phenotypes in Saccharomyces cerevisiae. Yeast *13*, 1099-1133.

Hansen, M., Taubert, S., Crawford, D., Libina, N., Lee, S.-J., and Kenyon, C. (2007). Lifespan extension by conditions that inhibit translation in Caenorhabditis elegans. Aging Cell *6*, 95-110.

Harrison, D.E., Strong, R., Sharp, Z.D., Nelson, J.F., Astle, C.M., Flurkey, K., Nadon, N.L., Wilkinson, J.E., Frenkel, K., Carter, C.S.*, et al.* (2009). Rapamycin fed late in life extends lifespan in genetically heterogeneous mice. Nature *460*, 392-395.

Hasin, N., Cusack, S.A., Ali, S.S., Fitzpatrick, D.A., and Jones, G.W. (2014). Global transcript and phenotypic analysis of yeast cells expressing Ssa1, Ssa2, Ssa3 or Ssa4 as sole source of cytosolic Hsp70-Ssa chaperone activity. BMC genomics *15*, 194.

Hassett, R., Dix, D.R., Eide, D.J., and Kosman, D.J. (2000). The Fe(II) permease Fet4p functions as a low affinity copper transporter and supports normal copper trafficking in Saccharomyces cerevisiae. Biochemical Journal *351*, 477-484.

Haurie, V., Boucherie, H., and Sagliocco, F. (2003). The Snf1 protein kinase controls the induction of genes of the iron uptake pathway at the diauxic shift in Saccharomyces cerevisiae. J Biol Chem *278*, 45391-45396.

Hawley, S.A., Ross, F.A., Chevtzoff, C., Green, K.A., Evans, A., Fogarty, S., Towler, M.C., Brown, L.J., Ogunbayo, O.A., Evans, A.M*., et al.* (2010). Use of cells expressing gamma subunit variants to identify diverse mechanisms of AMPK activation. Cell Metab *11*, 554-565.

Hawthorne, D.C. (1963). A Deletion in Yeast and Its Bearing on the Structure of the Mating Type Locus. Genetics *48*, 1727-1729.

Hedbacker, K., and Carlson, M. (2008). SNF1/AMPK pathways in yeast. Frontiers in bioscience : a journal and virtual library *13*, 2408-2420.

Hekimi, S., Lapointe, J., and Wen, Y. (2011). Taking a "good" look at free radicals in the aging process. Trends in cell biology *21*, 569-576.

Herker, E., Jungwirth, H., Lehmann, K.A., Maldener, C., Frohlich, K.U., Wissing, S., Buttner, S., Fehr, M., Sigrist, S., and Madeo, F. (2004). Chronological aging leads to apoptosis in yeast. J Cell Biol *164*, 501-507.

Hideyuki, M., Takayoshi, K., Hozumi, T., Dai, H., Tokichi, M., and Chikako, T. (1993). Isolation and characterization of SSE1 and SSE2, new members of the yeast HSP70 multigene family. Gene *132*, 57-66.

Howitz, K.T., Bitterman, K.J., Cohen, H.Y., Lamming, D.W., Lavu, S., Wood, J.G., Zipkin, R.E., Chung, P., Kisielewski, A., Zhang, L.-L*., et al.* (2003). Small molecule activators of sirtuins extend Saccharomyces cerevisiae lifespan. Nature *425*, 191-196.

Hsieh, C.C., and Papaconstantinou, J. (2004). Akt/PKB and p38 MAPK signaling, translational initiation and longevity in Snell dwarf mouse livers. Mech Ageing Dev *125*, 785-798.

Huhne, R., Thalheim, T., and Suhnel, J. (2014). AgeFactDB--the JenAge Ageing Factor Database--towards data integration in ageing research. Nucleic Acids Res *42*, D892-896.

Imai, S.-i., Armstrong, C.M., Kaeberlein, M., and Guarente, L. (2000). Transcriptional silencing and longevity protein Sir2 is an NAD-dependent histone deacetylase. Nature *403*, 795-800.

Jakubowski, W., Biliński, T., and Bartosz, G. (2000). Oxidative stress during aging of stationary cultures of the yeast Saccharomyces cerevisiae. Free Radical Biology and Medicine *28*, 659-664.

Jazwinski, S.M. (2005). Yeast longevity and aging--the mitochondrial connection. Mech Ageing Dev *126*, 243-248.

Jiang, J.C., Jaruga, E.W.A., Repnevskaya, M.V., and Jazwinski, S.M. (2000). An intervention resembling caloric restriction prolongs life span and retards aging in yeast. The FASEB Journal *14*, 2135-2137.

Jiao, R., Postnikoff, S., Harkness, T.A., and Arnason, T.G. (2015). The SNF1 Kinase Ubiquitin-associated Domain Restrains Its Activation, Activity, and the Yeast Life Span. J Biol Chem *290*, 15393-15404.

Kaeberlein, M. (2010). Lessons on longevity from budding yeast. Nature *464*, 513-519.

Kaeberlein, M., Hu, D., Kerr, E.O., Tsuchiya, M., Westman, E.A., Dang, N., Fields, S., and Kennedy, B.K. (2005a). Increased life span due to calorie restriction in respiratory-deficient yeast. PLoS Genet *1*, e69.

Kaeberlein, M., Kirkland, K.T., Fields, S., and Kennedy, B.K. (2005b). Genes determining yeast replicative life span in a long-lived genetic background. Mech Ageing Dev *126*, 491-504.

Kaeberlein, M., Powers, R.W., Steffen, K.K., Westman, E.A., Hu, D., Dang, N., Kerr, E.O., Kirkland, K.T., Fields, S., and Kennedy, B.K. (2005c). Regulation of Yeast Replicative Life Span by TOR and Sch9 in Response to Nutrients. Science *310*, 1193-1196.

Kamei, Y., Tamada, Y., Nakayama, Y., Fukusaki, E., and Mukai, Y. (2014). Changes in transcription and metabolism during the early stage of replicative cellular senescence in budding yeast. J Biol Chem *289*, 32081-32093.

Kanfi, Y., Naiman, S., Amir, G., Peshti, V., Zinman, G., Nahum, L., Bar-Joseph, Z., and Cohen, H.Y. (2012). The sirtuin SIRT6 regulates lifespan in male mice. Nature *483*, 218-221.

Kapahi, P., Chen, D., Rogers, A.N., Katewa, S.D., Li, P.W., Thomas, E.L., and Kockel, L. (2010). With TOR, less is more: a key role for the conserved nutrient-sensing TOR pathway in aging. Cell Metab *11*, 453-465.

Katajisto, P., Döhla, J., Chaffer, C.L., Pentinmikko, N., Marjanovic, N., Iqbal, S., Zoncu, R., Chen, W., Weinberg, R.A., and Sabatini, D.M. (2015). Asymmetric apportioning of aged mitochondria between daughter cells is required for stemness. Science *348*, 340-343.

Kathiresan, M., Martins, D., and English, A.M. (2014). Respiration triggers heme transfer from cytochrome c peroxidase to catalase in yeast mitochondria. Proceedings of the National Academy of Sciences *111*, 17468-17473.

Kennedy, B.K., Austriaco, N.R., and Guarente, L. (1994). Daughter cells of Saccharomyces cerevisiae from old mothers display a reduced life span. The Journal of Cell Biology *127*, 1985-1993.

Kenyon, C.J. (2010). The genetics of ageing. Nature *464*, 504-512.

Kim, S., Villeponteau, B., and Jazwinski, S.M. (1996). Effect of Replicative Age on Transcriptional Silencing Near Telomeres in Saccharomyces cerevisiae. Biochemical and Biophysical Research Communications *219*, 370-376.

Kowaltowski, A.J., and Vercesi, A.E. (1999). Mitochondrial damage induced by conditions of oxidative stress. Free Radical Biology and Medicine *26*, 463-471.

Lamming, D.W., Ye, L., Katajisto, P., Goncalves, M.D., Saitoh, M., Stevens, D.M., Davis, J.G., Salmon, A.B., Richardson, A., Ahima, R.S.*, et al.* (2012). Rapamycin-Induced Insulin Resistance Is Mediated by mTORC2 Loss and Uncoupled from Longevity. Science *335*, 1638-1643.

Laun, P., Ramachandran, L., Jarolim, S., Herker, E., Liang, P., Wang, J., Weinberger, M., Burhans, D.T., Suter, B., Madeo, F.*, et al.* (2005). A comparison of the aging and apoptotic transcriptome of Saccharomyces cerevisiae. FEMS Yeast Res *5*, 1261-1272.

Lawen, A., and Lane, D.J. (2013). Mammalian iron homeostasis in health and disease: uptake, storage, transport, and molecular mechanisms of action. Antioxid Redox Signal *18*, 2473-2507.

Leal, S.S., Botelho, H.M., and Gomes, C.M. (2012). Metal ions as modulators of protein conformation and misfolding in neurodegeneration. Coordination Chemistry Reviews *256*, 2253-2270.

Lesur, I., and Campbell, J.L. (2004). The Transcriptome of Prematurely Aging Yeast Cells Is Similar to That of Telomerase-deficient Cells. Molecular Biology of the Cell *15*, 1297-1312.

Li, L., and Kaplan, J. (1997). Characterization of Two Homologous Yeast Genes That Encode Mitochondrial Iron Transporters. Journal of Biological Chemistry *272*, 28485-28493.

Li, L., and Kaplan, J. (1998). Defects in the Yeast High Affinity Iron Transport System Result in Increased Metal Sensitivity because of the Increased Expression of Transporters with a Broad Transition Metal Specificity. Journal of Biological Chemistry *273*, 22181-22187.

Li, L., Miao, R., Jia, X., Ward, D.M., and Kaplan, J. (2014). Expression of the yeast cation diffusion facilitators Mmt1 and Mmt2 affects mitochondrial and cellular iron homeostasis: evidence for mitochondrial iron export. J Biol Chem *289*, 17132-17141.

Lill, R., Hoffmann, B., Molik, S., Pierik, A.J., Rietzschel, N., Stehling, O., Uzarska, M.A., Webert, H., Wilbrecht, C., and Muhlenhoff, U. (2012). The role of mitochondria in cellular iron-sulfur protein biogenesis and iron metabolism. Biochim Biophys Acta *1823*, 1491-1508.

Lin, S.-J., Defossez, P.-A., and Guarente, L. (2000). Requirement of NAD and SIR2 for Life-Span Extension by Calorie Restriction in Saccharomyces cerevisiae. Science *289*, 2126-2128.

Lin, S.-J., Ford, E., Haigis, M., Liszt, G., and Guarente, L. (2004). Calorie restriction extends yeast life span by lowering the level of NADH. Genes & Development *18*, 12-16.

Lin, S.-J., Kaeberlein, M., Andalis, A.A., Sturtz, L.A., Defossez, P.-A., Culotta, V.C., Fink, G.R., and Guarente, L. (2002). Calorie restriction extends Saccharomyces cerevisiae lifespan by increasing respiration. Nature *418*, 344-348.

Lin, S.S., Manchester, J.K., and Gordon, J.I. (2001). Enhanced Gluconeogenesis and Increased Energy Storage as Hallmarks of Aging in Saccharomyces cerevisiae. Journal of Biological Chemistry *276*, 36000-36007.

Lin, S.S., Manchester, J.K., and Gordon, J.I. (2003). Sip2, an N-myristoylated beta subunit of Snf1 kinase, regulates aging in Saccharomyces cerevisiae by affecting cellular histone kinase activity, recombination at rDNA loci, and silencing. J Biol Chem *278*, 13390-13397.

Lindegren, C.C. (1949). CHROMOSOME MAPS OF SACCHAROMYCES. Hereditas *35*, 338-355.

Lindegren, C.C., and Lindegren, G. (1943). Segregation, Mutation, and Copulation in Saccharomyces cerevisiae. Annals of the Missouri Botanical Garden *30*, 453-468.

Longo, V.D., Antebi, A., Bartke, A., Barzilai, N., Brown-Borg, H.M., Caruso, C., Curiel, T.J., de Cabo, R., Franceschi, C., Gems, D.*, et al.* (2015). Interventions to Slow Aging in Humans: Are We Ready? Aging Cell *14*, 497-510.

Lopez-Otin, C., Blasco, M.A., Partridge, L., Serrano, M., and Kroemer, G. (2013). The hallmarks of aging. Cell *153*, 1194-1217.

Lorenz, D.R., Cantor, C.R., and Collins, J.J. (2009). A network biology approach to aging in yeast. Proceedings of the National Academy of Sciences of the United States of America *106*, 1145-1150.

Mahadev, K., Zilbering, A., Zhu, L., and Goldstein, B.J. (2001). Insulin-stimulated hydrogen peroxide reversibly inhibits protein-tyrosine phosphatase 1b in vivo and enhances the early insulin action cascade. J Biol Chem *276*, 21938-21942.

Malyshev, I. (2013). HSP70 in Aging. In Immunity, Tumors and Aging: The Role of HSP70 (Springer), pp. 99-111.

Mann, H.B. (1945). Nonparametric tests against trend. Econometrica: Journal of the Econometric Society, 245-259.

Matecic, M., Smith, D.L., Pan, X., Maqani, N., Bekiranov, S., Boeke, J.D., and Smith, J.S. (2010). A microarray-based genetic screen for yeast chronological aging factors. PLoS Genet *6*, e1000921.

McClure, C.D., Zhong, W., Hunt, V.L., Chapman, F.M., Hill, F.V., and Priest, N.K. (2014). Hormesis results in trade-offs with immunity. Evolution *68*, 2225-2233.

McFaline-Figueroa, J.R., Vevea, J., Swayne, T.C., Zhou, C., Liu, C., Leung, G., Boldogh, I.R., and Pon, L.A. (2011). Mitochondrial quality control during inheritance is associated with lifespan and mother–daughter age asymmetry in budding yeast. Aging Cell *10*, 885-895.

Menzel, J., Malo, M.E., Chan, C., Prusinkiewicz, M., Arnason, T.G., and Harkness, T.A. (2014). The anaphase promoting complex regulates yeast lifespan and rDNA stability by targeting Fob1 for degradation. Genetics *196*, 693-709.

Mercken, E.M., Crosby, S.D., Lamming, D.W., JeBailey, L., Krzysik-Walker, S., Villareal, D.T., Capri, M., Franceschi, C., Zhang, Y., Becker, K.*, et al.* (2013). Calorie restriction in humans inhibits the PI3K/AKT pathway and induces a younger transcription profile. Aging Cell *12*, 645-651.

Michal Jazwinski, S., Egilmez, N.K., and Chen, J.B. (1989). Replication control and cellular life span. Experimental Gerontology *24*, 423-436.

Miller, R.A., Harrison, D.E., Astle, C.M., Fernandez, E., Flurkey, K., Han, M., Javors, M.A., Li, X., Nadon, N.L., Nelson, J.F.*, et al.* (2014). Rapamycin-mediated lifespan increase in mice is dose and sex dependent and metabolically distinct from dietary restriction. Aging Cell *13*, 468-477.

Milman, S., Atzmon, G., Huffman, D.M., Wan, J., Crandall, J.P., Cohen, P., and Barzilai, N. (2014). Low insulin-like growth factor-1 level predicts survival in humans with exceptional longevity. Aging Cell *13*, 769-771.

Mirisola, M.G., Braun, R.J., and Petranovic, D. (2014). Approaches to study yeast cell aging and death. FEMS Yeast Res *14*, 109-118.

Miyauchi, H., Minamino, T., Tateno, K., Kunieda, T., Toko, H., and Komuro, I. (2004). Akt negatively regulates the in vitro lifespan of human endothelial cells via a p53/p21-dependent pathway. The EMBO Journal *23*, 212-220.

Molon, M., Zadrag-Tecza, R., and Bilinski, T. (2015). The longevity in the yeast Saccharomyces cerevisiae: A comparison of two approaches for assessment the lifespan. Biochem Biophys Res Commun *460*, 651-656.

Morimoto, R.I. (2011). The heat shock response: systems biology of proteotoxic stress in aging and disease. Cold Spring Harb Symp Quant Biol *76*, 91-99.

Mortimer, R.K., and Johnston, J.R. (1959). Life Span of Individual Yeast Cells. Nature *183*, 1751-1752.

Müller, G., Rouveyre, N., Crecelius, A., and Bandlow, W. (1998). Insulin Signaling in the Yeast Saccharomyces cerevisiae. 1. Stimulation of Glucose Metabolism and Snf1 Kinase by Human Insulin. Biochemistry *37*, 8683-8695.

Murshid, A., Eguchi, T., and Calderwood, S.K. (2013). Stress proteins in aging and life span. Int J Hyperthermia *29*, 442-447.

Nicola, R.D., and Walker, G. (2009). Interaction Between Yeasts and Zinc. 237-257.

Nyström, T. (2005). Role of oxidative carbonylation in protein quality control and senescence. The EMBO Journal *24*, 1311-1317.

Nystrom, T., and Liu, B. (2014). The mystery of aging and rejuvenation - a budding topic. Current opinion in microbiology *18*, 61-67.

Nyström, T., and Liu, B. (2014). Protein quality control in time and space – links to cellular aging. FEMS Yeast Research *14*, 40-48.

Paradis, S., and Ruvkun, G. (1998). Caenorhabditis elegans Akt/PKB transduces insulin receptor-like signals from AGE-1 PI3 kinase to the DAF-16 transcription factor. Genes & Development *12*, 2488-2498.

Pattabiraman, S., and Kaganovich, D. (2014). Imperfect asymmetry: The mechanism governing asymmetric partitioning of damaged cellular components during mitosis. Bioarchitecture *4*, 203-209.

Pearson, K.J., Baur, J.A., Lewis, K.N., Peshkin, L., Price, N.L., Labinskyy, N., Swindell, W.R., Kamara, D., Minor, R.K., Perez, E.*, et al.* (2008). Resveratrol delays age-related

deterioration and mimics transcriptional aspects of dietary restriction without extending life span. Cell Metab *8*, 157-168.

Petti, A.A., Crutchfield, C.A., Rabinowitz, J.D., and Botstein, D. (2011). Survival of starving yeast is correlated with oxidative stress response and nonrespiratory mitochondrial function. Proceedings of the National Academy of Sciences *108*, E1089-E1098.

Philpott, C.C. (2012). Yeast Iron Metabolism. 653-667.

Piper, P.W. (2006). Long-lived yeast as a model for ageing research. Yeast *23*, 215-226.

Polge, C., and Thomas, M. (2007). SNF1/AMPK/SnRK1 kinases, global regulators at the heart of energy control? Trends Plant Sci *12*, 20-28.

Postnikoff, S.D., and Harkness, T.A. (2014). Replicative and chronological life-span assays. Methods Mol Biol *1163*, 223-227.

Postnikoff, S.D., Malo, M.E., Wong, B., and Harkness, T.A. (2012). The yeast forkhead transcription factors fkh1 and fkh2 regulate lifespan and stress response together with the anaphase-promoting complex. PLoS Genet *8*, e1002583.

Pugh, T.D., Klopp, R.G., and Weindruch, R. (1999). Controlling caloric consumption: protocols for rodents and rhesus monkeys. Neurobiology of aging *20*, 157-165.

R Core Team, T. (2012). R: A language and environment for statistical computing. R Foundation for Statistical Computing, Vienna, Austria, 2012 (ISBN 3-900051-07-0).

Raguzzi, F., Lesuisse, E., and Crichton, R.R. (1988). Iron storage in Saccharomyces cerevisiae. FEBS Letters *231*, 253-258.

Ralph, S.J., Rodriguez-Enriquez, S., Neuzil, J., Saavedra, E., and Moreno-Sanchez, R. (2010). The causes of cancer revisited: "mitochondrial malignancy" and ROS-induced oncogenic transformation - why mitochondria are targets for cancer therapy. Mol Aspects Med *31*, 145-170.

Raymond, C.K., Howald-Stevenson, I., Vater, C.A., and Stevens, T.H. (1992). Morphological classification of the yeast vacuolar protein sorting mutants: evidence for a prevacuolar compartment in class E vps mutants. Molecular biology of the cell *3*, 1389-1402.

Robertson, L.S., Causton, H.C., Young, R.A., and Fink, G.R. (2000). The yeast A kinases differentially regulate iron uptake and respiratory function. Proceedings of the National Academy of Sciences *97*, 5984-5988.

Rose, G., Dato, S., Altomare, K., Bellizzi, D., Garasto, S., Greco, V., Passarino, G., Feraco, E., Mari, V., Barbi, C.*, et al.* (2003). Variability of the SIRT3 gene, human silent information regulator Sir2 homologue, and survivorship in the elderly. Experimental Gerontology *38*, 1065-1070.

Roth, G., Hayek, M., Massimino, S., Davenport, G., Arking, R., Bartke, A., Bonkowski, M., and Ingram, D. (2009). Mannoheptulose: glycolytic inhibitor and novel caloric restriction mimetic. The FASEB Journal *23*, 553-551.

Roth, G.S., and Ingram, D.K. (2015). Manipulation of health span and function by dietary caloric restriction mimetics. Ann N Y Acad Sci.

Roudeau, S., Carmona, A., Perrin, L., and Ortega, R. (2014). Correlative organelle fluorescence microscopy and synchrotron X-ray chemical element imaging in single cells. Anal Bioanal Chem *406*, 6979-6991.

Sanchez de Groot, N., Gomes, R.A., Villar-Pique, A., Babu, M.M., Coelho, A.V., and Ventura, S. (2015). Proteome response at the edge of protein aggregation. Open Biol *5*, 140221.

Sardu, A., Treu, L., and Campanaro, S. (2014). Transcriptome structure variability in Saccharomyces cerevisiae strains determined with a newly developed assembly software. BMC Genomics *15*, 1-15.

Schieber, M., and Chandel, N.S. (2014). ROS function in redox signaling and oxidative stress. Current biology : CB *24*, R453-462.

Schmeisser, S., Zarse, K., and Ristow, M. (2011). Lonidamine extends lifespan of adult Caenorhabditis elegans by increasing the formation of mitochondrial reactive oxygen species. Horm Metab Res *43*, 687-692.

Scott, C.T., and DeFrancesco, L. (2015). Selling long life. Nat Biotech *33*, 31-40.

Sharma, P.K., Mittal, N., Deswal, S., and Roy, N. (2011). Calorie restriction up-regulates iron and copper transport genes in Saccharomyces cerevisiae. Molecular bioSystems *7*, 394-402.

Shibata, Y., Kumar, P., Layer, R., Willcox, S., Gagan, J.R., Griffith, J.D., and Dutta, A. (2012). Extrachromosomal MicroDNAs and Chromosomal Microdeletions in Normal Tissues. Science *336*, 82-86.

Silverman, G. (1996). Reconstruction of Large Genomic Segments of DNA by Meiotic Recombination Between YACs. In YAC Protocols, D. Markie, ed. (Humana Press), pp. 199-216.

Sinclair, D.A., and Guarente, L. (1997). Extrachromosomal rDNA Circles— A Cause of Aging in Yeast. Cell *91*, 1033-1042.

Smeal, T., Claus, J., Kennedy, B., Cole, F., and Guarente, L. (1996). Loss of Transcriptional Silencing Causes Sterility in Old Mother Cells of S. cerevisiae. Cell *84*, 633-642.

Soefje, S.A., Karnad, A., and Brenner, A.J. (2011). Common toxicities of mammalian target of rapamycin inhibitors. Target Oncol *6*, 125-129.

Soti, C., and Csermely, P. (2007). Aging cellular networks: chaperones as major participants. Exp Gerontol *42*, 113-119.

Spizzo, T., Byersdorfer, C., Duesterhoeft, S., and Eide, D. (1997). The yeast FET5 gene encodes a FET3-related multicopper oxidase implicated in iron transport. Mol Gen Genet *256*, 547-556.

Squier, T.C. (2001). Oxidative stress and protein aggregation during biological aging. Experimental Gerontology *36*, 1539-1550.

Stearman, R., Yuan, D.S., Yamaguchi-Iwai, Y., Klausner, R.D., and Dancis, A. (1996). A Permease-Oxidase Complex Involved in High-Affinity Iron Uptake in Yeast. Science *271*, 1552-1557.

Steffen, K.K., Kennedy, B.K., and Kaeberlein, M. (2009). Measuring replicative life span in the budding yeast. J Vis Exp.

Steinkraus, K.A., Kaeberlein, M., and Kennedy, B.K. (2008). Replicative aging in yeast: the means to the end. Annu Rev Cell Dev Biol *24*, 29-54.

Sturtz, L.A., Diekert, K., Jensen, L.T., Lill, R., and Culotta, V.C. (2001). A fraction of yeast Cu,Zn-superoxide dismutase and its metallochaperone, CCS, localize to the intermembrane space of mitochondria. A physiological role for SOD1 in guarding against mitochondrial oxidative damage. J Biol Chem *276*, 38084-38089.

Tacutu, R., Craig, T., Budovsky, A., Wuttke, D., Lehmann, G., Taranukha, D., Costa, J., Fraifeld, V.E., and de Magalhaes, J.P. (2013). Human Ageing Genomic Resources: integrated databases and tools for the biology and genetics of ageing. Nucleic Acids Res *41*, D1027-1033.

Tower, J. (2011). Heat shock proteins and Drosophila aging. Exp Gerontol *46*, 355-362.

Treco, D.A., and Winston, F. (2008). Growth and manipulation of yeast. Curr Protoc Mol Biol *Chapter 13*, Unit 13 12.

Urbanowski, J.L., and Piper, R.C. (1999). The Iron Transporter Fth1p Forms a Complex with the Fet5 Iron Oxidase and Resides on the Vacuolar Membrane. Journal of Biological Chemistry *274*, 38061-38070.

van den Hazel, H.B., Kielland-Brandt, M.C., and Winther, J.R. (1996). Review: Biosynthesis and function of yeast vacuolar proteases. Yeast *12*, 1-16.

van der Horst, A., and Burgering, B.M. (2007). Stressing the role of FoxO proteins in lifespan and disease. Nat Rev Mol Cell Biol *8*, 440-450.

van Deursen, J.M. (2014). The role of senescent cells in ageing. Nature *509*, 439-446.

Vassiliev, V., Harris, Z.L., and Zatta, P. (2005). Ceruloplasmin in neurodegenerative diseases. Brain Res Brain Res Rev *49*, 633-640.

Vijg, J., and Suh, Y. (2013). Genome instability and aging. Annu Rev Physiol *75*, 645-668.

Viswanathan, M., Kim, S.K., Berdichevsky, A., and Guarente, L. (2005). A role for SIR-2.1 regulation of ER stress response genes in determining C. elegans life span. Dev Cell *9*, 605-615.

Wach, A., Brachat, A., Pöhlmann, R., and Philippsen, P. (1994). New heterologous modules for classical or PCR-based gene disruptions in Saccharomyces cerevisiae. Yeast *10*, 1793-1808.

Wanichthanarak, K., Wongtosrad, N., and Petranovic, D. (2015). Genome-wide expression analyses of the stationary phase model of ageing in yeast. Mech Ageing Dev *149*, 65-74.

Willcox, B.J., Donlon, T.A., He, Q., Chen, R., Grove, J.S., Yano, K., Masaki, K.H., Willcox, D.C., Rodriguez, B., and Curb, J.D. (2008). FOXO3A genotype is strongly associated with human longevity. Proceedings of the National Academy of Sciences of the United States of America *105*, 13987-13992.

Winder, W.W., and Hardie, D.G. (1999). AMP-activated protein kinase, a metabolic master switch: possible roles in Type 2 diabetes. American Journal of Physiology - Endocrinology and Metabolism *277*, E1-E10.

Winterbourn, C.C. (1995). Toxicity of iron and hydrogen peroxide: the Fenton reaction. Toxicology Letters *82–83*, 969-974.

Winzeler, E.A., Shoemaker, D.D., Astromoff, A., Liang, H., Anderson, K., Andre, B., Bangham, R., Benito, R., Boeke, J.D., Bussey, H.*, et al.* (1999). Functional Characterization of the S. cerevisiae Genome by Gene Deletion and Parallel Analysis. Science *285*, 901-906.

Wood, J.G., Rogina, B., Lavu, S., Howitz, K., Helfand, S.L., Tatar, M., and Sinclair, D. (2004). Sirtuin activators mimic caloric restriction and delay ageing in metazoans. Nature *430*, 686-689.

Wuttke, D., Connor, R., Vora, C., Craig, T., Li, Y., Wood, S., Vasieva, O., Shmookler Reis, R., Tang, F., and de Magalhaes, J.P. (2012). Dissecting the gene network of dietary

restriction to identify evolutionarily conserved pathways and new functional genes. PLoS Genet *8*, e1002834.

Yip, C.K., Murata, K., Walz, T., Sabatini, D.M., and Kang, S.A. (2010). Structure of the human mTOR complex I and its implications for rapamycin inhibition. Mol Cell *38*, 768-774.

Zhou, C., Slaughter, B.D., Unruh, J.R., Guo, F., Yu, Z., Mickey, K., Narkar, A., Ross, R.T., McClain, M., and Li, R. (2014). Organelle-based aggregation and retention of damaged proteins in asymmetrically dividing cells. Cell *159*, 530-542.

Zong, H., Ren, J.M., Young, L.H., Pypaert, M., Mu, J., Birnbaum, M.J., and Shulman, G.I. (2002). AMP kinase is required for mitochondrial biogenesis in skeletal muscle in response to chronic energy deprivation. Proceedings of the National Academy of Sciences of the United States of America *99*, 15983-15987.